

3-24-2009

Moment-Dependent Pseudo-Rigid-Body Models for Beam Deflection and Stiffness Kinematics and Elasticity

Diego Alejandro Espinosa
University of South Florida

Follow this and additional works at: <https://scholarcommons.usf.edu/etd>



Part of the [American Studies Commons](#)

Scholar Commons Citation

Espinosa, Diego Alejandro, "Moment-Dependent Pseudo-Rigid-Body Models for Beam Deflection and Stiffness Kinematics and Elasticity" (2009). *Graduate Theses and Dissertations*.
<https://scholarcommons.usf.edu/etd/1955>

This Thesis is brought to you for free and open access by the Graduate School at Scholar Commons. It has been accepted for inclusion in Graduate Theses and Dissertations by an authorized administrator of Scholar Commons. For more information, please contact scholarcommons@usf.edu.

Moment-Dependent Pseudo-Rigid-Body Models for Beam Deflection and Stiffness

Kinematics and Elasticity

By

Diego Alejandro Espinosa

A thesis submitted in partial fulfillment
of the requirements for the degree of
Master of Science in Mechanical Engineering
Department of Mechanical Engineering
College of Engineering
University of South Florida

Major Professor: Craig P. Lusk, Ph.D.
Nathan Crane, Ph.D.
Rajiv Dubey, Ph.D.
Kathryn J De Laurentis, Ph.D.

Date of Approval:
March 24, 2009

Keywords: Flexible mechanisms, curved beam,
parametric model, ortho-planar motion, virtual work

©Copyright 2009, Diego Espinosa

Dedication

To my family and all of those who believed and supported me throughout this journey

Acknowledgements

I would like to express my gratitude to all of those who helped me and supported me throughout my education. I want to thank my mother, my father, and all the members of my family, who always believed in me and gave me courage to succeed and finish all of my goals. I want to give special thanks to Dr. Craig Lusk, who has been not only my mentor, but my friend and advisor. He was with me every step of the way, guiding me, teaching me, and showing me the right path for a successful career. I have learned so much from him and I am sure that without his caring dedication, knowledgeable advice and unceasing patience this thesis would not be a reality. Thank you very much, Dr. Lusk. I also would like to thank my committee members Dr. Rajiv Dubey, Dr. Nathan Crane, and Dr. De Laurentis, who took the time to review my thesis and gave me valuable advice to improve and complete my work. Finally, I would like to thank the Mechanical Engineering Department, the College of Engineering, and the University of South Florida for opening the door to me and giving me the opportunity to explore, discover and use the best of my potential. Thank you very much.

Table of Contents

List of Tables	iii
List of Figures	v
Abstract	vii
Chapter 1. Introduction	1
1.1 Objective	3
1.2 Motivation	4
1.3 Scope	5
1.4 Contributions	6
1.5 Roadmap	7
Chapter 2. Background	8
2.1 Pseudo-Rigid-Body Model	8
2.2 Kinematics of the Pseudo-Rigid-Body Model	9
2.3 Elasticity of the Pseudo-Rigid-Body Model	12
2.4 Trigonometric Relationships Between Planar and Spherical Mechanisms	13
2.5 Closure	18
Chapter 3. Methodology and Model Development	19
3.1 Theoretical Approach of Novel Parametric Beam Model for Straight and Curved Beams Kinematic Analysis	20
3.2 Computational Approach for Straight Compliant Beam Deflection	26
3.3 Kinematic Analysis Results Large Deflection Straight Beams	31
3.4 Computational Approach for Curved Compliant Beam Deflection	41
3.5 Curved Beam Kinematic Analysis	44
3.6 Kinematic Analysis Results Large Deflection Curved Beams	53
Chapter 4. Elasticity of a PRBM for Curved Beams	60
4.1 Principle of Virtual Work	60
4.2 Model Validation	65
4.3 Analysis of a Compliant Micro Helico-Kinematic Platform (MHKP) Device	68
Chapter 5. Conclusion	70
5.1 Conclusion and Summary of Contributions	70

References.....	72
Appendices.....	75
Appendix A: ANSYS Batch Code for a Vertical End-Loaded Beam	76
Appendix B: MATLAB Code for a Vertical End-Loaded Beam	88
Appendix C: ANSYS Batch Code for a Specific Horizontal Buckling End-Loaded Beam	93
Appendix D: MATLAB code for a Specific Horizontal Buckling End-Loaded Beam	105
Appendix E: ANSYS Batch Code for a Specific Horizontal Buckling End-Loaded Curved Beam.....	110
Appendix F: MATLAB Code for a Specific Horizontal Buckling End-Loaded Curved Beam.....	130
Appendix G: Tables of Summary of Results for a Specific Horizontal Buckling End-Loaded Curved Beam	152

List of Tables

Table 3.1	Notation of straight beam and curved beam variables.....	20
Table 3.2	Object data for FEA.....	27
Table 3.3	Values of the rational function coefficients for Case 1: Vertical end-load.....	31
Table 3.4	Results of statistic analysis for a vertical end load	36
Table 3.5	Values of the rational function coefficients for Case 2: Horizontal buckling end-load.....	37
Table 3.6	Results of statistic analysis for a horizontal buckling end-load	40
Table 3.7	Object data for FEA of curved beams.....	41
Table 3.8	Coordinate frames position and orientation.....	46
Table 3.9	Nomenclature.....	47
Table 3.10	Values of the rational function coefficients for a curved beam with a horizontal buckling end-load.....	54
Table 3.11	Results of statistic analysis for a horizontal buckling end-load curved beam.....	58
Table 4.1	Torque function coefficients.....	64
Table 4.2	Characteristics of the test beam	67
Table 4.3	MHKP material properties and cross-sectional area characteristics.....	68
Table 4.4	MHKP device simulation results	69
Table G.1	Summary of results of curved beam with $\lambda = 15^\circ$	152
Table G.2	Summary of results of curved beam with $\lambda = 30^\circ$	153

Table G.3	Summary of results of curved beam with $\lambda = 45^\circ$	153
Table G.4	Summary of results of curved beam with $\lambda = 60^\circ$	154
Table G.5	Summary of results of curved beam with $\lambda = 75^\circ$	154
Table G.6	Summary of results of curved beam with $\lambda = 90^\circ$	155
Table G.7	Summary of results of curved beam with $\lambda = 105^\circ$	155

List of Figures

Figure 2.1	A compliant cantilever beam with beam tip at $x=a$ and $y=b$	10
Figure 2.2	The PRBM of a compliant cantilever beam.....	10
Figure 2.3	Spherical triangle with sides k , m , and n ; and dihedral angles ϑ , σ , and ζ	15
Figure 2.4	Napier's Circle for a spherical right triangle with a right angle ζ	17
Figure 3.1	Shows the undeflected position of the beam Case 1	28
Figure 3.2	Shows the deflected position of beam Case 1.....	28
Figure 3.3	Shows the undeflected position of the beam Case 2.....	29
Figure 3.4	Shows the deflected position of beam Case 2.....	30
Figure 3.5	γ versus moment for Case 1: Vertical end-load	32
Figure 3.6	Case 1: Vertical end-load horizontal and vertical position of beam end.....	33
Figure 3.7	Case 1: Vertical end-load moment versus Θ	34
Figure 3.8	Shows the characteristic radius factor within the 95% confidence interval for Case 1: Vertical end load.....	35
Figure 3.9	γ versus moment for Case 2: Horizontal buckling end-load.....	37
Figure 3.10	Case 2: Horizontal buckling end-load, horizontal and vertical position of beam end.....	38
Figure 3.11	Case 2: Horizontal buckling end-load moment versus Θ	39
Figure 3.12	Shows the characteristic radius factor within the 95% confidence interval for Case 2: Horizontal buckling end-load.....	40

Figure 3.13	Shows the geometry, the loading, and the nodes of the undeflected curved beam	43
Figure 3.14	The deflected curved beam	43
Figure 3.15	The reference frames that describe the motion and orientation of positions on a compliant curved beam	45
Figure 3.16	The position coordinates and angles of nodes 3 and 12.....	49
Figure 3.17	The position coordinates and angles of nodes 4 and 8.....	49
Figure 3.18	The translation of the quarter segment on the planes A_2-A_1 and B_3-B_2	50
Figure 3.19	The spherical right triangle formed by a curved beam	52
Figure 3.20	γ versus moment for a curved beam with a horizontal buckling end-load.....	55
Figure 3.21	A horizontal end-load curved beam planar rotation, α versus out-of-plane rotation, β	56
Figure 3.22	Moment versus Θ for a horizontal buckling end-load curved beam.....	57
Figure 3.23	The characteristic radius factor within the 95% confidence interval for a horizontal buckling end-load curved beam	58
Figure 3.24	The approximation to \mathcal{G}_0 using the angle coefficient, C_ϑ and the Pseudo-Rigid-Body angle, Θ	59
Figure 4.1	The torque coefficient functions T_θ , T_f , and T_m versus Θ^*	64
Figure 4.2	The loads predicted by the parametric model and the loads acquired from the FEA analysis for a beam with an arc length of 105°	67
Figure 4.3	The loads predicted by the parametric model and the loads acquired from the FEA analysis for a beam with an arc length of 15°	68
Figure 4.4	Shows the MHKP device and outlines the curved beam being tested	69

Moment-Dependent Pseudo-Rigid-Body Models for Beam Deflection and Stiffness

Diego Alejandro Espinosa

ABSTRACT

This thesis introduces a novel parametric beam model for describing the kinematics and elastic properties of ortho-planar compliant Micro-Electro-Mechanical Systems (MEMS) with straight beams subject to specific buckling loads. Ortho-planar MEMS have the ability to achieve motion out the plane on which they were fabricated, characteristic that can be used to integrate optical devices such as variable optical attenuators and micro-mirrors. In addition, ortho-planar MEMS with large output forces and long strokes could be used to develop new applications such as tactile displays, active Braille, and actuation of micro-mirrors. In order to analyze the kinematics and elasticity of a curved beam contained in a Micro Helico-Kinematic Platform (MHKP) device, this thesis offers an improved model of straight and curved flexures under compressive loads. This model uses an approach similar to the one applied to develop a regular Pseudo-Rigid –Body Model but it differs in the definition of a key parameter, the *characteristic radius factor*, γ , which is not a constant, but a function of the moment, $\hat{\gamma} = \gamma(M)$. This approach allows for the Pseudo-Rigid-Body Model (PRBM) to describe the motion taken by the deflected beam precisely over a large range of motion. In developing the model, this thesis describes kinematic and elastic parameters such as the

angle coefficient, C_θ , the characteristic radius, γl , and the torque coefficient, T_θ .

Furthermore, the torque coefficient is divided into two component functions, T_f , and, T_m , which can be used to find the working loads (force and moment) on the beam. The input displacement is the only needed state variable, object variables, which describe the beam, include the material modulus of elasticity, E , the moment of inertia, I , and its length, l .

Chapter 1

Introduction

Mechanisms are “mechanical devices use to transfer or transform energy, force, or motion [1, 2]. We can distinguish between rigid-body mechanisms, which are “systems of rigid links connected by movable joints” such as cams, lever, and gears and *compliant mechanisms*, which “gain some of their mobility from the deflection of flexible members rather than from movable joints only” [3]. Compliant mechanisms offer advantages such as cost reduction and performance improvements, which are achieved by increasing the precision and reliability of the mechanism, reducing wear, weight, maintenance, assembly time and the number of parts needed for assembly [3]. These advantages are particularly important in devices fabricated at the micro scale, known as Micro-Electro-Mechanical Systems (MEMS).

MEMS technology offers ways to bridge fields that were previously unrelated, joining different branches of study such as biology and microelectronics. Some examples of the applications in which MEMS are currently being applied include biotechnology, where MEMS have facilitated new discoveries “such as Polymerase Chain Reaction (PCR) Microsystems for DNA amplification and identification, micro-machined Scanning Tunneling Microscopes (STMs), biochips for detection of hazardous chemical and biological agents, and micro-systems for drug screening and selection” [4]. MEMS

technology has also improved the overall performance of communication circuits and has reduced the cost and power consumption of such devices. Moreover, MEMS accelerometers are rapidly substituting for the conventional accelerometers used to trigger air-bag deployment systems in automobiles, due to their reliability, the ability to integrate the accelerometer and electronics in a single silicon chip, and reduction of the overall cost [4].

Generally MEMS are fabricated by depositing multiple planar layers of polysilicon, or polycrystalline silicon on a silicon wafer, then, by bulk micromachining, planar lithography is used to selectively etch and shaped the planar material layers into the micro-structure desired [3]. There are several challenges in the design phase and part assembly of mechanical devices at the micro level. Due to the planar nature of the fabrication process and the small scale in which MEMS are designed, it is hard to create hinges and pin joints that accurately move and stay in place. Additionally, it is also challenging to design three-dimensional motion devices that achieve their specific tasks without failing first. The performance of these devices greatly depend on the materials properties, yet the material choices for MEMS processes are very limited and their behavior and properties at the micro-scale are not completely understood [3].

Nevertheless, compliant mechanisms offer an answer to many of these problems due to advantages they offer in the designs of mechanisms at the micro level [5]. According to

Clements [5] “Compliant MEMS:

- Can be fabricated in a plane
- Required no assembly
- Required less space and are less complex

- Have less need for lubrication
- Have reduced friction and wear
- Have less clearances due to pin joints, resulting in higher precision
- Integrate energy storage elements (springs) with the other components”

One of the methods used to performed compliant beams deflection analysis is a mathematical approach based on elliptical integrals, a method that is difficult to use and does not produce much insight on the motion and the stiffness of the beam.

Consequently, alternative methods have been found in order to make the analysis simpler and more intuitive. One of these methods is a parametric approximation model called the Pseudo-Rigid-Body Model (PRBM) in which the compliant mechanism is modeled by an analogue rigid mechanism [3]. Some of the weaknesses of this model are:

- First, it only works on certain load and force configurations.
- Second, for some long and thin beams it does not model the compliant beam deflection throughout its complete range of motion.
- Finally, it does not work on curved beams.

1.1 Objective

The objectives of this thesis are:

- To create a more accurate parametric beam model for compliant MEMS using a rational function to represent the characteristic radius factor as a function of the moment load, $\hat{\gamma} = \gamma(M)$.
- Second, apply this model for the analysis of the kinematics and elasticity of the complete deflection range of motion of both straight and the curved beams.

- Third, find specific buckling loads on a compliant Micro Helico-Kinematic Platform (MHKP) device [6].
- Finally, develop software codes in order to produce a new parametric model and provide validation of its capabilities see appendixes A, C, and E (ANSYS codes), B, D, and F (MATLAB codes).

1.2 Motivation

Ortho-planar mechanisms are a subclass of mechanisms that are manufactured in a single plane and have the ability to achieve motion out of that plane [7]. Ortho-planar MEMS can be used to “integrated optical devices such as variable optical attenuators, micro Fresnel lenses, micro grating, multiplexers, and micro-mirrors” [8]. In addition, ortho-planar MEMS with a high integration ability and capability of moving in the out-plane direction with large output forces and long strokes could be used to develop new applications such as tactile displays, active Braille, and actuation of micro-mirrors [9]. Last but not least, ortho-planar MEMS could be implemented to developed new spatial light modulators [10] capable of manipulating optical wave fronts, which can be “used in image projectors, optical switching, and adaptive optics” [11].

Planar kinematics has been the method of choice when designing ortho-planar MEMS, leaving the benefits of spherical kinematics largely unnoticed and unexplored. “Using spherical kinematics, it is possible to design devices that move links to specified spatial orientations and can covert rotation in one plane to rotation in a different plane” [11]. The intent of this work is to provide tools that can help design and analyze curved

beams, furthering and facilitating the exploration and development of new compliant ortho-planar MEMS using spherical kinematics.

1.3 Scope

The Micro Helico-Kinematic Platform (MHKP) is an example of an ortho-planar mechanism. It was designed using spherical kinematic techniques in which three spherical crank-sliders with the same center and with an in-plane rotational input are used to vertically translate (in the out-plane direction) and rotate a platform. Due to the nature of the input, this device does not produce side-to-side motion, which allows for a closed packed array of similar devices and provides large vertical translation of the platform [6], making it a good candidate for movable pixels mirror [8]. To improve the design, manufacture process, and overall performance of this device, the rigid links, movable pins joints, and hinges were replaced by their compliant analogues; however, the kinematic and elastic analysis of the compliant analogues is more challenging due to the absence of a spherical Pseudo-Rigid-Body Model for curved compliant beams loaded with buckling loads [12]. As a consequence, there was a need for a new spherical Pseudo-Rigid-Body Model that would allow us to accurately analyze the kinematic and elastic behavior of the MKKP curved compliant beams.

This thesis introduces a novel parametric model for the kinematics and the elastic analysis of curved compliant beams using specific buckling loads. It focuses on the development of model parameters needed to accurately describe the behavior of a curved beam as it is deflects. Consequently, one can use this new model to accurately describe the

kinematics of the deflected MHKP's curved beams and computed the loads needed to actuate the device.

1.4 Contributions

The major contributions made by this research work in the analysis and design of compliant beams include:

- A novel parametric beam model for the kinematic analysis of buckled beams, where characteristic radius factor, γ , is a function of the moment load, $\hat{\gamma} = \gamma(M)$.
- Improvements in accuracy and range of this model compared with previous models by using a rational function model.
- The development of non-dimensional kinematic and elastic parameters, the angle coefficient, C_g , the characteristic radius factor, γ , and the torque coefficients, T_θ , T_f , and, T_m , that when combined with object data, the modulus of elasticity, E , the moment of inertia, I , the length of the beam, l , and state information, such as the input displacement, d , or the input rotation, Φ , can be use to determine the buckling behavior of the beam.
- This thesis also describes finite element analysis (FEA) procedures that were used to develop and validate the new parametric beam model.
- This thesis computes specific buckling loads needed to actuate a compliant Micro Helico-Kinematic Platform (MHKP) device.
- This thesis establishes the coordinates of the highest point reached by the MHKP once it is buckled.

- Finally, this work provides MATLAB codes used to analyze the output data produced by the finite element analysis, derive and validate the new parametric model, and obtain the kinematic and elastic parameters.

1.5 Roadmap

This first chapter has introduced the work developed in this thesis. Chapter 2 provides the background of PRBMs and spherical kinematics. Chapter 3 explains the relationships between a planar PRBM and a spherical PRBM. It also describes the approach taken to develop the new parametric beam model and its outcomes. Chapter 4 gives an overview of the principle of virtual work and how it was used to develop the torque coefficient, T_θ , and its components, T_f , and, T_m . Finally, Chapter 5 discusses the results and validation and provides the conclusions.

Chapter 2

Background

This chapter reviews previous work on Pseudo-Rigid-Body Models and spherical trigonometry. These are explained in detail because they are the starting point for this work and their overall understanding is essential for an easier comprehension of the details in this thesis.

2.1 Pseudo-Rigid-Body Model

In the past, elliptic integrals have been used to analyze end-loaded large deflection cantilever beams in order to obtain closed-form solutions [3]. However, this mathematical approach is difficult to use and produces little insight about the motion or stiffness of the beam. As a result, alternative methods of determining the beam deflection path have been developed, one of these is a parametric approximation model called the Pseudo-Rigid-Body Model (PRBM). This method consists in describing the compliant member's motion and stiffness by replacing it with a rigid-link analogue that has approximately the "same motion and stiffness for a known range of motion and to a known mathematical tolerance" [13]. In other words, the PRBM "provides a simplified but accurate method of analyzing the deflection of flexible beams and provides the designer a means of visualizing the deflection" [3], meaning that given a compliant beam,

its motion can be found by treating it as a mechanism with rigid links or given a specific motion, a PRBM that performs the same motion can be developed and transformed into its compliant analogue [13]. After the identification of the PRBM of the compliant member, its kinematic and elastic parameters are optimized and validated so that its range of applicability and level of error are known and acceptable [13].

2.2 Kinematics of the Pseudo-Rigid-Body Model

This PRBM approach is based on the fact that the deflection of the beam's free end follows a near-circular path with a center of curvature located at a point on the undeformed beam [3]. This allows the PRBM to determine "the relative positions of the end points of various compliant segments without precise modeling of the locations of interior points [8]. In addition, the PRBM is used to compute the amount of force required to achieve the desired deflection. An example of a PRBM for a straight cantilever beam with a vertical end load [3] is shown in Figure 2.1. This model was developed by Howell et al. [3,14] and is shown here to provide context for the current research.

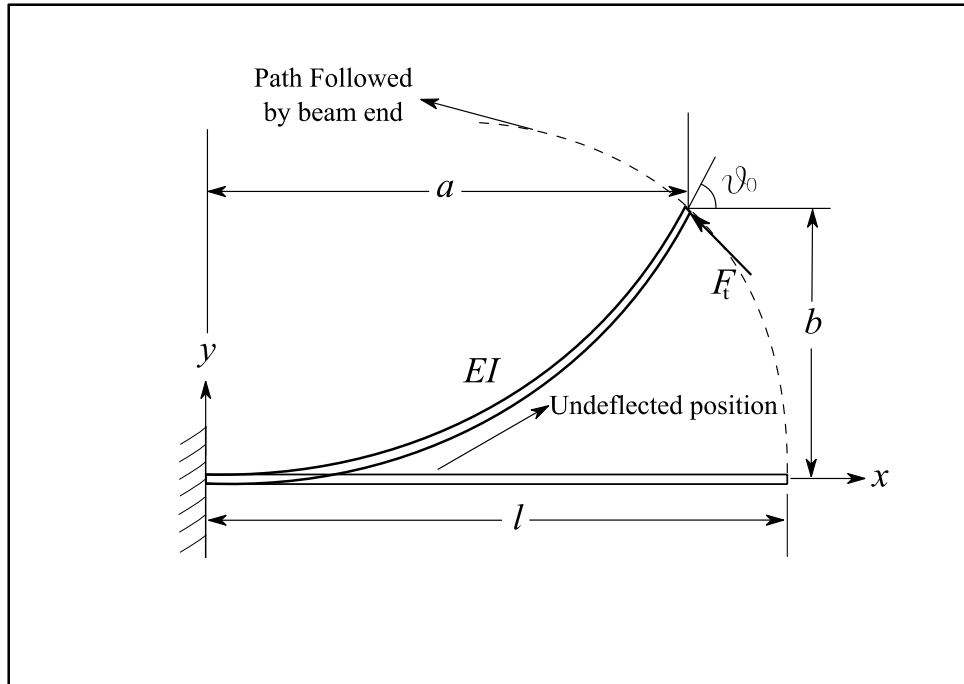


Figure 2.1. A compliant cantilever beam with beam tip at $x=a$ and $y=b$. Adapted from [3]

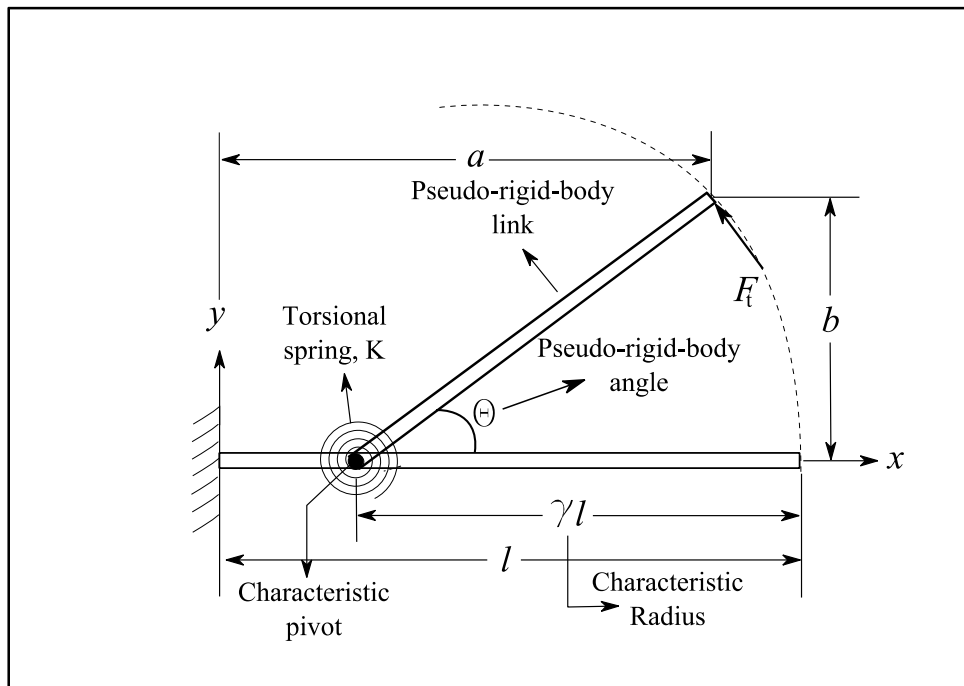


Figure 2.2. The PRBM of a compliant cantilever beam. (See Figure 2.1) adapted from [3]

Figure 2.1 shows the compliant cantilever beam and the large-deflection path of the beam end and Figure 2.2 shows a Pseudo-Rigid-Body Model that approximates the nearly circular path of the beam end. The Pseudo-Rigid-Body Model is created with two rigid links joined at a point along the beam called the *characteristic pivot*. The location of the characteristic pivot is chosen so that the path of the beam end of the rigid model matches, as closely as possible, the path of the beam end of the compliant beam. The distance from the beam end to the characteristic pivot is called the *characteristic radius*, γl , where the constant, γ , is named the *characteristic radius factor*. The angle Θ , known as the *Pseudo-Rigid-Body angle* is the amount of rotation that the rigid link must undergo to match the deflection of the compliant beam. Furthermore, the angle of inclination of the compliant beam at the beam end is given by \mathcal{G}_0 . In addition, the horizontal (x -coordinate) and the vertical (y -coordinate) coordinates of the end of the deflected beam are represented by the variables a and b , respectively, which are given in terms of the PRBM angle, Θ , in equations (2.1) and (2.2) Thus, the value of Θ can be calculated using equation (2.3). The relation between Θ and \mathcal{G}_0 is represented by (2.4), where C_g represents the *angle coefficient* with a value of 1.24.

$$\frac{a}{l} = 1 - \gamma(1 - \cos\Theta) \quad (2.1)$$

$$\frac{b}{l} = \gamma \sin\Theta \quad (2.2)$$

$$\Theta = \tan^{-1}\left(\frac{b}{a - l(1 - \gamma)}\right) \quad (2.3)$$

$$\mathcal{G}_0 = C_g \Theta \quad (2.4)$$

where C_g represents the *angle coefficient* with a value of 1.24.

In a research monograph by Howell [14], the characteristic radius factor, γ , was found by establishing the maximum acceptable percent error in the deflection at 0.5% equation (2.5); then, optimization was used to determine the value of γ that allows for a maximum value of PRBM angle, Θ , without violating the maximum error constraints. It was determined that an optimal value of γ is 0.8517, which maintains an error smaller than 0.5% at angular deflections less than $\Theta_{\max}=64.3^\circ$.

$$g(\Theta) = \frac{\text{error}}{\varepsilon_e} \leq \left(\frac{\text{error}}{\varepsilon_e} \right)_{\max} \quad \text{for } 0 < \Theta < \Theta_{\max} \quad (2.5)$$

Where $\frac{\text{error}}{\varepsilon_e}$ represents the error of the relative deflection between the PRBM

and the compliant member and ε_e represents is the vector difference of the deflected position of the beams end point and its undeflected position.

2.3 Elasticity of the Pseudo-Rigid-Body Model

In order to model the elasticity of the material and its resistance to deformation, a torsional spring with a constant spring-rate, K , is placed at the characteristic pivot, as shown in Figure 2.2. When a load is applied to a PRBM link at an angle, φ , the component of the force orthogonal to the beam's surface and tangent to the end point's path is represented by F_t , which is defined by equation (2.6) [3].

$$F_t = F \sin(\varphi - \Theta) = \frac{K\Theta}{\gamma l} \quad (2.6)$$

This transverse force, F_t , is responsible for the initial deflection of the rigid link, and creates a torque, T , about the characteristic pivot.

$$T = F_t \gamma l \quad (2.7)$$

Substituting (2.6) in (2.7) yields the torque required to deflect the flexural beam in terms of the constant spring-rate, K , and the PRBM angle, Θ .

$$T = K\Theta \quad (2.8)$$

The value of the torsional spring constant spring-rate, K , can be calculated as a function of the geometry of the beam, l/l , its material properties, E , the PRBM constants, γ , and the nondimensionalized spring constant, K_θ , defined as the *stiffness coefficient*, equation (2.9).

$$K = \gamma K_\theta \frac{EI}{l} \quad (2.9)$$

K_θ allows for an easy calculation of the force necessary to deflect the Pseudo-Rigid-Body Model; this force is approximately equal to the force required to deflect the compliant member equation (2.10), however, the elastic portion of the PRBM yields a $\Theta_{max}(K_\theta) < 58.5^\circ$ in order to have an accurate force prediction [15].

$$F_t = \frac{EIK_\theta\Theta}{l^2} \quad (2.10)$$

2.4 Trigonometric Relationships Between Planar and Spherical Mechanisms

This section reviews the basics of spherical trigonometry and introduces Napier's rules, which later are used to analyze spherical triangles.

Planar mechanisms are those in which joints axes are parallel and links are defined by the lengths between joints; in contrast, spherical mechanisms are those in which the joints axes intersect at the center of a sphere and links are defined by their great circles arcs [16]. A great circle is defined as one that has a radius equal to the radius of the sphere, and it is contained within a plane that intersects the sphere. For example, the earth longitudinal circles are great circles; the only latitudinal circle that is a great circle is the equator, which shares the same radius as the earth. Moreover, the angles between the planes containing the great circles are defined as dihedral angles. Relationships between planar and spherical configurations can be developed [17], often allowing the application of familiar planar kinematics concepts to spherical configurations. In spherical trigonometry the surface is not flat; instead, it is the curved surface of a sphere, where neither straight lines nor planar figures can be drawn [8]. However, “there are geometrical features on a spherical surface that have properties mathematically similar to their planar counterparts” [8]. For instance, a circle arcs drawn on a surface of a sphere possesses similar mathematical properties as a straight line drawn on a plane; furthermore, angles between intersecting circles can become analogues to the angles formed by straight lines [18]. These types of similarities allow the application of similar relationships and trigonometric rules, such as the Law of Sines, Law of Cosines, and rules for spherical right triangles, (Spherical triangle in which one of the dihedral angles is 90°). The following procedure follows Spiegel and Liu’s work [17] to describe the analogies between spherical trigonometry and plane trigonometry. During the discussion of these laws it is important to follow the nomenclature and differentiate between dihedral angles denoted by Greek letters, segment of great circles (arcs) denoted

by lower-case roman letter, and the points on great circles denoted by upper-case roman letters. The measurement of the dihedral angles and the great circles segments can be given in degrees or radians in order to facilitate the description of the spherical analogues of the Law of Sines and the Law of Cosines, simplified relations for spherical right triangles, and allows for the derivation of general results, which are independent of the radius of a particular sphere.

A spherical triangle is shown in Figure 2.3, where the arcs and the dihedral angles can be related by the Laws of Sines and Cosines.

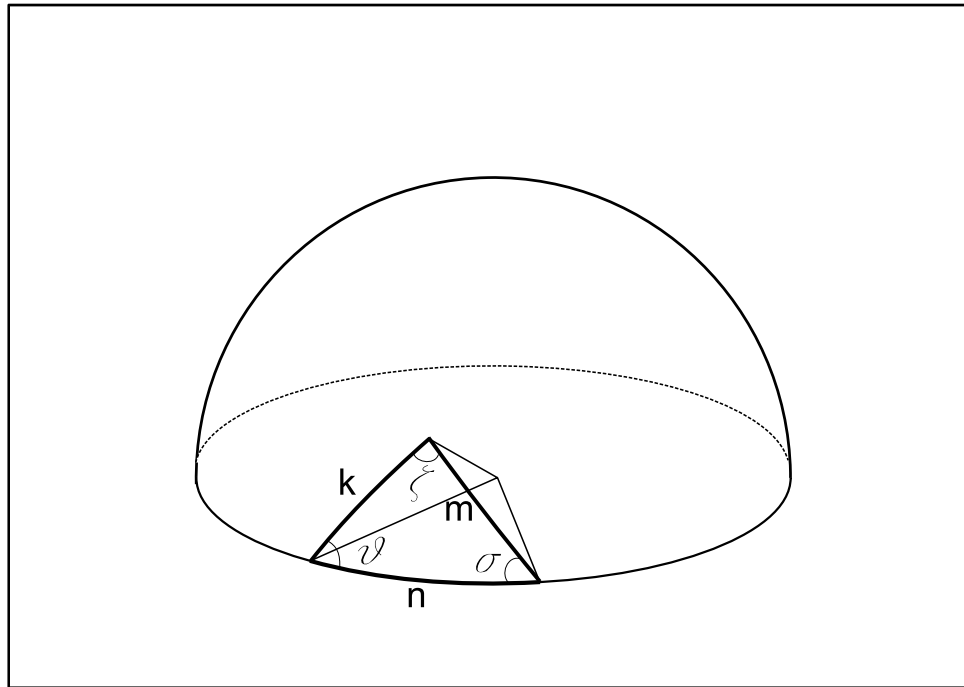


Figure 2.3. Spherical triangle with sides k , m , and n ; and dihedral angles ϱ , σ , and ζ . Adapted from [8]

The spherical Law of Cosines can relate the arcs and the dihedral angles in the following ways:

- Three arcs and one dihedral angle

$$\cos(\theta) = \cos(m)\cos(n) + \sin(m)\sin(n)\sin(\sigma) \quad (2.11)$$

- Three dihedral angles and one arc

$$\cos(\sigma) = -\cos(\vartheta)\cos(\xi) + \sin(\vartheta)\sin(\xi)\sin(k) \quad (2.12)$$

The spherical Law of Sines can relate two arcs and their respective opposing dihedral angles.

$$\frac{\sin(n)}{\sin(\zeta)} = \frac{\sin(m)}{\sin(\vartheta)} = \frac{\sin(k)}{\sin(\sigma)} \quad (2.13)$$

A spherical right triangle is one with at least one 90° dihedral angle, ζ , two other dihedral angles, ϑ and σ , and three arcs, k , m , and n , where n represents the hypotenuse of the spherical right triangle. If any two of these five parameters are known, one can find a third using *Napier's Rules* in spherical trigonometry. Napier's Rules are based on Figure 2.4, which arranges all five parameters around a circle. The hypotenuse and the two non-right dihedral angles carry the prefix "co", which represents the complement of the angle. Any segment of the circle can be considered as a *middle part*, the adjoining segments, are defined as the *adjacent parts*, and the two remaining segments are defined as the *opposite parts*.

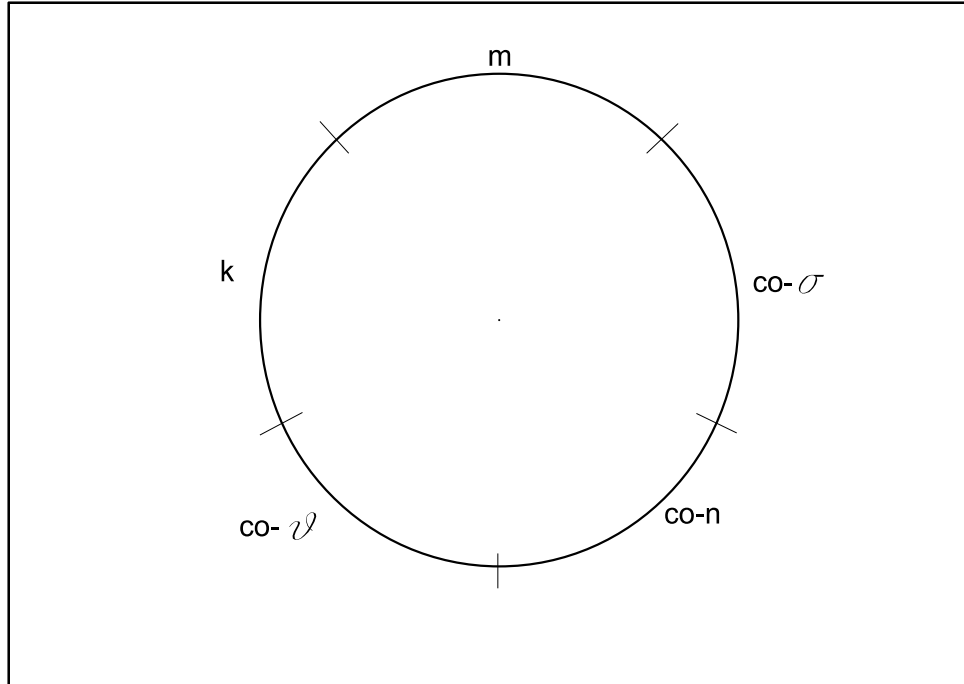


Figure 2.4. Napier's Circle for a spherical right triangle with a right angle ζ . Adapted from [17]

Napier's Rules summarizes ten equations that describe the relationships between any set of three of the five parameters in the Napier's Circle. The rules are:

- Rule 1: The sine of any middle part equals the product of the tangents of the adjacent parts.
- Rule 2: The sine of any middle part equals the product of the cosines of the opposite parts.

For instance, using Napier's Rules the value of k gives for Rule 1:

$$\sin(k) = \tan(\text{co} - \rho)\tan(m) = \cot(\rho)\tan(m) \quad (2.14)$$

and for Rule 2:

$$\sin(k) = \cos(\text{co} - n)\cos(\text{co} - \sigma) = \sin(n)\sin(\sigma) \quad (2.15)$$

2.5 Closure

This chapter has reviewed previous work on the Pseudo-Rigid-Body Model developed by Howell and the basics of spherical trigonometry. In the next chapter those concepts will be used to develop new parametric beam models for straight and curved beams.

Chapter 3

Methodology and Model Development

This section explains the theoretical approach taken for the straight beams deflection kinematic analysis. The notation of the variables of curved beam variables change due to the spherical nature of the beam and the need to express many of the variables as angles. However, there is a correspondence principle between planar and spherical PRBMs, which states that “when small angle assumption is used for spherical arcs i.e. the arc length is much smaller than the radius of the sphere, the spherical PRBM become identical to a planar PRBM.” [12]. For instance, the arc length, β , can be express to the planar length, b . Thus by small angle assumption:

$$\cos(\beta) = 1 \quad (3.1)$$

$$\sin(\beta) = \beta \rightarrow b \quad (3.2)$$

In the same way, the planar equivalents of α and λ are a and l respectively. Additionally, the terminology used to represent angles and ratios such as θ , γ , in spherical and planar PRBMs is the same for both cases. See Table 3.1.

The theoretical approach exposed in section 3.2 is analogues to the one of the curved beam. For practical reasons the equations on this section are only express on terms of the straight beam variables. The curved beam kinematic analysis will be study in more depth in sections 3.4, 3.5, and 3.6.

Table 3.1. Notation of straight beam and curved beam variables.

Parameter	Straight beam	Curved Beam
Characteristic radius factor	γ	γ
Length/Arc-length	l	λR
End-beam x-coordinate	b	β
End-beam y-coordinate	a	α
Pseudo-Rigid-Body angle	Θ	Θ

3.1 Theoretical Approach of Novel Parametric Beam Model for Straight and Curved Beams Kinematic Analysis

In this work, a different approach is implemented for finding the characteristic radius factor, γ , of straight and curved compliant beams with large deflections. It is possible to regard equations (2.1) and (2.2) as definitions of γ^* and Θ^* , rather than a convenient approximation. Thus, given the coordinates of the beam end, a and b , for a particular load condition, the values of γ^* and Θ^* can be found that satisfy equations (2.1) and (2.2) for that load.

By squaring equations (2.1) and (2.2), γ^* (3.3) and Θ^* (3.4) are defined in terms of a and b , as:

$$\gamma^* = \frac{-(a^2 - 2al + l^2 + b^2)}{2al - 2l^2} \quad (3.3)$$

$$\Theta^* = \tan^{-1}\left(\frac{b}{a - l(1 - \gamma^*)}\right) \quad (3.4)$$

The crucial difference between this approach and Howell's method is that γ^* is not a constant value throughout the deflection motion. Rather, it is a function of the load that allows for the PRBM to describe a closer approximation of the motion taken by the deflected beam. As a result, it is required to find a function that can closely match the

behavior of γ^* as the beam deflects and will not add significantly more complexity to the analysis of the PRBM. Our solution to that problem is to implement a rational function model that will fit the behavior of γ^* . This type of function was chosen over a polynomial function because of its numerous mathematical advantages, some of which include, the qualitative superiority of a rational function over a polynomial function [19], and its ability to fit complex shapes while keeping a low degree in both the numerator and denominator. This means that the function will required fewer coefficients giving it a relative simple form. Some other advantages of rational functions [20] include:

- Excellent interpolatory properties and extrapolatory powers.
- The tendency to be smoother and not as oscillatory as a polynomial functions.
- Accurate asymptotic properties, they can model a function not only within the domain of the data but also to represent theoretical/asymptotic behavior outside the domain of interest.

It is possible to created an expression of $\gamma(M)$, which contains both positive and negative powers of M . For example, we can approximate:

$$\gamma(M) \approx \hat{\gamma}(M) = b_{-2} \frac{1}{M^2} + \frac{b_{-1}}{M} + b_0 + b_1 M + b_2 M^2 \quad (3.5)$$

Where,

M_i = i th value of nondimensionalized M from data

γ_i^* = value of γ calculated form a_i and b_i from equation (3.1)

$\hat{\gamma}_i = \hat{\gamma}(M_i) =$ Rational fit to γ_i^*

In order to find the coefficients (b_i)

Let,

$$\bar{B} = [b_{-2} \quad b_{-1} \quad b_0 \quad b_1 \quad b_2]^T \quad (3.6)$$

$$\hat{\gamma}_i = [X] \bar{B} \quad (3.7)$$

Where,

$$X = \begin{bmatrix} \frac{1}{M_1^2} & \frac{1}{M_1} & 1 & M_1 & M_1^2 \\ \vdots & \vdots & 1 & \vdots & \vdots \\ \frac{1}{M_i^2} & \frac{1}{M_i} & 1 & M_i & M_i^2 \\ \vdots & \vdots & 1 & \vdots & \vdots \\ \frac{1}{M_n^2} & \frac{1}{M_n} & 1 & M_n & M_n^2 \end{bmatrix} \quad (3.8)$$

Using the method of least squares to find \bar{B} ,

$$\bar{B} = ([X]^T [X])^{-1} [X]^T \gamma_i^* \quad (3.9)$$

Once b_i is known, equation (3.5) can be used to find $\hat{\gamma}_B(M)$. Then, the Pseudo-Rigid-Body angle, Θ_B^* , can be found.

$$\hat{\gamma}_B(M) = b_{-2} + \frac{b_{-1}}{M} + \frac{b_0}{M^2} + b_1 M + b_2 M^2 \quad (3.10)$$

$$\Theta_B^* = \tan^{-1} \left(\frac{b}{a - l(1 - \hat{\gamma}_B(M))} \right) \quad (3.11)$$

In order to determine how well the parametric model, $\hat{\gamma}_B(M)$, truly represents the data, statistical analysis a two-sided t test with a 95% confidence interval and the coefficient of determination R_B^2 were performed. The R_B^2 is used to determine a proportion of the variance of one variable that is predictable from another variable; in addition, its measurement allows determination of how certain one can be in making

predictions based on certain model/graph. In other words, it represents the percent of the data that is closest to the line of best fit. The coefficient of determination is defined as the ratio of the explained variation to the total variation [21, 22].

$$\varepsilon_B = (\gamma^* - \hat{\gamma}_B(M))^2 \quad (3.12)$$

$$SST = \Sigma(\gamma_i^* - \bar{\gamma}_i^*)^2 \quad (3.13)$$

$$SSE_B = \Sigma(\varepsilon_i^2) \quad (3.14)$$

$$\sigma_B^2 = \frac{SSE}{\text{Number of data Points}} \quad (3.15)$$

$$R_B^2 = 1 - \frac{SSE_B}{SST} \quad (3.16)$$

Where σ_B^2 , represents the variance, ε_B , represent the squares explained, SSE represents the sum of the squares explained (explained variance), and SST represents the total sum of the squares (total variance). Then one can find the covariance matrix using,

$$\text{Var}B = \left([X]^T [X] \right)^{-1} \sigma_B^2 \quad (3.17)$$

However, computation of the variance of the coefficients of \bar{B} is complicated because $\text{Var}B$ is not a diagonal matrix (i.e. the basis functions chosen for X are not orthogonal).

We can find an orthogonal set of basis functions by finding the eigenvectors of $(X^T X)^{-1}$, which is a symmetric matrix and has eigenvalues that are real and its eigenvectors are orthogonal.

We express the eigenvectors as an orthogonal (rotation) matrix of eigenvectors and the eigenvalues as a diagonal matrix such that:

$$(X^T X)^{-1} V = VD \quad (3.18)$$

Where,

V = Eigenvectors matrix

D = Diagonal Eigenvalues matrix

We then can change the set of basis functions from the non-orthogonal set in X to an orthogonal set in X_2 , where

$$X_2 = [X]V \quad (3.19)$$

We can find the coefficients in the orthogonal basis by computing

$$\bar{C} = \left([X_2]^T [X_2] \right)^{-1} [X_2]^T \gamma_i^* \quad (3.20)$$

Then, the parametric model's function for the characteristic radius factor and the PRBM angle functions becomes

$$\hat{\gamma}_c(M) = \bar{C}X_2 \quad (3.21)$$

$$\Theta_c^* = \tan^{-1} \left(\frac{b}{a - l(1 - \hat{\gamma}_c(M))} \right) \quad (3.22)$$

The statistical two-side t test and the examination of the coefficient of determination R_c^2 can now be performed using the new variables

$$\varepsilon_c = \left(\gamma_i^* - \hat{\gamma}_c(M) \right)^2 \quad (3.23)$$

$$SST = \sum \left(\gamma_i^* - \bar{\gamma}_i^* \right)^2 \quad (3.24)$$

$$SSE_c = \sum \left(\varepsilon_i^2 \right) \quad (3.25)$$

$$\sigma_c^2 = \frac{SSE_c}{\text{Number of data values}} \quad (3.26)$$

$$R_c^2 = 1 - \frac{SSE_c}{SST} \quad (3.27)$$

It can be shown that

$$\vec{C} = V^T B \quad (3.28)$$

and that: $\sigma_C^2 = \sigma_B^2$ because X_2 is a orthogonal transformation (rotation) of X and $\det(V)=1$.

Therefore, the variance of C is:

$$\text{Var}C = \left([X_2]^T [X_2] \right)^{-1} \sigma_C^2 \quad (3.29)$$

or

$$\text{Var}C = D^{-1} \sigma_C^2 \quad (3.30)$$

because $\text{Var}C$ is a diagonal matrix, the standard deviation of i th component of \vec{C} can be found as:

$$C_i \pm \sqrt{\text{Var}C_{ii}} \quad (3.31)$$

or

$$C_i \pm \sigma_{C,i} \quad (3.32)$$

Where the standard deviation of the i th component of \vec{C} is the square root of the matrix element in the i th row and the i th column of $\text{Var}C$.

$$\sigma_{C,i} = \sqrt{\text{Var}C_{ii}} \quad (3.33)$$

from equation (3.25), it can then be shown that variance, $\sigma_{B,i}^2$ and the standard deviation $\sigma_{B,i}$ of the i th element of B are related to the standard deviation, σ_{C_j} , of the coefficients C_j of the orthogonal basis the elements by:

$$\sigma_{B,i}^2 = \left(\sum_{ij} V_{ij} \sigma_{C_j} \right)^2 \quad (3.34)$$

$$\sigma_{B,i} = \sqrt{\sigma_{Bi}^2} \quad (3.35)$$

Once the variance and the standard deviation have been found, one can proceed to perform a two-sided t test with a confidence interval of 95%; these interval estimates are often useful because the accuracy of estimate of the mean varies. The confidence interval generates a lower and upper limit for the mean which gives an indication of how much uncertainty there is in the estimate of the mean. The narrower the interval, the more precise the estimate is [23].

3.2 Computational Approach for Straight Compliant Beam Deflection

Two models of straight beams with different loading conditions were developed using FEA in order to obtain the data required to create the PRBM of each mechanisms (Case 1: Vertical end-load and Case 2: Horizontal buckling end-loaded). The horizontal buckling end-loaded case was considered because:

- Most of the PRBMs developed before focused only on cantilever beams vertically end-loaded. In addition, the PRBM for a beam with specific horizontal buckling end-loads has only been published for a beam with initial curvature. Reason being, the used of a constant γ does not yield accurate results for this type of problems. As a result, it was desired to develop a new PRBM for horizontal buckling end-loaded beams and study their behavior.
- A PRBM for horizontal buckling end-loaded beams will help to study the legs of Micro Helico-Kinematic Platform device, which are loaded with horizontal buckling loads.

The geometry and the material properties of the beams were defined as follows.

(See appendixes A and C).

Table 3.2. Object data for FEA.

	Case 1: Vertical end-load	Case 2: Horizontal end-load
Length, l	25 μm	100 μm
Width, w	10 μm	10 μm
Thickness, t	1 μm	1 μm
Modulus, E	169 GPa	169 GPa

The reason why there is a difference between the lengths of the two cases is because the beam in Case 2 is being buckled and just a fourth of the beam is analyzed this will be explained in further detail later in this chapter.

The ANSYS 3D beam element beam4 was used on these models; in order to take into account the complete 3D flexibility of the beams. In other words, the bending deformations, axial deformations, and torsional deformations occurring on the two principal bending planes were allowed for these analyses.

For Case 1 the boundary conditions defining this model were specified as follows. Node1 at the beginning of the beam was constrained in all directions so it remained fixed throughout the deflection motion. A vertical displacement was applied to node 5, rotation about the y -axis and translation on the x and z -directions were allowed, all other degrees of freedom were constrained. Moreover, the remaining nodes on the beam were left unconstrained allowing the observation and analysis of the beam's motion as it was deflected see Figures 3.1 and 3.2.

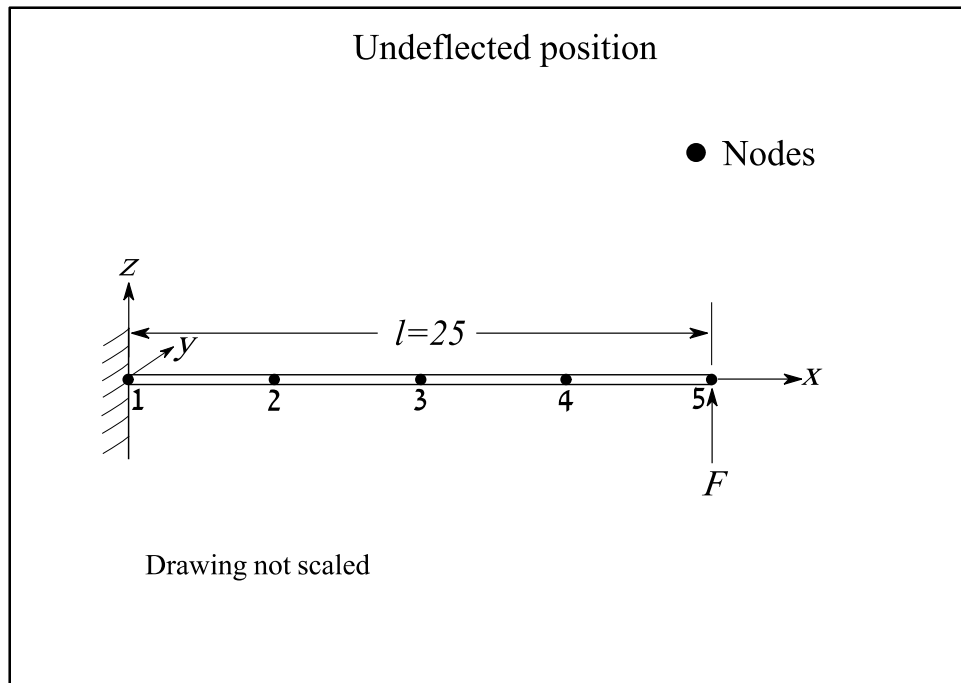


Figure 3.1. Shows the undeformed position of the beam Case 1.

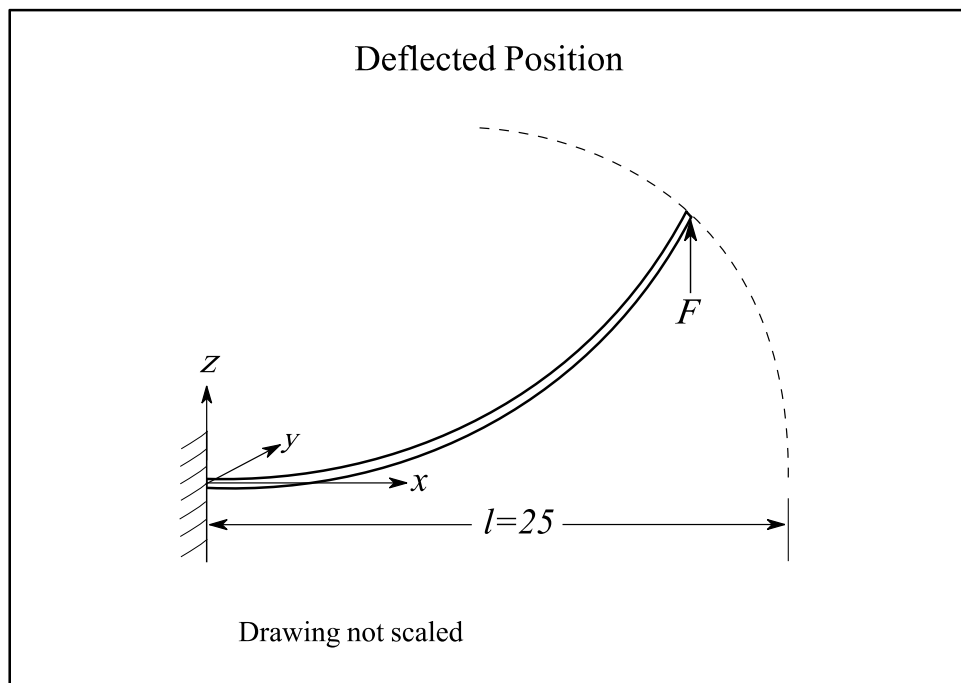


Figure 3.2. Shows the deflected position of beam Case 1.

For Case 2, the boundary conditions were identical to those of Case 1 with the exception that node 5 at the end of the beam was allow to move in x -direction and all other translations and rotations were prevented, resulting in the motion shown in Figures 3.3 and 3.4.

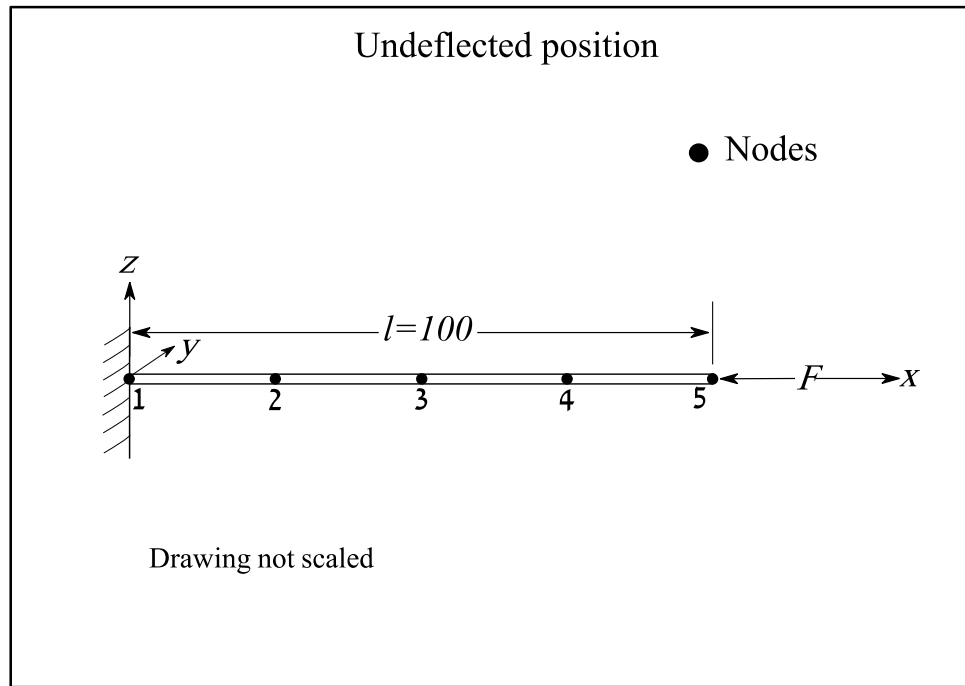


Figure 3.3. Shows the undeformed position of the beam Case 2.

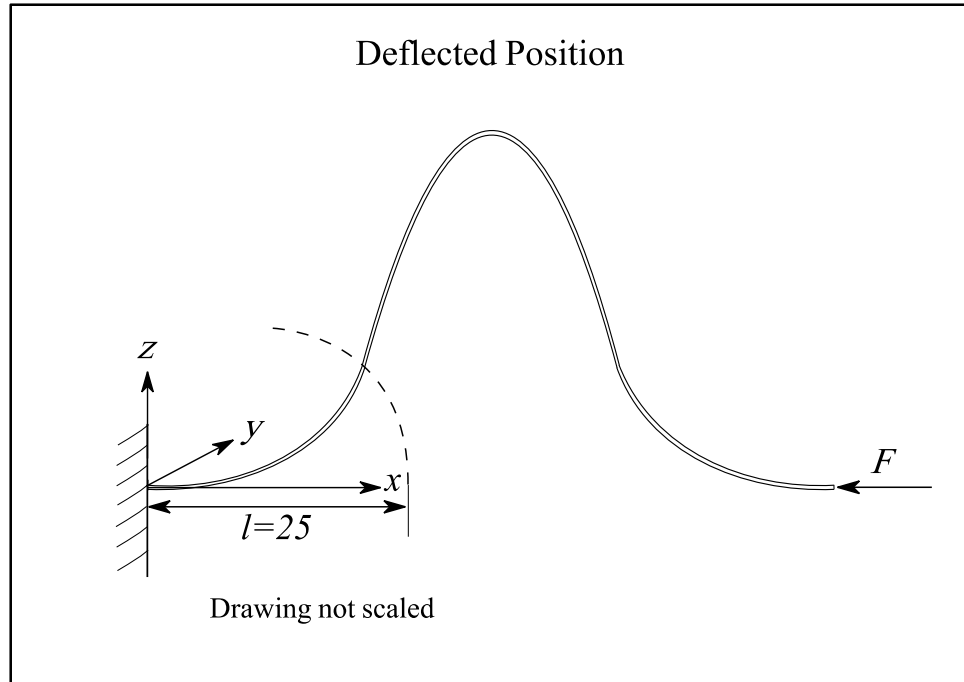


Figure 3.4. Shows the deflected position of beam Case 2.

The different loading conditions cases were defined as follows. Case 1 includes a vertical displacement load applied perpendicularly to the beam's end. Case 2 includes a buckling horizontal displacement applied horizontally to the beam's end as well. In both cases the beam's moving end was represented by node 5, which displacement caused the translation and rotation of the rest of the nodes, the deflection of the beam, and reaction forces to take place at node 1 and node 5. This information was collected over a range of 300 load steps in an ANSYS data output file. This file contains the displacements of the nodes in the x , y , and z directions, their rotations about the x , y , and z axes, their reaction forces in the x , y , and z directions, and their reaction moments about the x , y , and z axes as the beams were deflected.

Once the ANSYS information was acquired, an analysis program was written in MATLAB; this program used the output information file from ANSYYS to develop the

new parametric beam model introduced in Section 3.2 (see appendixes B and D). This part of the model predicts the kinematic behavior of the deflected beams.

3.3 Kinematic Analysis Results Large Deflection Straight Beams

This section provides a summary of the kinematic analysis of the deflection of a straight beam under different loading conditions.

For a vertical end-loaded beam Case 1, Howell's model, which uses a constant characteristic radius factor, γ , is accurate when the force acting on the beam is perpendicular to its neutral axis. However, as the end of the beam deflects and rotates, more of the beam becomes parallel to the direction of the applied load, and the accuracy of the values predicted by his PRBM decreases dramatically. In other words, a PRBM that uses a constant γ works well for the initial part of the deflection and its accuracy diminishes as the beam undergoes larger deflections as shown in Figure 3.5. On the other hand, in our new model, which uses a characteristic radius factor defined as a rational function of the moment, $\hat{\gamma} \approx \hat{\gamma}(M)$, with coefficient constants b_i , Table 3.3 the predicted values remain accurate throughout most of the deflection range.

Table 3.3. Values of the rational function coefficients for Case 1: Vertical end-load.

	Rational function Coefficients
b_{-2}	8.2e-1
b_{-1}	1.0e-4
b_0	-1.0e-5
b_1	4.1e-1
b_2	-1.9e-1

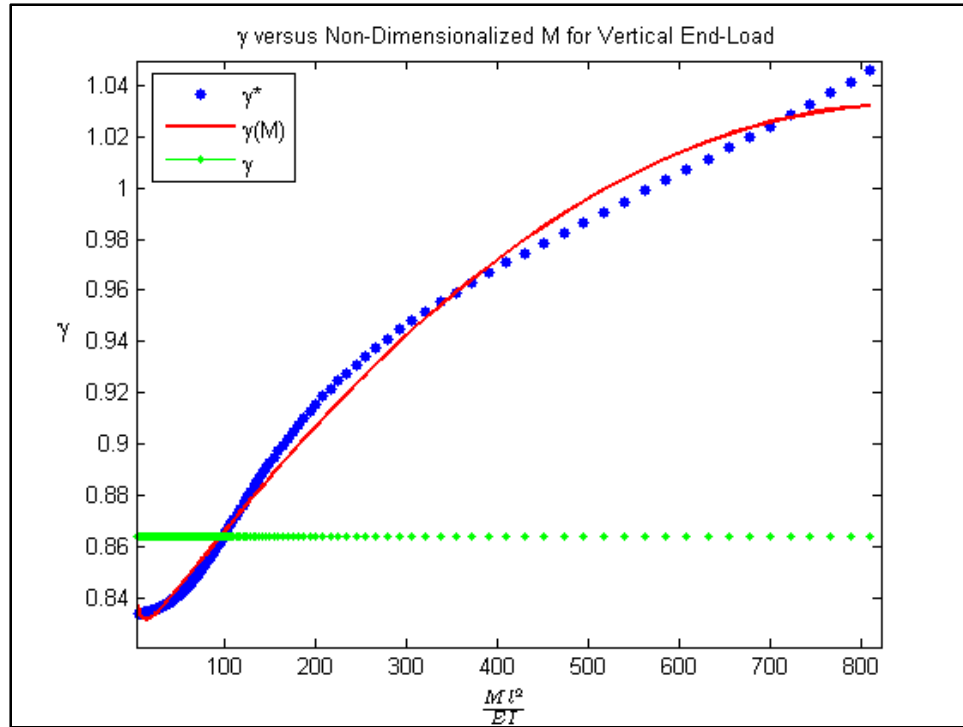


Figure 3.5. γ versus moment for Case 1: Vertical end-load.

Figure 3.6 shows the different PRBM approximations of the end-beam deflection path. As the beam's vertical deflection becomes large, significant portions of it become parallel to the applied force, this causes the beam to elongate as is shown in the final vertical height being larger than the original length of the beam. Consequently, the PRBM using the constant γ does not describe the complete deflection motion nor the elongation of the member; in contrast, the new parametric model approximation is able to accurately describe the complete path of the end-beam and its elastic deformation.

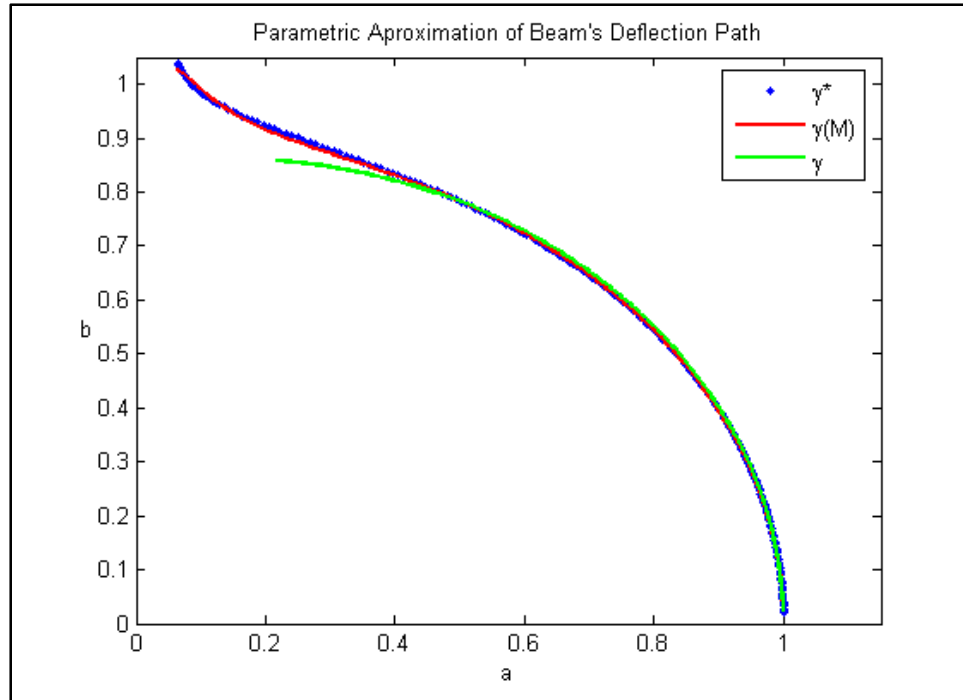


Figure 3.6. Case 1: Vertical end-load horizontal and vertical position of beam end.

Figure 3.7 shows the approximation of the PRBM angle, θ , found with the different parametric models. During the initial deflection motion of the beam, the PRBM using a constant γ exhibits an accurate prediction of the PRBM angle; however, as the deflection progresses the accuracy of this model diminishes giving a larger percent error for the prediction. Conversely, the new parametric model shows a constant and accurate prediction of the PRBM angle throughout the complete deflection of the beam.

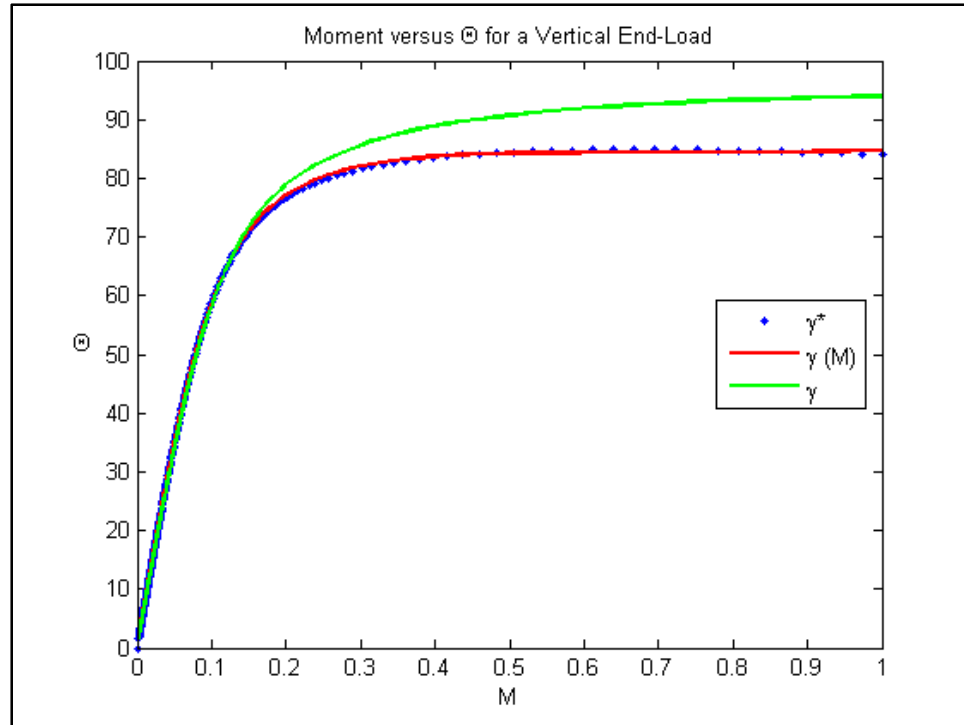


Figure 3.7. Case 1: Vertical end-load moment versus Θ .

A statistical analysis was performed to determine how well the new parametric model predicts the kinematics of the beam. Consequently, a two-sided t test with a 95% confidence interval was developed; Figure 3.8 shows the characteristic radius factor within the 95% confidence interval. The coefficient of determination R_B^2 was calculated to measure the amount of certainty of the model prediction, the rational function prediction maximum error and total error, and the constant g prediction total error in the deflection approximation were also calculated as shown in Table 3.4.

The 95% confidence interval produces an upper and lower limit for each coefficient of the rational function used in the PRBM to model the beam. This interval indicates how much uncertainty there is in the estimate of the mean; the narrower the interval, the more precise is the estimate. The coefficient of determination R_B^2 represents

the percentage of data that is closest to the line of best fit describing how certain one can be in making a prediction using our model. Finally, the total error represents the error in the kinematic prediction of our model compared to the actual data provided by the FEA analysis.

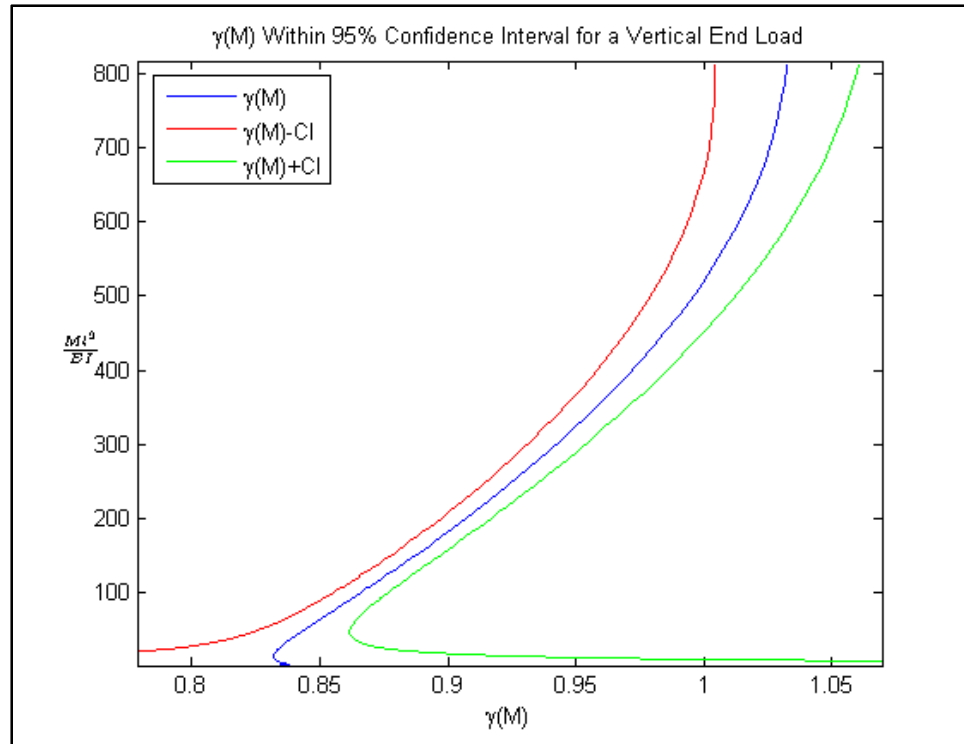


Figure 3.8. Shows the characteristic radius factor within the 95% confidence interval for Case 1: Vertical end load.

Table 3.4. Results of statistic analysis for a vertical end load.

	Rational function Coefficients	95% Confidence Interval
$b_{.2}$	8.2e-1	$\pm 3.9e-3$
$b_{.1}$	1.0e-4	$\pm 5.0e-4$
b_0	-1.0e-5	$\pm 1.0e-5$
b_1	4.1e-1	$\pm 1.2e-2$
b_2	-1.9e-1	$\pm 1.2e-2$
Coefficient of Determination, R_B^2		99.48%
Rational Function Prediction Maximum Error		0.1495e-1 %
Rational Function Prediction Total Error		2.7994e-3 %
Constant γ Total Error		0.3160 %

In Case 2, where a straight beam was loaded with specific horizontal buckling loads, just the first fourth segment of the beam was analyzed, that is from node 1 to node 2 as shown in Figures 3.3 and 3.4. This approach describes a cantilever beam loaded horizontally and at the same time permits the description of the buckled beam using symmetry. After testing with a constant- γ PRBM it was noticed that a constant γ does not produce an accurate PRBM for the initial part of the beam deflection. Interestingly, the constant γ PRBM approximation improves when the beam deflects sufficiently, so that the force is more perpendicular to the neutral axis of the beam. Furthermore, when γ is represented as a function of the load, i.e. as $\hat{\gamma} \approx \hat{\gamma}(M)$, a more accurate PRBM can be achieved throughout the whole range of the deflection. That is, regardless of the direction of the load or if the beam is being evaluated at the beginning or at the end of its deflection, $\hat{\gamma} \approx \hat{\gamma}(M)$ with coefficient constants b_i Table 3.5, can always produce an accurate PRBM for the prediction of the beam behavior Figure 3.9.

Table 3.5. Values of the rational function coefficients for Case 2: Horizontal buckling end-load.

	Rational function Coefficients
b_{-2}	8.216e-1
b_{-1}	-1.27e-2
b_0	-1.0e-4
b_1	-1.72e-2
b_2	-6.0e-3

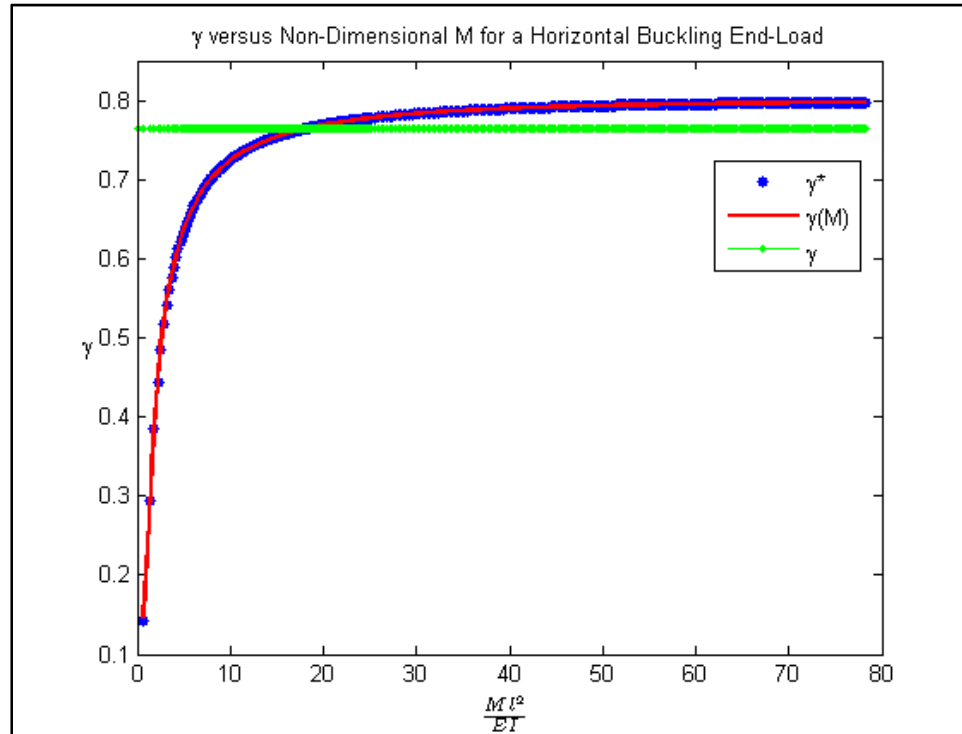


Figure 3.9. γ versus moment for Case 2: Horizontal buckling end-load.

Figure 3.10 shows the parametric approximations of the end-beam deflection path of the beam loaded with specific buckling loads. The new model is able to improve the accuracy of the PRBM in comparison with a constant γ model.

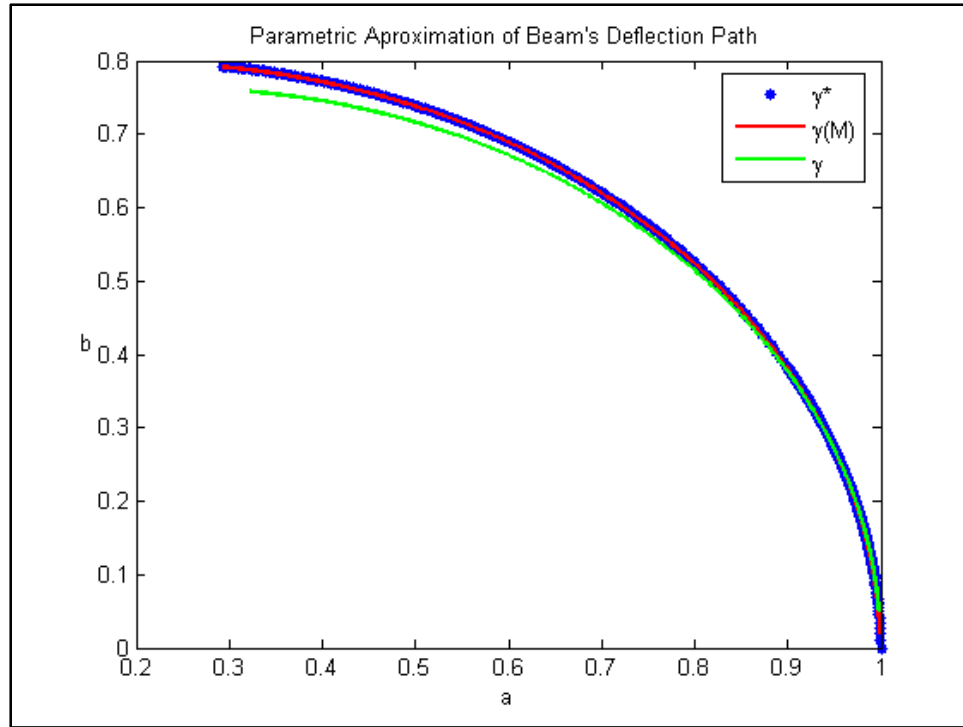


Figure 3.10. Case 2: Horizontal buckling end-load, horizontal and vertical position of beam end.

Figure 3.11 shows the approximation of the deflected member PRBM angle, θ .

Once again, the new parametric model demonstrates more accurate large deflection kinematic model predictions than a PRBM using the constant γ .

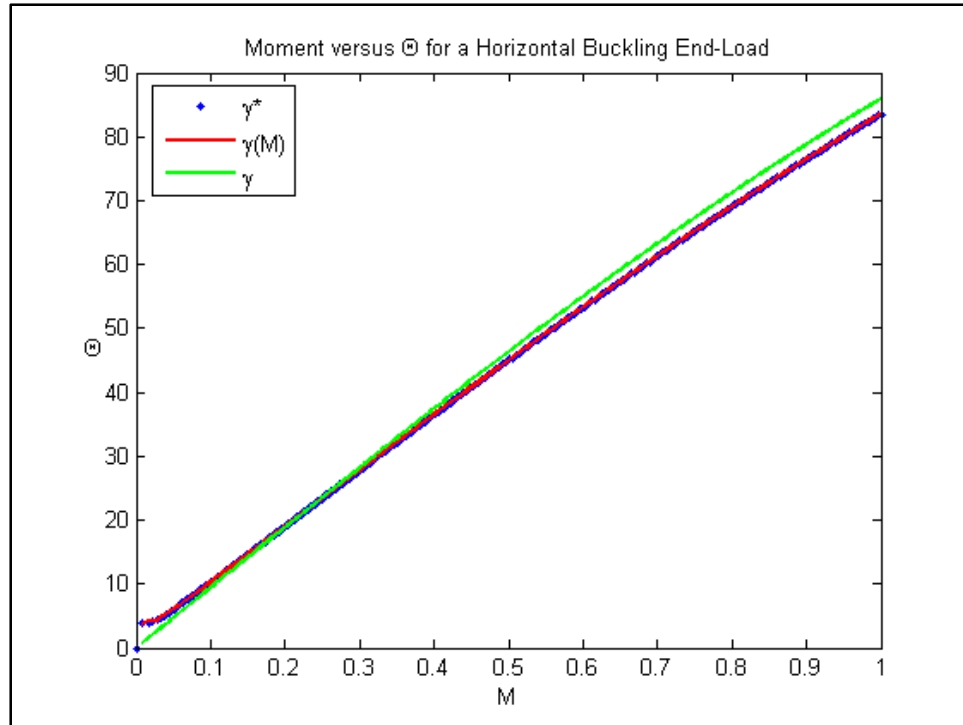


Figure 3.11. Case 2: Horizontal buckling end-load moment versus Θ .

For Case 2 a statistical analysis was performed as well; a two-sided t test with a 95% confidence interval was developed; Figure 3.12 shows the characteristic radius factor within the 95% confidence interval. The coefficient of determination R_B^2 , the rational function prediction maximum error and total error, and the constant γ prediction total error in the deflection approximation were also calculated as shown in Table 3.6.

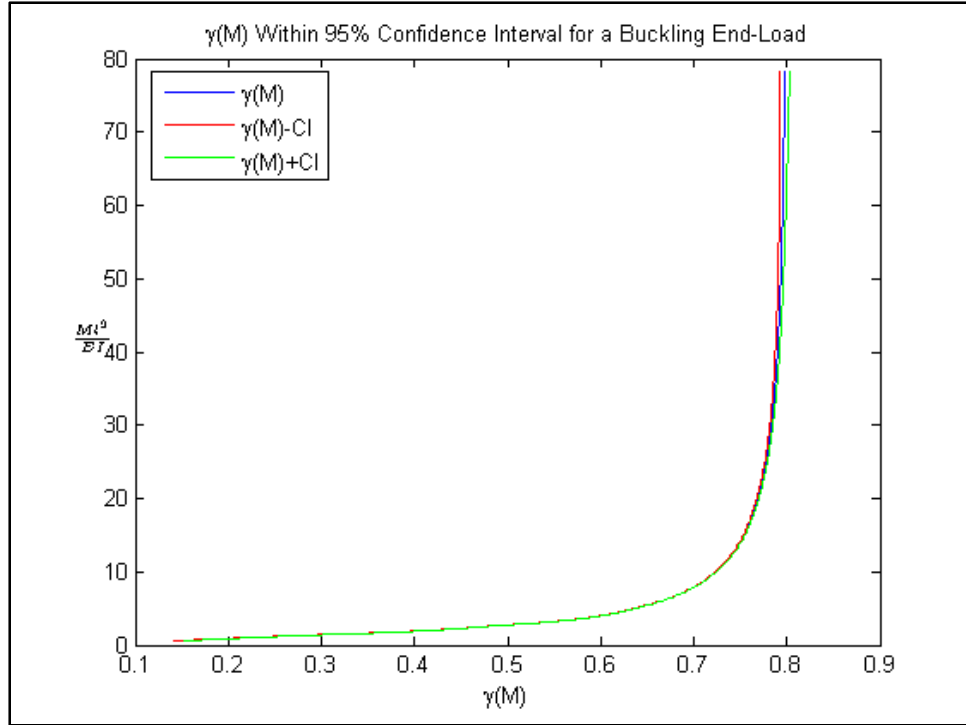


Figure 3.12. Shows the characteristic radius factor within the 95% confidence interval for Case 2: Horizontal buckling end-load.

Table 3.6. Results of statistic analysis for a horizontal buckling end-load.

	Rational function Coefficients	95% Confidence Interval
b_{-2}	8.216e-1	$\pm 3.0e-43$
b_{-1}	-1.27e-2	$\pm 1.0e-5$
b_0	1.0e-4	$\pm 1.0e-5$
b_1	-1.72e-2	$\pm 2.5e-3$
b_2	6.0e-31	$\pm 2.4e-3$
Coefficient of Determination, R_B^2		99.96%
Rational Function Prediction Maximum Error		0.1704e-5 %
Rational Function Prediction Total Error		1.6502e-7%
Constant γ Total Error		0.3187 %

A PRBM for a beam with specific horizontal buckling end-loads has only been previously published for a beam with initial curvature. This is because a constant γ , which was used for previous PRBMs does not yield accurate results. Consequently,

taking this new approach, we can improve the accuracy of the PRBMs for the analysis of end-loaded cantilever beams undergoing large deflections [24].

3.4 Computational Approach for Curved Compliant Beam Deflection

A model of a curved beam was developed in ANSYS in order to obtain the data required to create the PRBM of a spherical mechanism. The geometry and the material properties of the beam were defined as follows.

Table 3.7. Object data for FEA of curved beams.

	Data	Comments
Arc angle, λ	15°, 30°, 45°, 60°, 75°, and 90°	Different arc angles were use in order to broaden the analysis of curved beams and develop a model that would work with any arc angle.
Arc Length, s	10	The arc length was held constant throughout the analysis.
Radius, R	$\frac{s}{\lambda}$	The radius was defined as a function of the arc angle.
Width w	$\frac{s}{20}$	
Height, h	$(0.1) \times \frac{s}{\lambda}$	
Modulus, E	169 GPa	

The ANSYS 3D beam element beam4 was used in the FEA model in order to study the bending axial and torsional deflections occurring in the beam.

The geometry and boundary conditions of the spherical model were specified as shown in figure 3.13: Node 1 was defined as the fixed center of the sphere; thus, it was constrained in all directions.

In order to have the opportunity to test the symmetry of the deflected beam, the arc was divided in four segments of equal length formed by nodes 2, 3, 4, 8, and 12. Node 4 was placed at the middle of the beam and nodes 8 and 12 were placed at the first and final quarters of the structure allowing collection of strategic data from these symmetric points on the arc. Node 2 defined the fixed edge of the beam; therefore, it was constrained in all directions causing it to remain stationary throughout the deflection motion; in addition, nodes 4, 8 and 12 were free allowing for the study and observation of the beam's structure as it was deflected. Moreover, node 3 was a guided end of the curved beam, where a horizontal buckling displacement load was applied and motion was prevented in the z -direction as were rotations about the y and x -axes. These boundary conditions allowed for translation and rotation of the other nodes, and for reaction forces and moments to be obtained at the constrained nodes. Three orthogonal axes, a rotational reference frame were placed on nodes 4, 8, and 12 in order to track the motion of these nodes and to determine the twist about the beam's neutral axis. The reference frame at node 8 was defined by nodes 9, 10, and 11; the frame at node 4 was defined by nodes 5, 6, and 7; and the frame at node 12 was defined by nodes 13, 14, and 15.

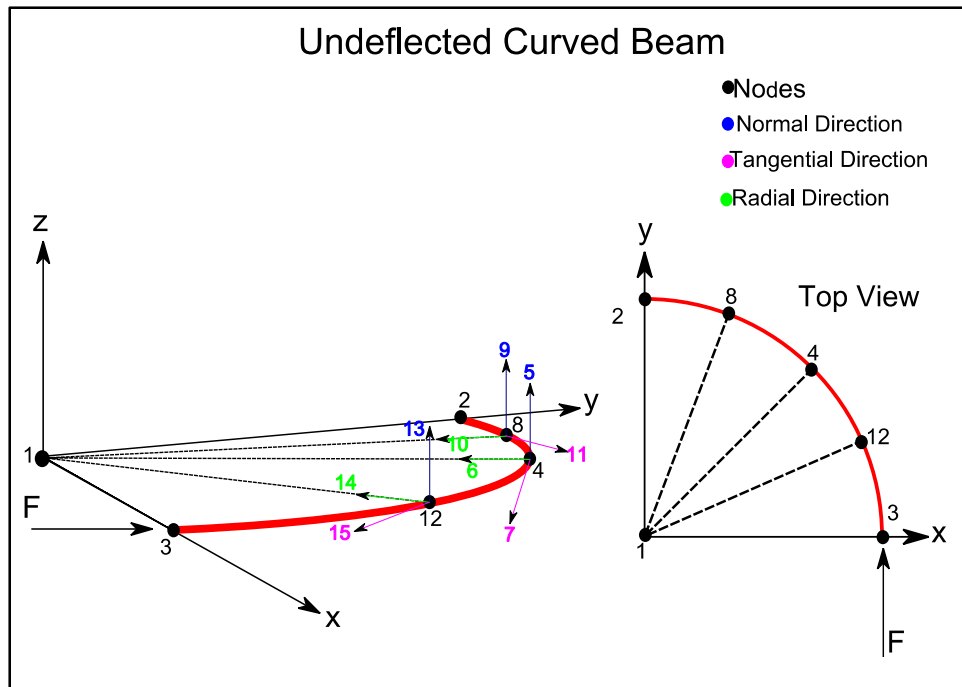


Figure 3.13. Shows the geometry, the loading, and the nodes of the undeformed curved beam.

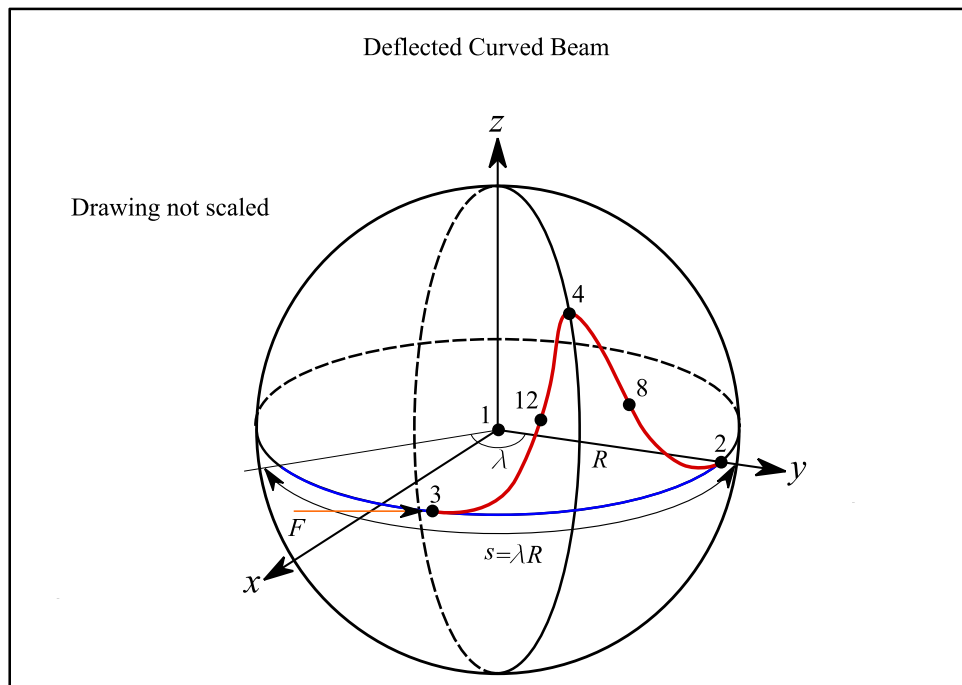


Figure 3.14. The deflected curved beam.

Once the beam was deflected the information containing the nodes' reaction forces, rotations, and displacements on the x , y , and z directions was collected over a range of 70 load steps in an ANSYS data output file. In addition, an analysis program was written; which used the output for the development and application of the new parametric beam model for curved beams that will be introduced in section 3.5. This model produces a prediction of the kinematics and the elasticity of the deflected curved beam.

3.5 Curved Beam Kinematic Analysis

In order to accurately use the spherical PRBM to perform the kinematic and elastic analysis of a compliant curved beam with horizontal buckling loads, a specific analysis criterion was defined and reference frames were established based on the nomenclature developed by Saurabh Jagirdar [13]. The analysis criterion, the position, and the coordinate frames are related as follows:

- It was established that the beam deflects symmetrically meaning that the half and quarter segments of the beam are their mirror images of each other. As a result we chose to analyze the segment from node 3 to node 12, which is a fourth of the beam and can be interpreted as a cantilever curved beam. Then, the remaining beam points' characteristics could be calculated using symmetry.
- Moments about the x and y axes are equal and opposite at node 2 and node 3.
- The radial displacement of all nodes stays the same, meaning that the radius of curvature does not change as the beam deflects.

- Moments about the z axis at node 12 are close to zero meaning that there is no twist on the beam.

The compliant curved beam, PG , Figure 3.15 is described by using the following coordinate frames given in Table 3.8:

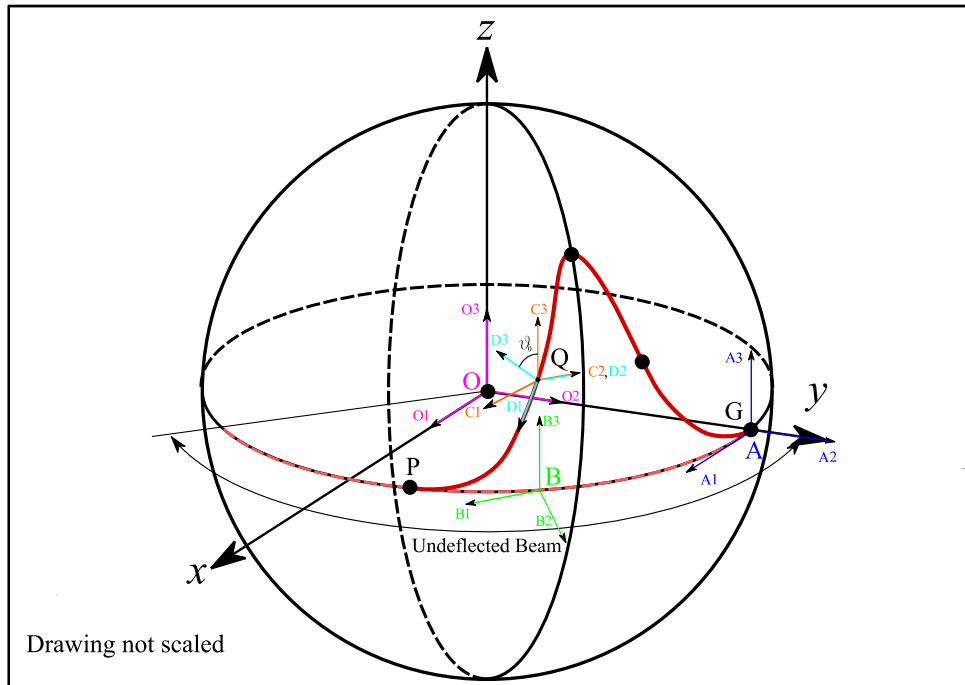


Figure 3.15. The reference frames that describe the motion and orientation of positions on a compliant curved beam.

The center of the sphere is defined by the O frame; the frames A , B , C , and D are located on the surface of the sphere. The curved beam is denoted by the points P , Q , and G , where P is on node 3; the free end of the beam, G is on node 2; the fixed end of the beam and Q is on node 12 which is the first quarter segment of the beam. The description of the coordinate frames is described on Table 3.6.

Table 3.8. Coordinate frames position and orientation.

Frame	Frame Description
<i>O</i>	This is a non-moving frame at the center of the sphere and is established by the x , y , and z coordinate system program in the ASNSYS batch code. The O_2 axis passes through the fix end of the beam at node 2 denote by G . The O_3 axis is normal to the plane containing the undeflected beam. The O_1 axis lies on the x axis of the coordinate system.
<i>A</i>	This frame has identical orientation as O frame; however it is located at the fixed end of the beam on G , is on the O_2 axis.
<i>B</i>	This frame is in the same plane as O and A and underneath point Q in order to locate its deflected position in the A_2 - A_1 plane.
<i>C</i>	This frame is located on point Q and describes the movement of this point in the B_3 - B_2 plane.
<i>D</i>	This frame is also located on point Q ; however, it is represented by the skew axis placed on node 12. This frame can be used to track the rotation about the C_2 axis

Table 3.9 provides a summary of the nomenclature used in the analysis of the curved beam to facilitate the understanding of the geometry.

Table 3.9. Nomenclature.

Variable	Description
α_{12}	Represents the translation of the quarter segment, node 12, in the A_2-A_1 plane, this translation is analogous to, a , the translation in the x -direction, in the planar model. Using symmetry α is defined in equation (3.35). See Figure 3.18
α_{total}	Represents the translation of the half segment, node 4, in the A_2-A_1 plane. α_{total} is defined in equation (3.36).
β_{12}	Represents the translation of the quarter segment, node 12, in the B_3-B_2 plane, this translation is analogous to, b , the translation in the y -direction, in the planar model. Using symmetry β_{12} is defined in equation (3.37). See Figure 3.16
β_{total}	Represents the translation of the half segment, node 4, in the B_3-B_2 plane. β_{total} is defined in equation (3.38). See Figure 3.18
ψ	Represents the angles that the nodes make with the x -axis as the beam deflects. See Figure 3.16 and 3.17
λ_{12}	Represents the arc angle of the quarter segment and it is defined on equation (3.39).
λ_{total}	Represents the arc angle of the entire curved beam and it is defined on equation (3.40). See Figure 3.14
ϕ_{12}	Represent the total change of translation of the quarter segment, node 12, in the A_2-A_1 plane and it is defined on equation (3.41).
Φ	Represent the total change of translation of the beam, in the A_2-A_1 plane and it is defined on equation (3.42).
Θ	Represents the amount of rotation that the rigid model must undergo to match the deflection of the compliant curved beam.
g_0	Represents the “deflection of the beam end about an axis normal to the tangent plane to the sphere at the beam end” [12]. See Figure 3.15
s	Represents the arc length of the curved beam.
R	Represents the radius of the sphere.

$$\alpha_{12} = \left(\frac{\psi_4 - \psi_3}{2} \right) \quad (3.36)$$

$$\alpha_{total} = \psi_4 - \psi_3 \quad (3.37)$$

$$\beta_{12} = \left(\frac{\tan^{-1} \left(\frac{z_4}{\sqrt{x_4^2 + y_4^2}} \right)}{2} \right) = \tan^{-1} \left(\frac{z_{12}}{\sqrt{x_{12}^2 + y_{12}^2}} \right) \quad (3.38)$$

$$\beta_{total} = \tan^{-1} \left(\frac{z_4}{\sqrt{x_4^2 + y_4^2}} \right) \quad (3.39)$$

$$\lambda_{12} = \frac{s}{4R} \quad (3.40)$$

$$\lambda_{total} = \frac{s}{R} = 4\lambda_{12} \quad (3.41)$$

$$\phi_{12} = \alpha_{12.i} - \alpha_{12.f} = \lambda_{12} - \alpha_{12} \quad (3.42)$$

$$\Phi = 2\alpha_{total.i} - 2\alpha_{total.f} = \frac{\psi_3}{4} \quad (3.43)$$

Figures 3.16, 3.17, and 3.18 provide a graphical explanation of the approach taken to define the geometry of the curved beam.

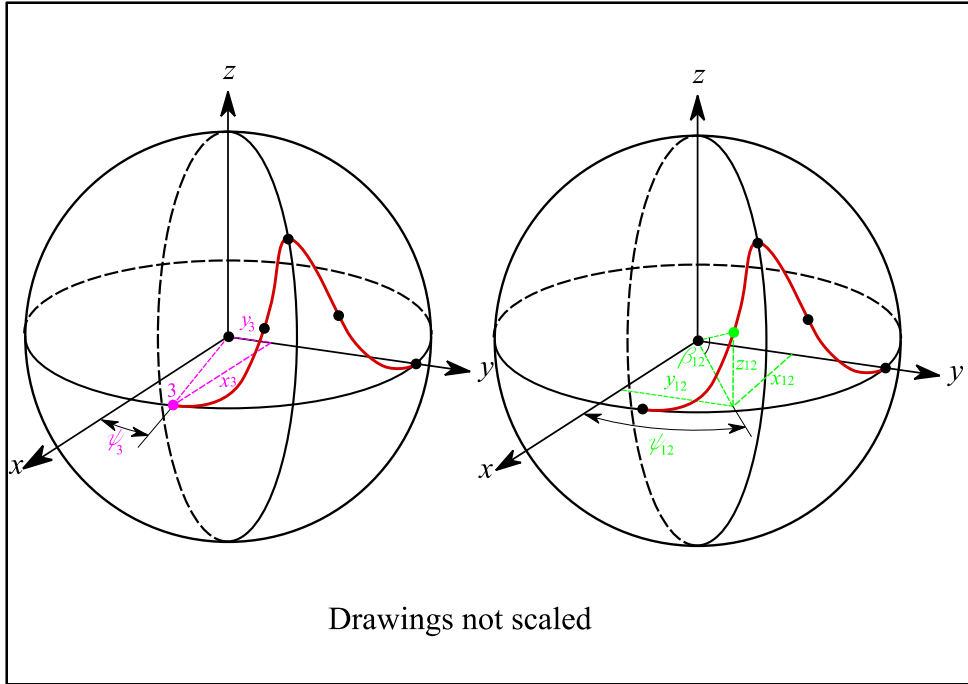


Figure 3.16. The position coordinates and angles of nodes 3 and 12.

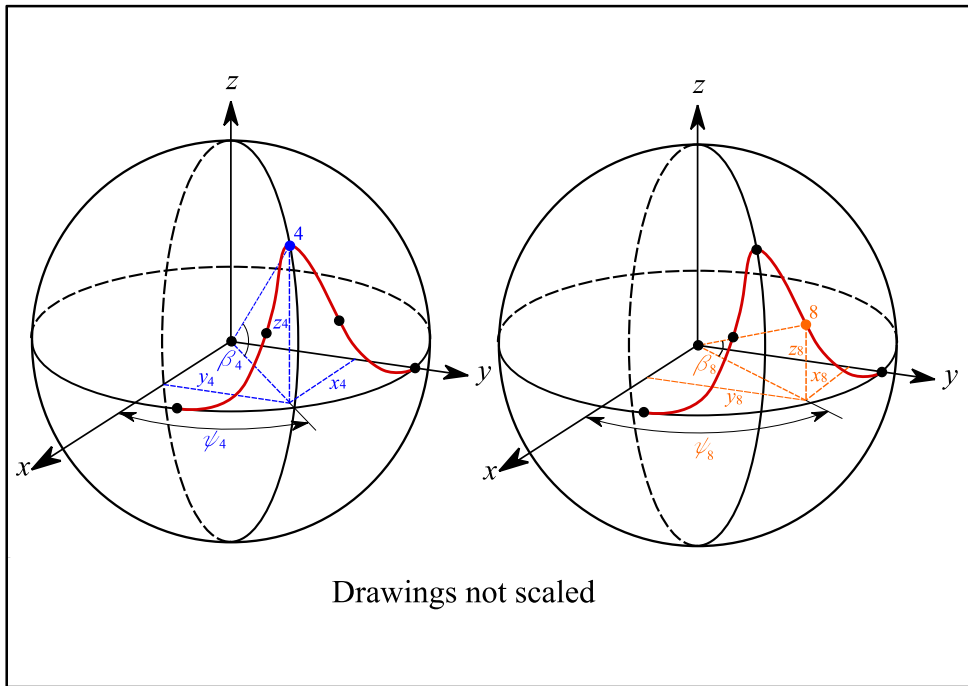


Figure 3.17. The position coordinates and angles of nodes 4 and 8.

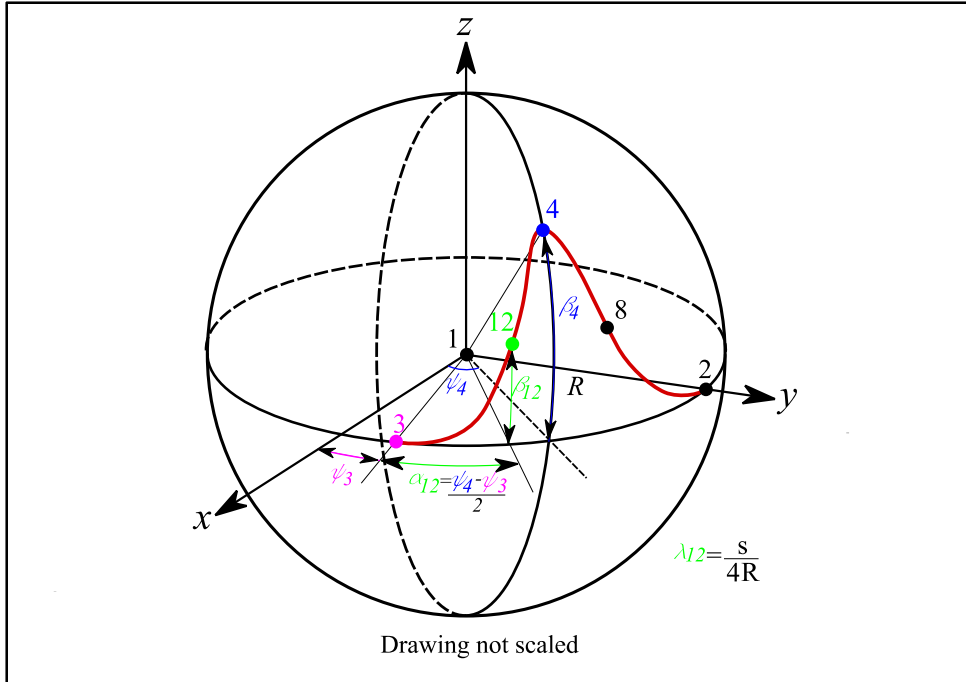


Figure 3.18. The translation of the quarter segment on the planes A_2-A_1 and B_3-B_2 .

The reference frames are defined by the matrices A , B , C , and D , where each of their columns represents a basis vector. The following equations represent the transformations that relate the frames.

$[A]$ is the identity matrix,

$$[A] = \begin{bmatrix} 1 & 0 & 0 \\ 0 & 1 & 0 \\ 0 & 0 & 1 \end{bmatrix} \quad (3.44)$$

$[B]$ is defined by

$$[B] = [R_B][A] \quad (3.45)$$

Where $[R_B]$ (3.44) is a rotation matrix that transforms the vectors in plane A_2-A_1 such that they align with those in frame B .

$$[R_B] = \begin{bmatrix} \cos\left(\psi_{12} - \frac{\pi}{2}\right) & -\sin\left(\psi_{12} - \frac{\pi}{2}\right) & 0 \\ \sin\left(\psi_{12} - \frac{\pi}{2}\right) & \cos\left(\psi_{12} - \frac{\pi}{2}\right) & 0 \\ 0 & 0 & 1 \end{bmatrix} \quad (3.46)$$

[C] is given by

$$[C] = [R_C][B] \quad (3.47)$$

where $[R_C]$ (3.46) is the rotation matrix that rotates vectors in the B_3 - B_2 such that they align with the vectors in frame C .

$$[R_C] = \begin{bmatrix} 1 & 0 & 0 \\ 0 & \cos(\beta_{12}) & -\sin(\beta_{12}) \\ 0 & \sin(\beta_{12}) & \cos(\beta_{12}) \end{bmatrix} \quad (3.48)$$

Equation (3.49) was used in order to calculate the amount of rotation that frame C must undergo about the C_2 to match frame D and compute the value of \mathcal{G}_0 .

$$[R_D] = [D][C]^{-1} \quad (3.49)$$

Where $[D]$ is given by the coordinates of the frame placed at node 12 and $[R_D]$ is specified in equation (3.50). \mathcal{G}_0 is found using the trace of $[R_D]$ in equation (3.50).

$$[R_D] = \begin{bmatrix} \cos(\mathcal{G}_0) & 0 & \sin(\mathcal{G}_0) \\ 0 & 1 & 0 \\ -\sin(\mathcal{G}_0) & 0 & \cos(\mathcal{G}_0) \end{bmatrix} \quad (3.50)$$

$$\mathcal{G}_0 = \cos^{-1}\left(\frac{\text{Trace}[R_D]-1}{2}\right) \quad (3.51)$$

Thus, the behavior of the curved compliant beam can be described by the parameters ϕ_{12} , λ , α_{12} , β_{12} , and \mathcal{G}_0 . Using Napier's Rules for spherical right triangles and trigonometric

identities (See Figure 3.19) we can find relationships to define γ^* (3.52) and Θ^* (3.53) in terms of β_{12} , λ_{12} , and ϕ_{12} .

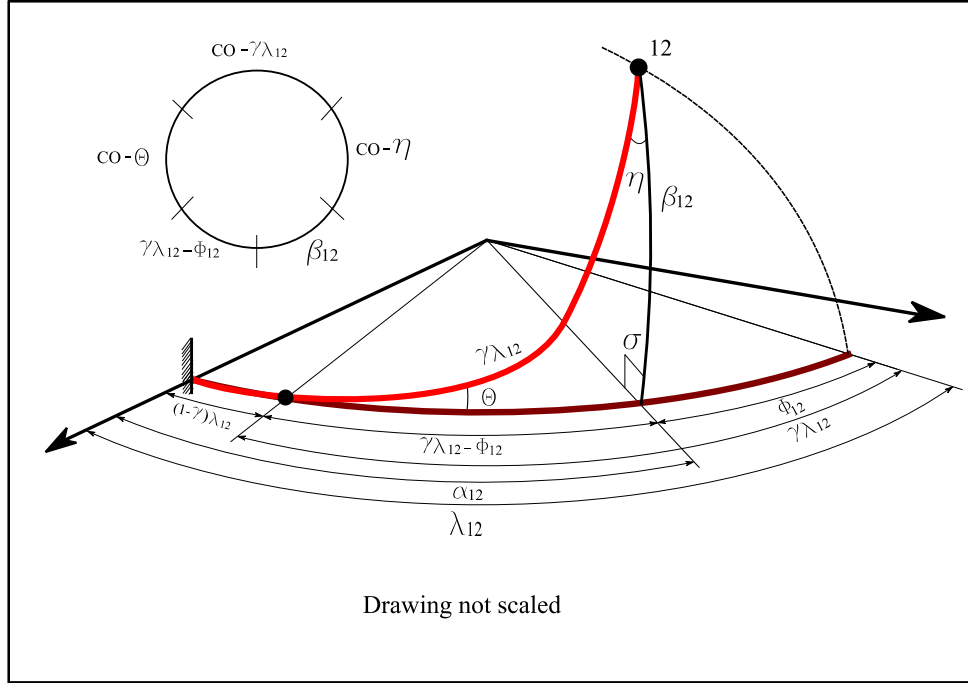


Figure 3.19. The spherical right triangle formed by a curved beam.

$$\gamma^* = \frac{1}{\lambda_{12}} \tan^{-1} \left(\frac{1 - \cos(\beta_{12}) \cos(\phi_{12})}{\cos(\beta_{12}) \sin(\phi_{12})} \right) \quad (3.52)$$

$$\Theta^* = \tan^{-1} \left(\frac{\tan(\beta_{12})}{\sin(\gamma^* \lambda_{12} - \phi_{12})} \right) \quad (3.53)$$

Once γ^* and Θ^* are defined, one can apply the statistical fitting technique explained in section 3.2 to represent the characteristic radius factor as a function of the moment load. Then, using the fit and Napier's Rules the parameters ϕ_{12} , α_{12} , Θ^* , and β_{12} can be found as follows.

$$\hat{\gamma} \approx \hat{\gamma}(M) = b_{-2} \frac{1}{M^2} + \frac{b_{-1}}{M} + b_0 + b_1 M + b_2 M^2 \quad (3.54)$$

$$\phi_{12} = \tan^{-1} \left(\frac{1 - \cos(\Theta^*)}{\cot(\hat{\gamma}\lambda_{12} + \cos(\Theta^*)\tan(\hat{\gamma}\lambda_{12}))} \right) \quad (3.55)$$

$$\alpha_{12} = \lambda_{12} - \phi_{12} \quad (3.56)$$

$$\Theta^* = \tan^{-1} \left(\frac{\tan(\beta_{12})}{\sin(\hat{\gamma}\lambda_{12} - \phi_{12})} \right) \quad (3.57)$$

$$\beta_{12} = \sin^{-1}(\sin(\hat{\gamma}\lambda_{12})\sin(\Theta^*)) \quad (3.58)$$

Finally using symmetry one can calculate the parameters of the half segment node 4, ϕ_4 , β_4 , α_4 , and its final output coordinate Z_4 , which represent the highest point reached by the mechanism for a given input.

$$\phi_4 = 2\phi_{12} \quad (3.59)$$

$$\beta_4 = 2\beta_{12} \quad (3.60)$$

$$\alpha_4 = 2\alpha_{12} \quad (3.61)$$

$$Z_4 = [R \cos(\pi - 2\lambda_{12} + 2\phi_{12}) \quad R \sin(\pi - 2\lambda_{12} + 2\phi_{12}) \quad R \sin(2\beta_{12})] \quad (3.62)$$

3.6 Kinematic Analysis Results Large Deflection Curved Beams

This section provides a summary of the kinematic analysis of the deflection of a curved beam under specific horizontal buckling end-loads. The results shown in this section correspond to a curved beam with an arc angle, λ , of 105° . The reason why this angle was used is because it was the largest arc angle in the analysis; therefore, it was perceived as the worse case scenario yielding to the highest errors. In other words, we based the model on this case because if the model works for a beam with an arc angle of

105° it would work for any beam with a smaller arc angle producing smaller errors as the size of the arc angle decreased. The results of curved beams with angles 15°, 30°, 45°, 60°, 75°, and 90° are shown on the results summary tables in the Appendix G.

For a curved beam loaded with specific horizontal buckling loads a constant γ does not produce an accurate PRBM for the initial part of the beam deflection. Interestingly, this model behaves as Case 2 in the straight beams study; the constant γ PRBM approximation improves when the beam deflects significantly, so that the force is perpendicular to the neutral axis of the beam. In the other hand, when γ is represented as a function of the load, as $\hat{\gamma} \approx \hat{\gamma}(M)$ with coefficient constants b_i Table 3.10, the PRBM produces a more accurate prediction throughout the complete range of the deflection, meaning that regardless of the deflection magnitude or the direction in which the force is applied, this parametric model can provide an accurate prediction of the behavior of the beam Figure 3.20.

Table 3.10. Values of the rational function coefficients for a curved beam with a horizontal buckling end-load.

	Rational function Coefficients
b_{-2}	-142.1823
b_{-1}	78.0177
b_0	-15.7772
b_1	115.4554
b_2	-34.7151

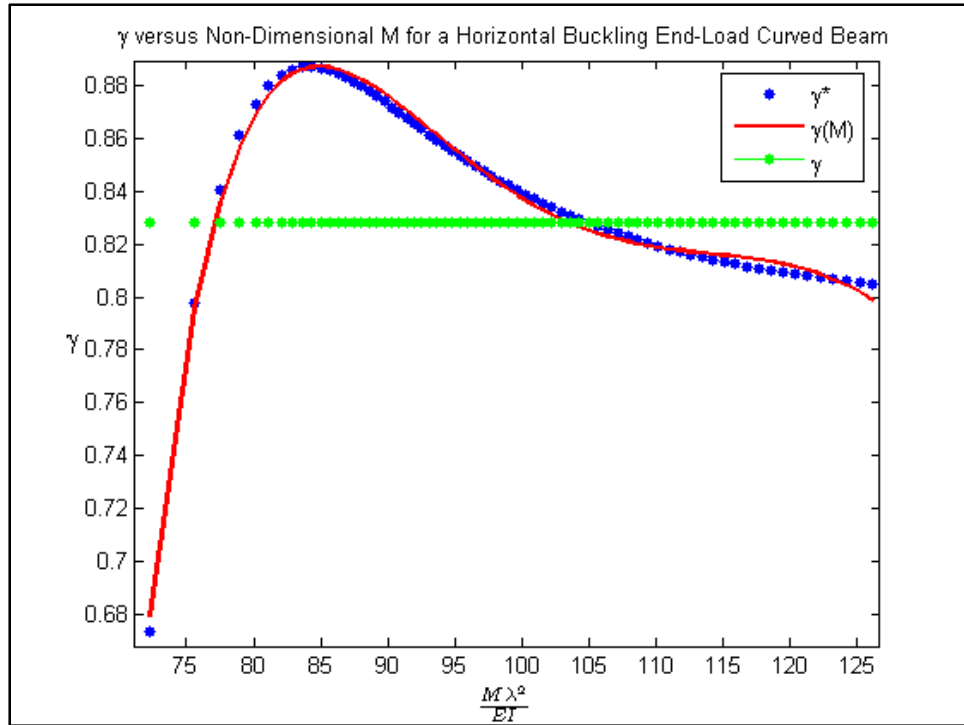
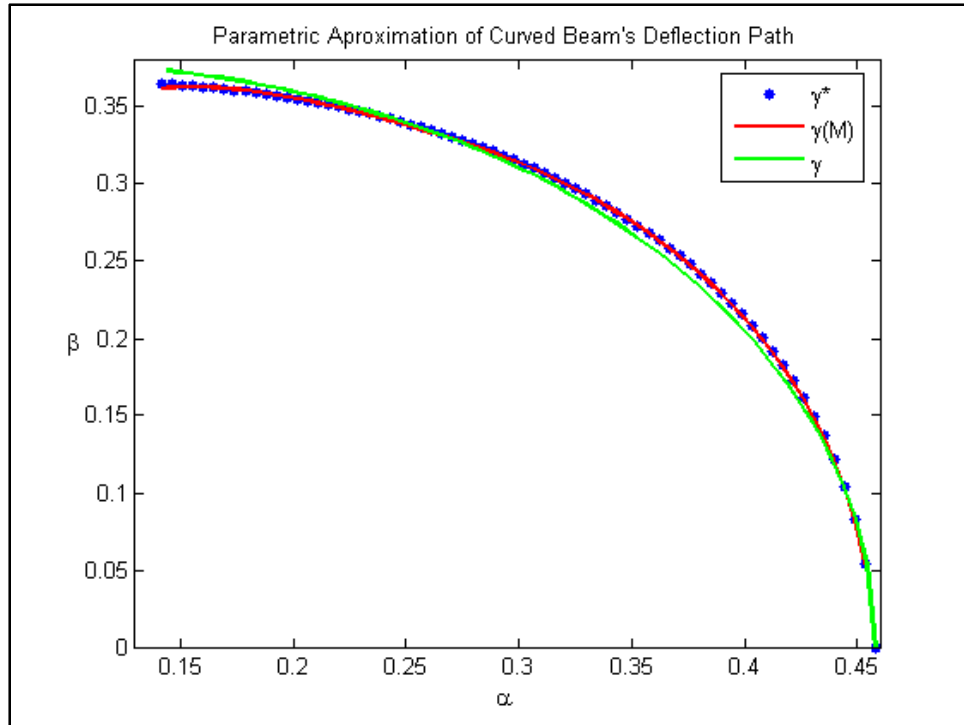


Figure 3.20. γ versus moment for a curved beam with a horizontal buckling end-load.

Figure 3.21 shows the parametric approximations of the end-beam deflection path of the curved beam loaded with specific buckling loads. Just as with the horizontal loaded straight beam, the new model is capable to improve the accuracy of the PRBM in comparison with a constant γ model.



3.21. A horizontal end-load curved beam planar rotation, α versus out-of-plane rotation, β .

Figure 3.22 shows the approximation of the deflected member PRBM angle, θ . As with the straight beam case the new parametric model yields more accurate large deflection kinematic model predictions than a PRBM using the constant γ .

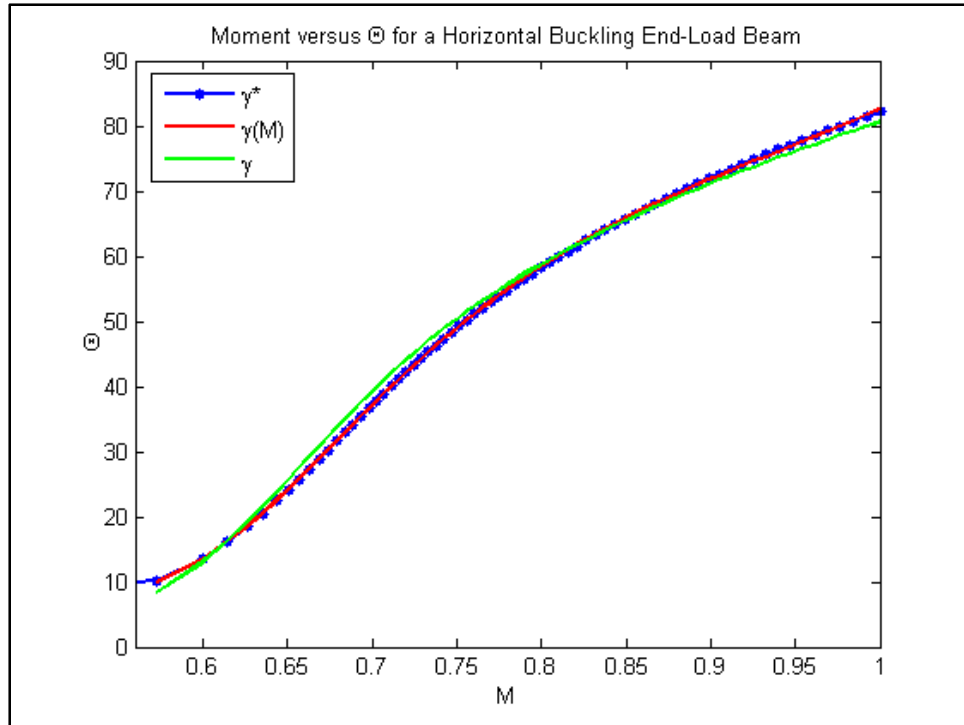


Figure 3.22. Moment versus Θ for a horizontal buckling end-load curved beam.

A statistical analysis was performed on the curved beam PRBM as well; a two-sided t test with a 95% confidence interval was developed; Figure 3.23 shows the characteristic radius factor within the 95% confidence interval. The coefficient of determination R_B^2 , the rational function prediction maximum error and total error, and the constant γ prediction total error in the deflection approximation were also calculated as shown in Table 3.11.

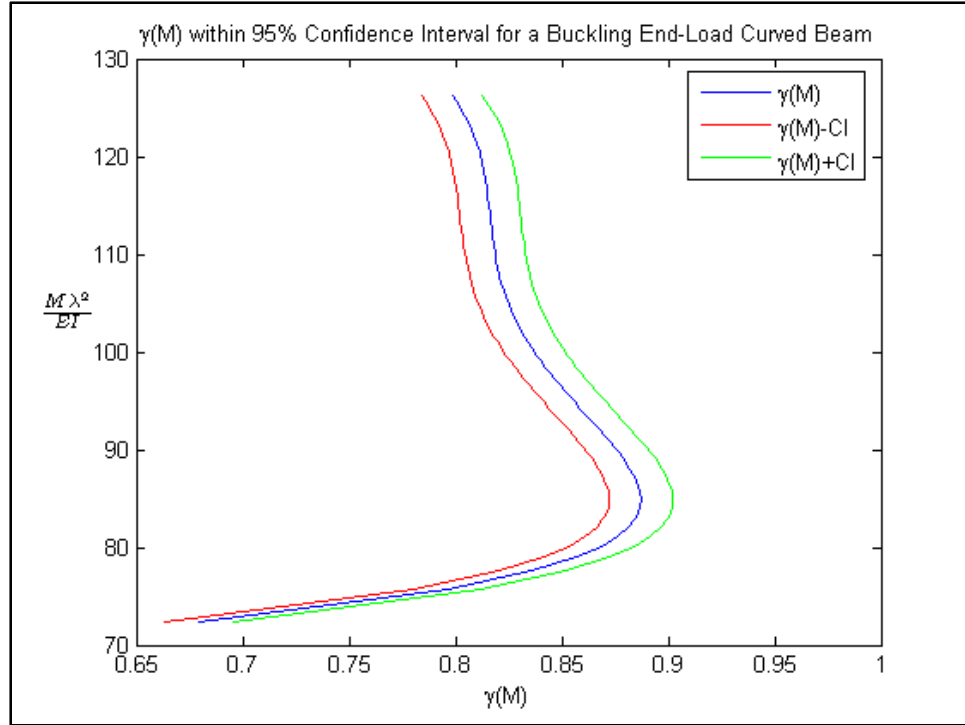


Figure 3.23. The characteristic radius factor within the 95% confidence interval for a horizontal buckling end-load curved beam.

Table 3.11. Results of statistic analysis for a horizontal buckling end-load curved beam.

	Rational function Coefficients	95% Confidence Interval
b_{-2}	-142.1823	± 4.1447
b_{-1}	78.0177	± 3.0046
b_0	-15.7772	± 1.3276
b_1	115.4554	± 3.7958
b_2	-34.7151	± 2.1215
Coefficient of Determination, R_B^2		99.44%
Rational Function Prediction Maximum Error		$1.1067e-3 \%$
Rational Function Prediction Total Error		$1.5795e-5\%$
Constant γ Total Error		0.3843%

In order to calculate the angle coefficient, C_g , a plot of Θ versus \mathcal{G}_0 was performed Figure 3.24; then, a linear fit was made to the curved yielding to the constant

value of C_g needed to obtain the value of \mathcal{G}_0 in terms of the Pseudo-Rigid-Body angle, θ .

$$C_g = 1.3427 \quad (3.63)$$

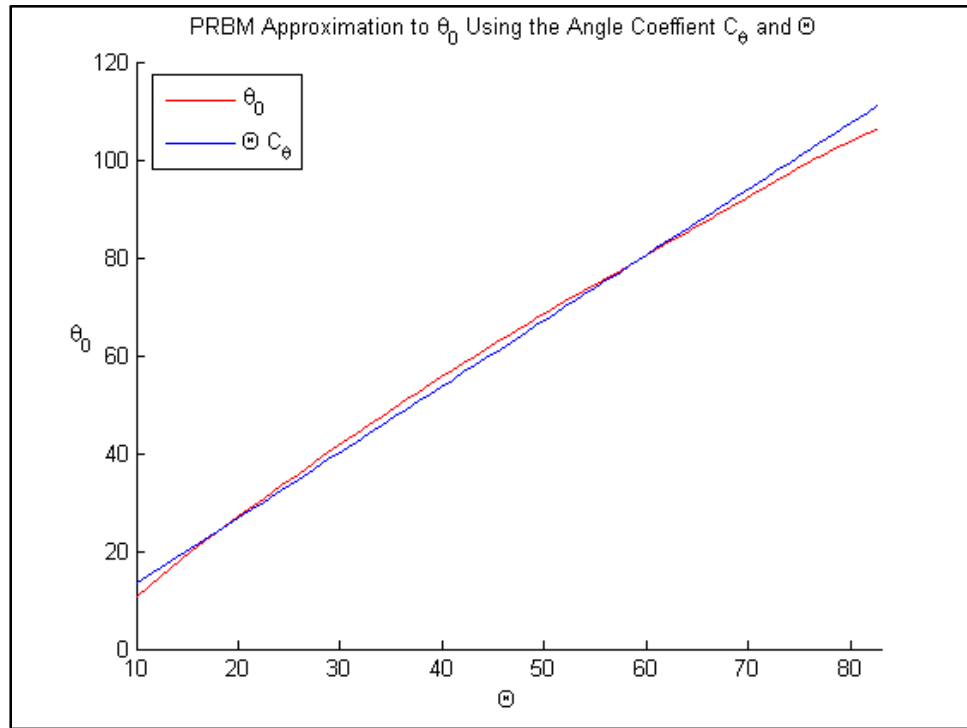


Figure 3.24. The approximation to \mathcal{G}_0 using the angle coefficient, C_g and the Pseudo-Rigid-Body angle, θ .

A PRBM for a curved beam under specific horizontal buckling end-loads has not been published before because PRBMs using a constant γ do not yield accurate predictions for this type of beams and loading configurations. This new approach appears to fill the gap.

Chapter 4

Elasticity of a PRBM for Curved Beams

This Chapter uses the principle of virtual work used in to develop elasticity parameters such as the torque coefficient, T_θ , and its components functions, T_f , and, T_m . According to Paul [25] “The net virtual work for all active forces is zero if and only if an ideal mechanical system is in equilibrium.” The compliant mechanism analyzed in this thesis is assume to be ideal, meaning that the constrains on the mechanism do not do work.

$$\sum \delta W = 0 \quad (4.1)$$

4.1 Principle of Virtual Work

In order to apply the principle of virtual work to this model, first an arbitrary virtual linear displacement, $\delta \vec{z}$, and an arbitrary virtual angular displacement, $\delta \Phi$, must be defined as functions of the generalized coordinates (4.2).

From (3.62) we expressed the virtual linear displacement as:

$$\delta \vec{z}_3 = \left(-R \sin\left(\frac{\pi}{2} - \lambda + \Phi\right) \delta \Phi \hat{i} + R \cos\left(\frac{\pi}{2} - \lambda + \Phi\right) \delta \Phi \hat{j} + 0 \delta \Phi \hat{k} \right) \quad (4.2)$$

Then, the virtual work, δW_F , due to the applied force, \vec{F} , and a virtual linear displacement, $\delta \vec{z}_3$, is:

$$\delta W_F = (\vec{F} \bullet \delta \vec{z}_3) \delta \Phi \quad (4.3)$$

In a like manner, the virtual work due to the applied moment, \vec{M} , and the virtual angular displacement, $\delta \Phi$, is:

$$\delta W_M = \vec{M} \delta \Phi \quad (4.4)$$

According to Howell [3] the PRBM can be used to model the compliant beam's resistance to bending by using the stiffness coefficient, K_θ , which represents a nondimensionalized torsional spring. This constant combined with the material properties and the geometry of the beam can be employed to calculate the value of the PRBM spring constant, K (4.5). In order to calculate the value of T_θ the principle of virtual work and the PRBM concepts are used to establish force-deflection relationships for compliant mechanisms as describe by Howell and Midha in [26].

$$K = K_\theta \frac{EI}{R\lambda} \quad (4.5)$$

Where $\frac{EI}{R\lambda}$ represents the non-dimensionalization factor.

Moreover, all the store energy in the springs of the PRBM must be taken into consideration in order to have a complete energy balance equation. Due to the symmetry of the deflected beam, the PRBM behaves as if it had four identical springs acting on each of its quarter segments' characteristic pivots; therefore, the total energy store on the springs, U_s , is:

$$U_s = -4K\Theta \frac{d\Theta^*}{d\Phi} \delta \Phi \quad (4.6)$$

Where, K represents the spring constant and $\frac{d\Theta^*}{d\Phi}$ represent the change of the Pseudo-

Rigid-Body Angle, Θ , as a function of the beams' rotation in the plane A_1 - A_3 , Φ .

Because the quarter model is the object being analyzed one can express $\frac{d\Theta^*}{d\Phi}$, and U_s in terms of the ϕ_{12} .

$$\frac{d\Theta}{d\Phi} = \frac{1}{4} \frac{d\Theta^*}{d\phi_{12}} \quad (4.7)$$

Therefore,

$$U_s = -K\Theta \frac{d\Theta^*}{d\phi_{12}} \delta\Phi \quad (4.8)$$

Then, the total virtual work is

$$\sum \delta W = \delta W_F + \delta W_M + U_s = 0 \quad (4.9)$$

or

$$\sum \delta W = (\vec{F} \bullet \vec{\delta z}_3) + \vec{M} + K\Theta^* \frac{d\Theta^*}{d\phi_{12}} = 0 \quad (4.10)$$

Solving for K and the resultant torque, T , due to the force and the moment we obtained:

$$K = \left(\frac{(\vec{F} \bullet \vec{\delta z}_3) + \vec{M}}{\Theta^*} \right) \frac{d\phi_{12}}{d\Theta^*} \quad (4.11)$$

$$T = K\Theta^* = \left((\vec{F} \bullet \vec{\delta z}_3) + \vec{M} \right) \frac{d\phi_{12}}{d\Theta^*} \quad (4.12)$$

Furthermore, $\frac{d\phi_{12}}{d\Theta^*}$ can be found using equations (3.55) and Napier's Rules for spherical

right triangles as follows:

$$\frac{d\phi_{12}}{d\Theta^*} = \frac{1}{\sec^2(\phi_{12})} \left[\left(\frac{\sin(\Theta^*)}{\cot(\hat{\gamma}\lambda_{12})\cos(\Theta^*)\tan(\hat{\gamma}\lambda_{12})} \right) + \left(\frac{(1 - \cos(\Theta^*))\sin(\Theta^*)\tan(\hat{\gamma}\lambda_{12})}{(\cot(\hat{\gamma}\lambda_{12}) + \cos(\Theta^*)\tan(\hat{\gamma}\lambda_{12}))^2} \right) \right] \quad (4.13)$$

Consequently, by substituting equation (4.5) into equation (4.11) one can find a torque coefficient function, T_θ , in terms of the virtual work.

$$T_\theta = \left(\left(\vec{F} \cdot \delta\vec{x}_3 \right) \frac{d\phi_{12}}{d\Theta^*} \frac{R\lambda_{12}}{EI} \right) + \left(\vec{M} \frac{d\phi_{12}}{d\Theta^*} \frac{R\lambda_{12}}{EI} \right) \quad (4.14)$$

Additionally, T_θ can be separated into its component functions, T_f (4.15) (the torque contributed by the force \vec{F}) and T_m (4.16) (the torque contributed by the moment \vec{M}); then, the polynomial function of Θ^* that best fits the torque is found as shown in Table 4.1 as the fits are shown in Figure 4.1.

$$T_f = \left(\left(\vec{F} \cdot \delta\vec{x}_3 \right) \frac{d\phi_{12}}{d\Theta^*} \frac{R\lambda_{12}}{EI} \right) \quad (4.15)$$

$$T_m = \left(\vec{M} \frac{d\phi_{12}}{d\Theta^*} \frac{R\lambda_{12}}{EI} \right) \quad (4.16)$$

$$T_\theta = T_f + T_m \quad (4.17)$$

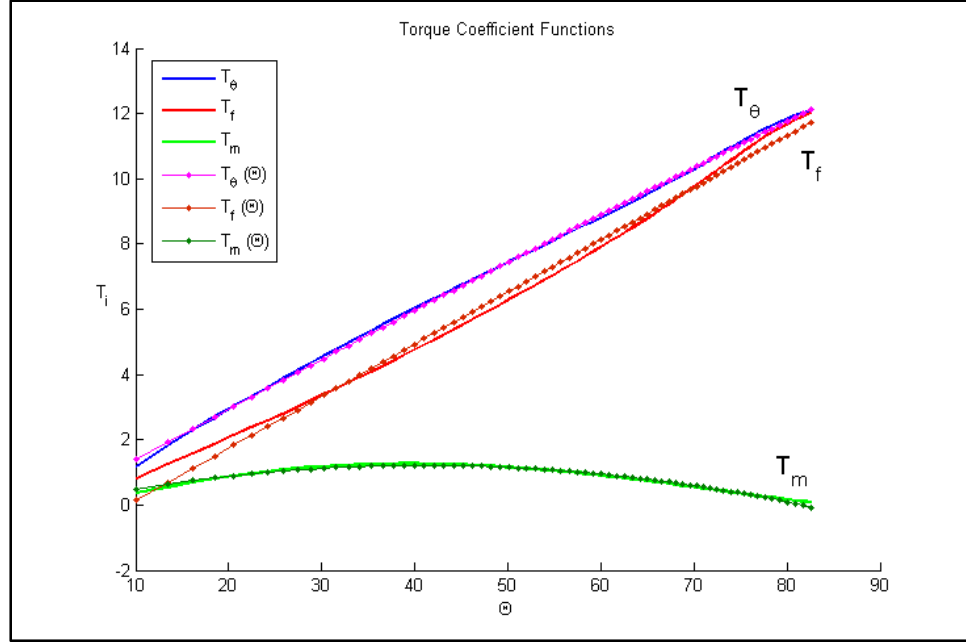


Figure 4.1. The torque coefficient functions T_θ , T_f , and T_m versus Θ^* .

Table 4.1. Torque function coefficients.

Function	Function constant coefficients
$\hat{T}_\theta (\Theta^*)$	$-0.3244 \Theta^{*2} + 8.9923 \Theta^* - 0.1640$
$\hat{T}_f (\Theta^*)$	$9.1455 \Theta^* - 1.4521$
$\hat{T}_m (\Theta^*)$	$-2.4524 \Theta^{*2} + 3.5246 \Theta^* - 0.0498$

Once these component functions have been established, one can determine the force (4.18) and the moment (4.19) applied a node 12 (quarter model). After these loads have been found, one can determine the values of the actual moment (4.21) and the actual force (4.22) applied at node 3.

$$F_{12} = \hat{T}_f (\Theta^*) \frac{EI}{R\lambda} \quad (4.18)$$

$$M_{12} = \hat{T}_m (\Theta^*) \frac{EI}{R^2\lambda} \quad (4.19)$$

$$M_3 = M_{12} \frac{d\Theta^*}{d\Phi} \quad (4.20)$$

$$F_3 = F_{12} \frac{d\Theta^*}{d\Phi} \quad (4.21)$$

4.2 Model Validation

In order to validate the stiffness model a test was performed on a beam with different material properties and different cross-sectional area from the original beam used to derived the model Table 4.2. Subsequently, the kinematic parameter Θ^* was determined using the following expression

$$\Theta^* = \tan^{-1} \left(\frac{\tan(\beta_{12})}{\sin(\hat{\gamma}\lambda_{12} - \phi_{12})} \right)$$

Where Φ was the input rotation of the beam and γ was the kinematic model $\hat{\gamma}$. After that, using Θ^* the force and moments loads were calculated using the torque function coefficients, T_f , T_m .in the following manner:

First, the values of the torque function confidents were calculated using Θ^* as an input

$$\begin{aligned} \hat{T}_\theta(\Theta^*) &= -0.3244\Theta^{*2} + 8.9923\Theta - 0.1640 \\ \hat{T}_f(\Theta^*) &= 9.1455\Theta^* + 1.4521 \\ \hat{T}_m(\Theta^*) &= -2.4524\Theta^{*2} + 3.5246\Theta - 0.0498 \end{aligned}$$

Then, using the non-dimensional torque coefficient function and the dimensionalization

factor $\frac{EI}{R\lambda}$ the force and the moment loads applied at node 12 were computed

$$F_{12} = \hat{T}_f(\Theta^*) \frac{EI}{R\lambda}$$

$$M_{12} = \hat{T}_m(\Theta^*) \frac{EI}{R^2\lambda}$$

Finally, using the loads applied at node 12 and the kinematic coefficient $\frac{d\Theta^*}{d\Phi}$ the loads applied at node 3 were determined.

$$M_3 = M_{12} \frac{d\Theta^*}{d\Phi}$$

$$F_3 = F_{12} \frac{d\Theta^*}{d\Phi}$$

In order to determine how well the loads were predicted by the model, the predicted loads were compared and plotted against the values of the loads acquired from the FEA analysis as shown in Figures 4.2 and 4.3. Finally, after doing an error analysis it was established that the elastic prediction error of the force and moment loads for a beam with an arc angle of 105° were 14.04 % and 14.53 % respectively, when compared to the data provided by the FEA analysis. However, when the error analysis was applied to the force and moment loads predicted for a beam with an arc angle of 15° it was found that the error decreased; the error of the force and moment loads were 1.2218e-3% and 0.21 % respectively, when compared with the FEA data analysis. This suggests that the reason the errors on the predictions decrease for different arc angles, is because as the arc angles get smaller the spherical PRBM behaves more as a planar PRBM simplifying the model and reducing the error.

Table 4.2. Characteristics of the test beam.

Arc angle, λ	15°, 30°, 45°, 60°, 75°, 90°, 105°	
Radius, R	100 μm	
Arc length, s	10	
Height, h	$s/15$	
Width, w	$w \times 0.1$	
Modulus, E	180GPa	
	$\lambda=105^\circ$	$\lambda=15^\circ$
Maximum force load prediction error	18.38%	1.8%
Average force load prediction error	14.04 %	1.2218e-3%
Maximum moment load prediction error	17.07%	1.57%
Average moment load prediction error	14.53 %	0.21 %

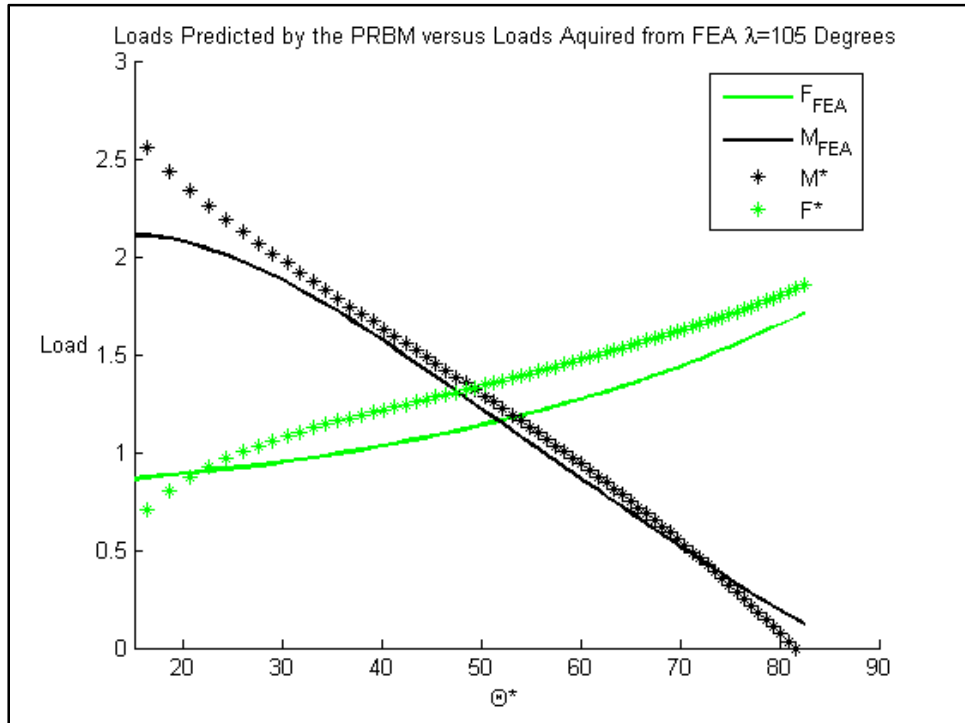


Figure 4.2. The loads predicted by the parametric model and the loads acquired from the FEA analysis for a beam with an arc length of 105°.

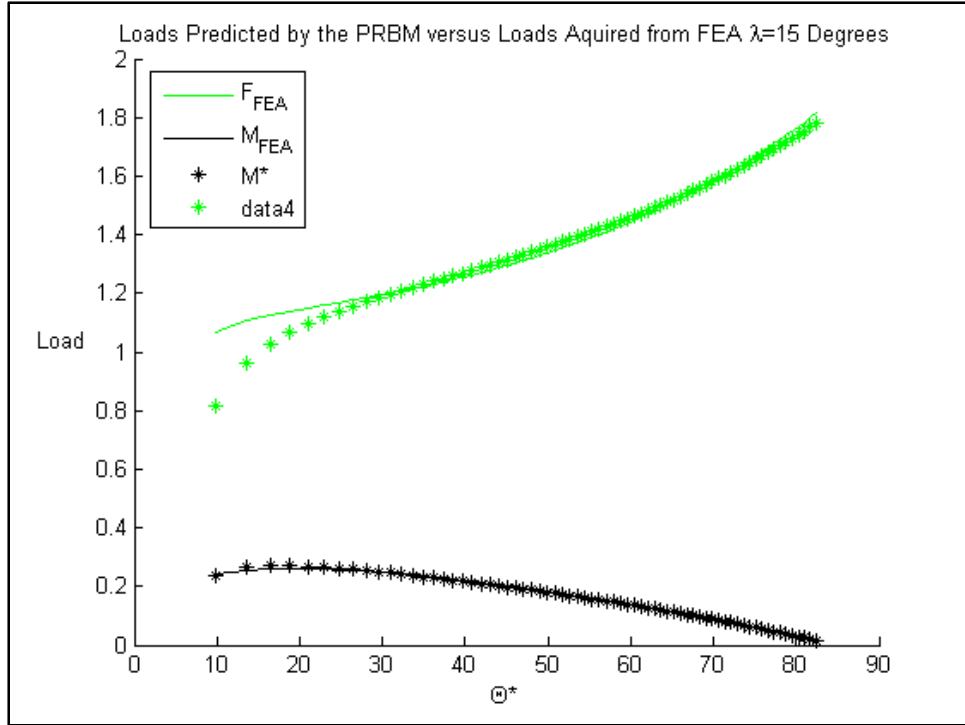


Figure 4.3. The loads predicted by the parametric model and the loads acquired from the FEA analysis for a beam with an arc length of 15°.

4.3 Analysis of a Compliant Micro Helico-Kinematic Platform (MHKP) Device

In order to analyze a compliant MHKP device with the new parametric beam model, the model was used to predict the motion and stiffness of a prototype with the properties given in Table 4.3, which was designed and manufactured using the PolyMUMPs process [27] and is shown in Figures 4.4.

Table 4.3. MHKP material properties and cross-sectional area characteristics.

Arc angle, λ	90°
Radius, R	100 μm
Arc length, s	$s = R\lambda$
Height, h	2 μm
Width, w	2 μm
Modulus, E	169GPa

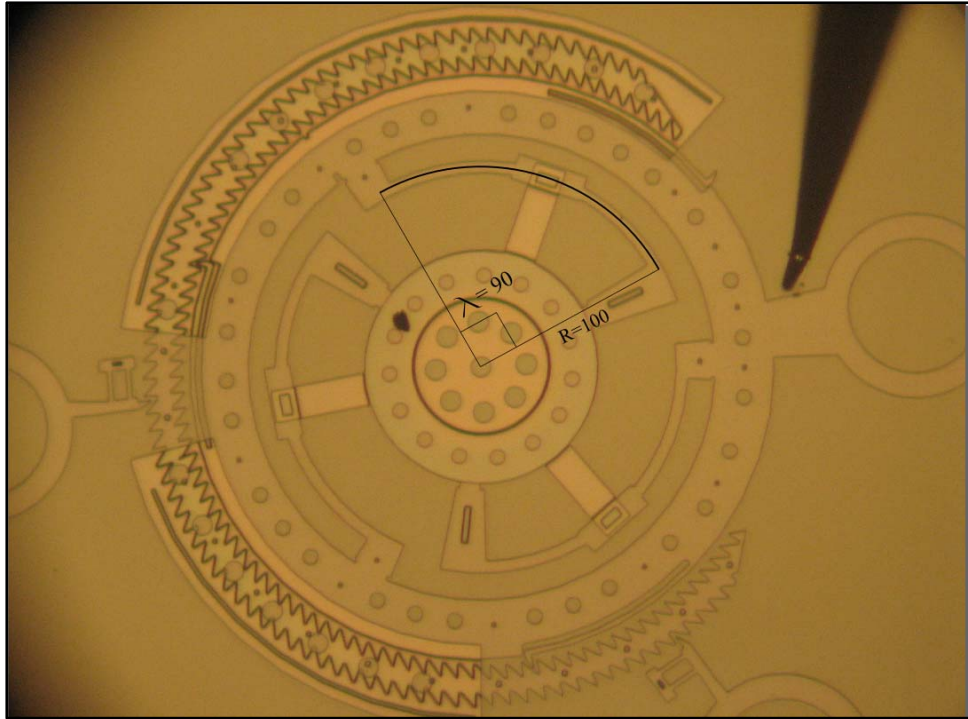


Figure 4.4. Shows the MHKP device and outlines the curved beam being tested.

After performing simulation we were able to determine the specific loads needed to actuate the device and the output coordinates of the center of the beam, where z is the highest point reached by the beam once it is actuated as given in Table 4.4.

Table 4.4. MHKP device simulation results.

Output coordinates	$x = 24.1031$
	$y = 97.05217$
	$z = 57.0909$ (Vertical displacement)
F_{initial}	$143.35 \mu\text{N}$
F_{final}	$430.77 \mu\text{N}$
M_{initial}	$356.17 \mu\text{N} \mu\text{m}$
M_{final}	$8.90 \mu\text{N} \mu\text{m}$

Chapter 5

Conclusion

This chapter provides a conclusion to the work developed in this thesis and gives a summary of the major contributions offered by this work.

5.1 Conclusion and Summary of Contributions

This thesis provides a novel, more accurate beam model for straight and curved compliant beams with vertical and horizontal buckling end-loads. The model uses a rational function to represent the characteristic radius factor as a function of the moment load, $\hat{\gamma} = \gamma(M)$, which improves the accuracy and the range of it when compared with previous models. The new parametric model is used to analyze the kinematics and elasticity of the complete deflection range of motion of both the straight and curved beams developing non-dimensional kinematic and elastic parameters such as the angle coefficient, C_θ , the characteristic radius factor, $\hat{\gamma}$, the characteristic radius, $\hat{\gamma}l$, and the torque coefficients functions, T_θ , T_m , T_f . In addition, the model is used to calculate the working loads on the curved beam using the input angle of rotation ϕ .

Furthermore, a compliant MHKP device was analyzed in order to determine specific buckling loads needed to actuate the device and the coordinates of the center of

its curved beams, so one could establish the highest point it could reach once it was buckled.

Finally, software codes were developed in ANSYS and MATLAB in order to produce the new parametric model and provide validation of its capabilities.

References

- [1] Shigley, J. E. and Uicker, J. J. *Theory of Machines and Mechanisms*. 2nd. New York : McGraw-Hill, 1995.
- [2] Erdman, A.G. and Sandor, G.N. *Mechanism Design: Analysis and Synthesis*. 3rd. Upper Saddle River : Prentice Hall, 1997. Vol. 1.
- [3] Howell, Larry L. *Compliant Mechanisms*. New York : Wiley-Interscience, 2001.
- [4] Memsnet.org. *MEMS and Nanotechnology Applications*. [Online] [Cited: 1 12, 2009.] <http://www.memsnet.org/mems/applications.html>.
- [5] Clements, D. *Implementing Compliant Mechanisms in Micro-Electro-Mechanical Systems (MEMS)*. Brigham Young University. Provo, UT : s.n., 2000. M.S. Thesis.
- [6] *A Micro Helico-kinematic Platform via Spherical Crank-slider*. Lusk, Craig P. and Howell, Larry L. 4, s.1. : ASME, 4 2008, Journal of Mechanical Design, Vol. 130.
- [7] *Ortho-planar mechanisms*. Pairese, J., Howell, L. and Magleby, S. 2000. Proceedings of the 2000 ASME Design Engineering Technical Conferences, DETC2000/MECH-14193. pp. 1-15.
- [8] Lusk, Craig P. *Ortho-Planar Mechanisms for Microelectromechanical Systems*. Brigham Young University. Provo, UT : s.n., 2005. Ph.D Dissertation.
- [9] *A MEMS conical spring actuator array*. Fukushinge, T., Hata, S. and Shimokohbe, A. April 2005, Journal of Microelectromechanical Systems, Vol. 14, pp. 243.
- [10] *MEMS Spatial Light Modulator Development at the Center of Adaptive Optics*. Krulevitch, P., et al. 2003. SPIE. pp. 227-233.
- [11] *Components, Building Blocks, and Demonstrations of Spherical Mechanisms in Microelectromechanical Systems*. Lusk, Craig P. and Howell, Larry L. s.1. : ASME, March 2008, Journal of Mechanical Design, Vol. 130.
- [12] Leon, Alejandro. *A Pseudo-Rigid-Body Model for Spherical Mechanisms: The Kinematics and Elasticity of a Curved Compliant Beam*. University of South Florida. Tampa, FL : s.n., 2007. M.S. Thesis.

- [13] Jagirdar, Saurabh. *Kinematics of Curved Flexible Beam*. University of South Florida. Tampa, FL : s.n., 2006. M.S. Thesis.
- [14] *Parametric Deflection Approximations for End-Loaded, Large-Deflection Beams in Compliant Mechanisms*. Howell, L. L. and Midha, A. 1, s.l. : ASME, March 1995, Journal of Mechanical Design, Vol. 117, pp. 156-165.
- [15] *Preliminaries for a spherical compliant mechanism: Pseudo-Rigid-Body Model Kinematics*. Lusk, C.P. and Jagirdar, S. Las Vegas, NV : s.n., 2007. ASME IDECT/CIE.
- [16] *Spherical Kinematics in Contrast to Planar Kinematics*. Chiang, C. H. Taipei, Taiwan : s.n., May 3, 1992, Mechanical Machine Theory, Vol. 27, pp. 243-250.
- [17] Spiegel, M. R. and Liu, J. *Schaum's Outlines: Mathematical Handbook of Formulas and Tables*. New York : McGraw-Hill, 1999.
- [18] Henderson, D. W. *Experiencing Geometry: In Euclidean, Spherical, and Hyperbolic spaces*. 2nd edition. Upper Saddle River : Prentice Hall, 2001.
- [19] Newman, Donald J. Approximation with Rational Functions. *Regional Conference series in Mathematics*. Providence, Rhode Island : Published for the Conference Board of Mathematical Sciences by the American Mathematical Society, 1979, 41, p. 52.
- [20] Contributors, Wikipedia. Polynomial and rational function modeling. *Wikipedia, The Free Encyclopedia*. [Online] 6 5, 2009. [Cited: January 5, 2009.] http://en.wikipedia.org/wiki/rational_function_modeling?oldid=217267798.
- [21] Mathbits.com. *Statistics 2 - Correlation Coefficient and Coefficient of Determination*. [Online] [Cited: February 19, 2009.] <http://mathbits.com/Mathbits/TISection/Statistics2/correlation.htm>.
- [22] Montgomery, Douglas C, Runger, George C and Faris, Norma. *Engineering Statistics*. New York : John Wiley & Sons, Inc, 2004.
- [23] Engineering Statistics Handbook. *NIST SAMTECH*. [Online] [Cited: February 19, 2009.] : <http://www.itl.nist.gov/div898/handbook/eda/section3/eda352.htm> .
- [24] *Methodology of compliant mechanisms and its current developments in applications: a review.(Report)*. Shuib, Solehuddin, Ridzwan and M.I.Z. Kadarman, Halim A. 3, 3 1, 2007, American Journal of Applied Sciences, Vol. 4, p. 160(8).

- [25] Paul, B. *Kinematics and Dynamics of Planar Machinery*. Upper Saddle River : Prentice Hall, 1979.
- [26] *The Development of Force-Deflection Relationships for Compliant Mechanisms*. Howell, Larry. L. and Midha, Ashok. s.l. : ASME, 1994. Machine Elements and Machine Dynamics. Vol. 71, pp. 501-508.
- [27] Koester, David, et al. *PolyMUMPs Design Handbook*. 2003.

Appendices

Appendix A: ANSYS Batch Code for a Vertical End-Loaded Beam

```
!*****
*****
/CONFIG,NRES,10000
!/CWD,'C:\Documents and Settings\despinos\Desktop\Work'

!*****
*****

!*****
*****

!*****Set Up Model
Variables*****

*

!*****
*****

!*DO,asp, .1,.7,.3
asp =.1
aspect = 10*asp
!*DO,beamlength,10,20,1
beamlength=25

/PREP7
!LCLEAR, ALL
!LDELE, ALL
!KDELE, ALL

R=25
PI=acos(-1.)
h1=25
b1=100
```

Appendix A: (continued)

```
b2=10
h2=asp*b2
beamhigh=26.1-h2/2
!***** Area properties
*****

A1 = h1*b1
Iz1= 1/12*b1*h1*h1*h1
Iy1= 1/12*h1*b1*b1*b1

E1= 300000

!*****
*****

A2= h2*b2

Iy2= 1/12*h2*b2*b2*b2
Iz2= 1/12*b2*h2*h2*h2

E2= 169000

!*****Declare an element type: Beam 4 (3D
Elastic)*****

ET,1,BEAM4
KEYOPT,1,2,1
KEYOPT,1,6,1

!*****Set Real Constants and Material
Properties*****

R,1,A1,Iy1,Iz1,h1,b1, , !Check on the assumptions being made

R,2,A2,Iy2,Iz2,h2,b2, ,

MPTEMP,1,0
MPDATA,EX,1,,E1
MPDATA,PRXY,1,,0.35 ! Material properties for material 1 and 2

MPTEMP,1,0
MPDATA,EX,2,,E2
```

Appendix A: (continued)

MPDATA,PRXY,2,,0.35

!*****

!xcoor=R*cos((90-arclength)*PI/180)

!zcoor=R*sin((90-arclength)*PI/180)

zcoor=0

xcoor=beamlenght

!*****Create Keypoints 1 through 7: K(Point #, X-Coord, Y-Coord, Z-Coord)*****

K,1, 0,0,0

K,2, beamlenght/4,0,0

K,3, beamlenght/2,0,0

K,4, 3*beamlenght/4,0,0

K,5, beamlenght,0,0

k,6, beamlenght/2, -1,h2/2

K,7, beamlenght/2, 0,h2/2+1

K,8, beamlenght/2, 1,h2/2

!*****Create Beam using Lines and an Arc and divide into segments*****

LSTR, 1,2

LSTR, 2,3

LSTR, 3,4

LSTR, 4,5 ! Draws lines connecting keypoints

!1 through 6

LSTR, 3, 6

LSTR, 3, 7

LSTR, 3, 8

LESIZE, 5,,1

LESIZE, 6,,1

LESIZE, 7,,1

LESIZE, 1,,30

LESIZE, 2,,30

LESIZE, 3,,30

LESIZE, 4,,30

Appendix A: (continued)

```
!*****MESH*****  
*****
```

```
!rigid part, skew axis
```

```
real, 1          ! Use real constant set 1  
type, 1          ! Use element type 1  
mat, 1          ! use material property set 1  
LMESH, 5,7      ! mesh lines 3-5
```

```
!compliant part!
```

```
real, 2          ! Use real constant set 2  
type, 1          ! Use element type 1  
mat, 2          ! use material property set 2  
LMESH, 1,4      ! mesh line 1,3
```

```
!*****Get Node Numbers at chosen  
keypoints*****
```

```
ksel,s,kp,,1  
nslk,s  
*get,nkp1,node,0,num,max  
nset,all  
ksel,all
```

```
ksel,s,kp,,2  
nslk,s  
*get,nkp2,node,0,num,max      !Retrieves a value and stores it as a scalar parameter or  
part of an array parameter  
nset,all  
ksel,all
```

```
ksel,s,kp,,3  
nslk,s  
*get,nkp3,node,0,num,max  
nset,all  
ksel,all
```

```
ksel,s,kp,,4  
nslk,s
```

Appendix A: (continued)

*get,nkp4,node,0,num,max !Retrieves a value and stores it as a scalar parameter or
part of an array parameter
nset,all
kset,all

kset,s,kp,,5
nslk,s
*get,nkp5,node,0,num,max
nset,all
kset,all
kset,s,kp,,6
nslk,s
*get,nkp6,node,0,num,max
nset,all
kset,all

FINISH

```
!*****  
*****  
!***** SOLUTION *****  
*****  
!*****  
*****
```

/SOL
ANTYPE,0 ! Specifies the analysis type and restart status and "0" means
that it Performs a static analysis. Valid for all degrees of freedom

NLGEOM,1 ! Includes large-deflection effects in a static or full transient
analysis

!CNVTOL,U,,0.000001,,0
!CNVTOL,F,,0.0001,,0
 !Sets convergence values for nonlinear analyses

```
!*****Constraints*****  
*****
```

DK,1, ,0, , , ,UX,UY,UZ,ROTX,ROTY,ROTz

Appendix A: (continued)

DK,5, ,0, , , ,UY,ROTX,ROTz

!*****

increments=250
loadsteps=250
DO,step,1,loadsteps,1
position1=(step-1)*beamhigh/increments

!DDELE,12,ALL

!*****

newz=h2/2+position1

dispz=newz+zcoor

DK,5,UZ,dispz

LSWRITE,step
*ENDDO
LSSOLVE,1,loadsteps

FINISH

!*****

!*****GET RESULTS

!*****

!*****Displacements nodes
2,3,5*****

/POST1

!*DIM,rotx2,TABLE,loadSteps
!*DIM,roty2,TABLE,loadSteps
!*DIM,rotz2,TABLE,loadSteps

Appendix A: (continued)

!*DIM,disX2, TABLE,loadSteps
!*DIM,disY2, TABLE,loadSteps
!*DIM,disZ2, TABLE,loadSteps
!*DIM,disX3, TABLE,loadSteps
!*DIM,disY3, TABLE,loadSteps
!*DIM,disZ3, TABLE,loadSteps
!no y displame on 5
DIM,roty5, TABLE,loadSteps
*DIM,disX5, TABLE,loadSteps
*DIM,disZ5, TABLE,loadSteps

!*****Reactions forces node
1*****

*DIM,momx1, TABLE,loadsteps
*DIM,momy1, TABLE,loadsteps
*DIM,momz1, TABLE,loadsteps
*DIM,fx1, TABLE,loadsteps
*DIM,fy1, TABLE,loadsteps
*DIM,fz1, TABLE,loadsteps

!*****Reactions forces node
2*****

!*DIM,momy2, TABLE,loadsteps
!*DIM,momz2, TABLE,loadsteps
!*DIM,fx2, TABLE,loadsteps
!*DIM,fy2, TABLE,loadsteps
!*DIM,fz2, TABLE,loadsteps

!*****Reactions forces node
5*****

*DIM,momx5, TABLE,loadsteps
*DIM,momy5, TABLE,loadsteps
*DIM,momz5, TABLE,loadsteps
*DIM,fx5, TABLE,loadsteps
*DIM,fy5, TABLE,loadsteps
*DIM,fz5, TABLE,loadsteps

Appendix A: (continued)

*Do,nn,1,loadSteps

set,nn

!*****Displacements node

2,3,5*****

!*GET,rotx,Node,nkp2,ROT,X

!*SET,rotx2(nn),rotx

!*GET,roty,Node,nkp2,ROT,Y

!*SET,roty2(nn),roty

!*GET,rotz,Node,nkp2,ROT,Z

!*SET,rotz2(nn),rotz

!*GET,disX,Node,nkp2,U,X

!*SET,disX2(nn),disX

!*GET,disY,Node,nkp2,U,Y

!*SET,disY2(nn),disY

!*GET,disz,Node,nkp2,U,Z

!*SET,disZ2(nn),disz

!*GET,disX,Node,nkp3,U,X

!*SET,disX3(nn),disX

!*GET,disY,Node,nkp3,U,Y

!*SET,disY3(nn),disY

!*GET,disz,Node,nkp3,U,Z

!*SET,disZ3(nn),disz

*GET,roty,Node,nkp5,ROT,y

*SET,roty5(nn),roty

*GET,disX,Node,nkp5,U,X

*SET,disX5(nn),disX

*GET,disz,Node,nkp5,U,Z

*SET,disZ5(nn),disz

!*****Reactions forces node

1*****

*GET,momx,Node,nkp1,RF,MX

Appendix A: (continued)

*SET,momx1(nn),momx
*GET,fx,Node,nkp1,RF,FX
*SET,fx1(nn),fx
*GET,momy,Node,nkp1,RF,MY
*SET,momy1(nn),momy
*GET,fy,Node,nkp1,RF,FY
*SET,fy1(nn),fy
*GET,momz,Node,nkp1,RF,MZ
*SET,momz1(nn),momz
*GET,fz,Node,nkp1,RF,FZ
*SET,fz1(nn),fz

!*****Reactions forces node
2*****

!*GET,momx,Node,nkp2,RF,MX
!*SET,momx2(nn),momx
!*GET,fx,Node,nkp2,RF,FX
!*SET,fx2(nn),fx
!*GET,momy,Node,nkp2,RF,MY
!*SET,momy2(nn),momy
!*GET,fy,Node,nkp2,RF,FY
!*SET,fy2(nn),fy
!*GET,momz,Node,nkp2,RF,MZ
!*SET,momz2(nn),momz
!*GET,fz,Node,nkp2,RF,FZ
!*SET,fz2(nn),fz

!*****Reactions forces node
5*****

*GET,momx,Node,nkp5,RF,MX
*SET,momx5(nn),momx
*GET,fx,Node,nkp5,RF,FX
*SET,fx5(nn),fx
*GET,momy,Node,nkp5,RF,MY
*SET,momy5(nn),momy
*GET,fy,Node,nkp5,RF,FY
*SET,fy5(nn),fy
*GET,momz,Node,nkp5,RF,MZ
*SET,momz5(nn),momz
*GET,fz,Node,nkp5,RF,FZ
*SET,fz5(nn),fz

Appendix A: (continued)

*ENDDO

/output,forcevertical2%_asp% aspect%,txt,,Append

!*****

!*****FILE HEADER: BEAM

DATA*****

!*****

*MSG,INFO,'h2','b2','R','E','beamlengt','beamhigh'
%-8C %-8C %-8C %-8C %-8C %-8C

*VWRITE,h2,b2,R,E2,beamlengt,beamhigh
% 16.8G %-16.8G %-16.8G %-16.8G %-16.8G %-16.8G

!*****

!*****DISPLACEMENT DATA

SET*****

!*****

!*MSG,INFO,'rotX2','rotY2','rotZ2','disX2','disY2','disZ2'
!%-8C %-8C %-8C %-8C %-8C %-8C

!*VWRITE,rotx2(1),roty2(1),rotz2(1),disX2(1),disY2(1),disZ2(1)
!% 16.8G %-16.8G %-16.8G %-16.8G %-16.8G %-16.8G

*MSG,INFO,'roty5','disX5','disZ5'
%-8C %-8C %-8C

*VWRITE,roty5(1),disX5(1),disZ5(1)
% 16.8G %-16.8G %-16.8G

!*****

Appendix A: (continued)

```
!*****REACTIONS AT NODE
2*****
!*****
*****
```

```
*MSG,INFO,'momx2','momy2','momz2','fx2','fy2','fz2'
!%-8C %-8C %-8C %-8C %-8C %-8C
```

```
*VWRITE,momx2(1),momy2(1),momz2(1),fx2(1),fy2(1),fz2(1)
!% 16.8G %-16.8G %-16.8G %-16.8G %-16.8G %-16.8G
```

```
!*****
*****
```

```
!*****REACTIONS AT NODE
5*****
!*****
*****
```

```
*MSG,INFO,'momx5','momy5','momz5','fx5','fy5','fz5'
%-8C %-8C %-8C %-8C %-8C %-8C
```

```
*VWRITE,momx5(1),momy5(1),momz5(1),fx5(1),fy5(1),fz5(1)
% 16.8G %-16.8G %-16.8G %-16.8G %-16.8G %-16.8G
```

```
!*****
*****
```

```
!*****REACTIONS AT NODE
1*****
!*****
*****
```

```
*MSG,INFO,'momx1','momy1','momz1','fx1','fy1','fz1'
%-8C %-8C %-8C %-8C %-8C %-8C
```

```
*VWRITE,momx1(1),momy1(1),momz1(1),fx1(1),fy1(1),fz1(1)
% 16.8G %-16.8G %-16.8G %-16.8G %-16.8G %-16.8G
```

```
!*****
*****
```

Appendix A: (continued)

```
!*****  
*****  
!*****  
*****
```

/output

FINISH

*ENDDO

*ENDDO

Appendix B: (continued)

```

momy5 = DATA2(:,2);
momz5 = DATA2(:,3);
fx5   = DATA2(:,4);
fy5   = DATA2(:,5);
fz5   = DATA2(:,6);
momx1 = DATA3(:,1);
momy1 = DATA3(:,2);
momz1 = DATA3(:,3);
fx1   = DATA3(:,4);
fy1   = DATA3(:,5);
fz1   = DATA3(:,6);

%%%%%%%%%DEFINING l,a,b,gamma,Captheta,theta0,torque%%%%%%%%%
%%%%%%%%%

l = 25;
a= l+disx5;
b =disz5;
gamma = -(a.^2 - 2*a*l+l^2+b.^2)./(2*a*l-2*l^2);
theta = atan2(b,a-(1-gamma)*l);
theta(1) =0;
Torque = -momy1;
theta0 = roty5;

E = 169000;
h = 1;
b1 = 10;
l = 25;
I = (b1*h^3)/12;

M = (momy1*l^2)/(E*I); % Nondimensionalization
M_max = max(M);

%Scales moment between 0 and 1
M = M/M_max;
R = normrnd(0.1,.1,[size(M)]);

X = [ones(size(M(2:end))) 1./M(2:end) 1./M(2:end).^2 1.*M(2:end)
1.*M(2:end).^2];
Y = gamma(2:end);

B = inv(X'*X)*X'*Y;

%Gamma =
1./(B(1)+B(2)./M+B(3)./M.^2+B(4)./M.^3+B(5)./M.^4+B(6)./M.^5);
Gamma = B(1)+B(2)./M+B(3)./M.^2 +B(4).*M +B(5).*M.^2;

Csgamma=polyfit(M*M_max,gamma,0);

Theta = atan2(b,a-(1-Gamma)*l);

```

Appendix B: (continued)

```
ThetaC= atan2(b,a-(1-Csgamma)*1);

epsilon = gamma(2:end)-Gamma(2:end);
SST = sum((gamma(2:end)-mean(gamma(2:end))).^2);
SSE = sum(epsilon.^2);
s_squared = SSE/(length(gamma(2:end))-length(B));
s = sqrt(s_squared);
rsqrd = 1- SSE/SST;

Var_b = inv(X'*X)*s_squared;
X_ortho = X'*X;
[V,D] = eig(X_ortho);

X2(:,1) = X*V(:,1);
X2(:,2) = X*V(:,2);
X2(:,3) = X*V(:,3);
X2(:,4) = X*V(:,4);
X2(:,5) = X*V(:,5);

C = inv(X2'*X2)*X2'*Y;
%Gamma2 =
C(1)*X2(:,1)+C(2)*X2(:,2)+C(3)*X2(:,3)+C(4)*X2(:,4)+C(5)*X2(:,5);
Gamma2 =
C(1)*X2(:,1)+C(2)*X2(:,2)+C(3)*X2(:,3)+C(4)*X2(:,4)+C(5)*X2(:,5);

Theta2 = atan2(b(2:end),a(2:end)-(1-Gamma2)*1);

epsilon2 = gamma(2:end)-Gamma2;
SSE2 = sum(epsilon2.^2);
s_squared2 = SSE2/(length(gamma(2:end))-length(C));
s2 = sqrt(s_squared2);
rsqrd2 = 1- SSE2/SST;

Var_c = inv(X2'*X2)*s_squared2;

B1_prime =
C(1)*V(1,1)+C(2)*V(1,2)+C(3)*V(1,3)+C(4)*V(1,4)+C(5)*V(1,5); % compare
with B(1)
B2_prime =
C(1)*V(2,1)+C(2)*V(2,2)+C(3)*V(2,3)+C(4)*V(2,4)+C(5)*V(2,5); % compare
with B(2)
B3_prime =
C(1)*V(3,1)+C(2)*V(3,2)+C(3)*V(3,3)+C(4)*V(3,4)+C(5)*V(3,5); % compare
with B(3)
B4_prime =
C(1)*V(4,1)+C(2)*V(4,2)+C(3)*V(4,3)+C(4)*V(4,4)+C(5)*V(4,5); % compare
with B(4)
B5_prime =
C(1)*V(5,1)+C(2)*V(5,2)+C(3)*V(5,3)+C(4)*V(5,4)+C(5)*V(5,5); % compare
with B(5)
```

Appendix B: (continued)

```

B_var(1) =
abs(Var_c(1,1)*V(1,1)+Var_c(2,2)*V(1,2)+Var_c(3,3)*V(1,3)+Var_c(4,4)*V(
1,4)+Var_c(5,5)*V(1,5));
    B_var(2) =
abs(Var_c(1,1)*V(2,1)+Var_c(2,2)*V(2,2)+Var_c(3,3)*V(2,3)+Var_c(4,4)*V(
2,4)+Var_c(5,5)*V(2,5));
    B_var(3) =
abs(Var_c(1,1)*V(3,1)+Var_c(2,2)*V(3,2)+Var_c(3,3)*V(3,3)+Var_c(4,4)*V(
3,4)+Var_c(5,5)*V(3,5));
    B_var(4) =
abs(Var_c(1,1)*V(4,1)+Var_c(2,2)*V(4,2)+Var_c(3,3)*V(4,3)+Var_c(4,4)*V(
4,4)+Var_c(5,5)*V(4,5));
B_var(5) =
abs(Var_c(1,1)*V(5,1)+Var_c(2,2)*V(5,2)+Var_c(3,3)*V(5,3)+Var_c(4,4)*V(
5,4)+Var_c(5,5)*V(5,5));

    B_std = sqrt(B_var);
    % 95 % 2 sided confidence interval ie mean + or - interval

    t_statistic = tinv(.975,length(Y)-length(B));
    CI = t_statistic*B_std;
    Gamma_minus = B(1)-CI(1)+(B(2)-CI(2))./M+(B(3)-CI(3))./M.^2 +(B(4)-
CI(4)).*M +(B(5)-CI(5)).*M.^2;
    Gamma_plus = B(1)+CI(1)+(B(2)+CI(2))./M+(B(3)+CI(3))./M.^2
+(B(4)+CI(4)).*M +(B(5)+CI(5)).*M.^2;

    %%%%%%%%%%%FIGURE 4 %%%%%%%%%%%
    %%%%%%%%%%%

    figure(4)
    plot([Gamma(2:end) Gamma_minus(2:end) Gamma_plus(2:end)]);

    %%%%%%%%%%%FIGURE 1 a vs b
    %%%%%%%%%%%

    %%%%%%%%%%%
    figure(1)
    clf
    plot(a/1,b/1,'b*',((1-
Gamma2(2:end))+Gamma2(2:end)).*cos(Theta2(2:end))),Gamma2(2:end).*sin(Th
eta2(2:end)), 'R', ((1-
Csgamma)+Csgamma*cos(Theta2)),Csgamma*sin(Theta2), 'G-');

```

Appendix B: (continued)

```

%%%%%%%%%%%%%%%%%%%%%%%%%%%%%%%%%%%%%%%%%%%%%%%%%%%%%%%%%%%%%%%%%%%%%%%%%
%%%%%%%%%%%%%%FIGURE 2 M vs theta
%%%%%%%%%%%%%%%%%%%%%%%%%%%%%%%%%%%%%%%%%%%%%%%%%%%%%%%%%%%%%%%%%%%%%%%%%
figure(2)
clf

plot(M,theta*180/pi,'b*',M(2:end),Theta2*180/pi,'R',M(2:end),ThetaC(2:
end)*180/pi,'G*-');

%%%%%%%%%%%%%%%%%%%%%%%%%%%%%%%%%%%%%%%%%%%%%%%%%%%%%%%%%%%%%%%%%%%%%%%%%
%%%%%%%%%%%%%%FIGURE 3 M vs gamma
%%%%%%%%%%%%%%%%%%%%%%%%%%%%%%%%%%%%%%%%%%%%%%%%%%%%%%%%%%%%%%%%%%%%%%%%%
figure (3)
plot(gamma,M*M_max,'b*',Gamma2,M(2:end)*M_max,'R',Csgamma,M*M_max,'G-
');
mytexstr = '$\frac{M l^2}{EI}$';
Gc=
ylabel(mytexstr,'interpreter','latex','fontsize',10,'units','norm');
G4c = legend('Data','\gamma*','\gamma');

%%%%%%%%%%%%%%%%%%%%%%%%%%%%%%%%%%%%%%%%%%%%%%%%%%%%%%%%%%%%%%%%%%%%%%%%%
%%%%%%%%%%%%%%ERROR %%%%%%%%%%%%%%%
%%%%%%%%%%%%%%%%%%%%%%%%%%%%%%%%%%%%%%%%%%%%%%%%%%%%%%%%%%%%%%%%%%%%%%%%%

        erroro = ( a/l - ((1-Gamma)+Gamma.*cos(Theta))).^2 +
(b/l - Gamma.*sin(Theta)).^2;
        %disp_mag = (((1-Gamma)+Gamma.*cos(Theta))-
a(round(end/3))/l).^2+(Gamma.*sin(Theta)-b(round(end/3))/l).^2).^5;

        total_erroro =
trapz(M(2:end),erroro(2:end));%+trapz(Gamma(2:end),erroro(2:end));
        %total_erroro = sqrt(max(erroro(2:end)./diff(M)))

rsqrd
Csgamma
total_erroro
CI

```

Appendix C: ANSYS Batch Code for a Specific Horizontal Buckling End-Loaded

Beam

```
!*****
*****
/CONFIG,NRES,10000
!/CWD,'C:\Documents and Settings\despinos\Desktop\Work'

!*****
*****

!*****
*****
!*****Set Up Model
Variables*****
*

!*****
*****

!*DO,asp, .1,.7,.3
asp =.1
aspect = 10*asp
!*DO,beamlenght,10,20,1
beamlenght=100
/PREP7
!LCLEAR, ALL
!LDELE, ALL
!KDELE, ALL

R=100
PI=acos(-1.)
h1=25
b1=100

b2=10
```

Appendix C: (continued)

$$h2=asp*b2$$

!***** Area properties

$$A1 = h1*b1$$

$$Iz1= 1/12*b1*h1*h1*h1$$

$$Iy1= 1/12*h1*b1*b1*b1$$

$$E1= 300000$$

!*****

$$A2= h2*b2$$

$$Iy2= 1/12*h2*b2*b2*b2$$

$$Iz2= 1/12*b2*h2*h2*h2$$

$$E2= 169000$$

!*****Declare an element type: Beam 4 (3D

Elastic)*****

ET,1,BEAM4

KEYOPT,1,2,1

KEYOPT,1,6,1

!*****Set Real Constants and Material

Properties*****

R,1,A1,Iy1,Iz1,h1,b1, , !Check on the assumptions being made

R,2,A2,Iy2,Iz2,h2,b2, ,

MPTEMP,1,0

MPDATA,EX,1,,E1

MPDATA,PRXY,1,,0.35 ! Material properties for material 1 and 2

MPTEMP,1,0

MPDATA,EX,2,,E2

MPDATA,PRXY,2,,0.35

Appendix C: (continued)

```
*****  
*****
```

```
xcoor=beamlenght
```

```
!*****Create Keypoints 1 through 7: K(Point #, X-Coord, Y-Coord, Z-  
Coord)*****
```

```
K,1, 0,0,0  
K,2, beamlenght/4,0,h2/4  
K,3, beamlenght/2,0,h2/2  
K,4, 3*beamlenght/4,0,h2/4  
K,5, beamlenght,0,0  
k,6, beamlenght/2, -1,h2/2  
K,7, beamlenght/2, 0,h2/2+1  
K,8, beamlenght/2, 1,h2/2
```

```
!*****Create Beam using Lines and an Arc and divide into  
segments*****
```

```
LSTR, 1,2  
LSTR, 2,3  
LSTR, 3,4  
LSTR, 4,5 ! Draws lines connecting keypoints
```

```
1 through 6
```

```
LSTR, 3, 6  
LSTR, 3, 7  
LSTR, 3, 8  
LESIZE, 5,,1  
LESIZE, 6,,1  
LESIZE, 7,,1  
LESIZE, 1,,30  
LESIZE, 2,,30  
LESIZE, 3,,30  
LESIZE, 4,,30
```

```
!*****MESH*****  
*****
```

Appendix C: (continued)

!rigid part, skew axis

```
real, 1      ! Use real constant set 1
type, 1      ! Use element type 1
mat, 1      ! use material property set 1
LMESH, 5,7   ! mesh lines 3-5
```

!compliant part!

```
real, 2      ! Use real constant set 2
type, 1      ! Use element type 1
mat, 2      ! use material property set 2
LMESH, 1,4   ! mesh line 1,3
```

!*****Get Node Numbers at chosen

keypoints*****

```
ksel,s,kp,,1
nslk,s
*get,nkp1,node,0,num,max
nset,all
ksel,all
```

```
ksel,s,kp,,2
nslk,s
*get,nkp2,node,0,num,max      !Retrieves a value and stores it as a scalar parameter or
part of an array parameter
nset,all
ksel,all
```

```
ksel,s,kp,,3
nslk,s
*get,nkp3,node,0,num,max
nset,all
ksel,all
```

```
ksel,s,kp,,4
nslk,s
*get,nkp4,node,0,num,max      !Retrieves a value and stores it as a scalar parameter or
part of an array parameter
```

Appendix C: (continued)

nsl,all
ksel,all

ksel,s,kp,,5
nslk,s
*get,nkp5,node,0,num,max
nsl,all
ksel,all

ksel,s,kp,,6
nslk,s
*get,nkp6,node,0,num,max
nsl,all
ksel,all

FINISH

```
!*****  
*****  
!***** SOLUTION  
*****  
!*****  
*****
```

/SOL
ANTYPE,0 ! Specifies the analysis type and restart status and "0" means
that it Performs a static analysis. Valid for all degrees of freedom

NLGEOM,1 ! Includes large-deflection effects in a static or full transient
analysis

!CNVTOL,U,,0.000001,,0
!CNVTOL,F,,0.0001,,0
!Sets convergence values for nonlinear analyses

```
!*****Constraints*****  
*****
```

DK,1, ,0, , , ,UX,UY,UZ,ROTX,ROTY,ROTz

Appendix C: (continued)

DK,5, ,0, , , ,UZ,UY,ROTY,ROTX,ROTz

!*****

increments=3000
loadsteps=300
*DO,step,1,loadsteps,1
position=(step-1)*beamlengt/increments

!DDELE,12,ALL

!*****

newx=beamlengt-position
dispX=newx-xcoor
DK,5,UX,dispX

LSWRITE,step
*ENDDO

increments=400
loadsteps=284
*DO,step,41,loadsteps,1
position=(step-1)*beamlengt/increments

!DDELE,12,ALL

!*****

newx=beamlengt-position
dispX=newx-xcoor
DK,5,UX,dispX

LSWRITE,step+260
*ENDDO

LSSOLVE,1,loadsteps+260

Appendix C: (continued)

/STATUS,SOLU
FINISH

loadsteps= loadsteps+260

!*****

!*****GET RESULTS

!*****

!*****Displacements nodes

2,3,5*****

/POST1

*DIM,rotx2, TABLE, loadSteps

*DIM,roty2, TABLE, loadSteps

*DIM,rotz2, TABLE, loadSteps

*DIM,disX2, TABLE, loadSteps

*DIM,disY2, TABLE, loadSteps

*DIM,disZ2, TABLE, loadSteps

*DIM,disX3, TABLE, loadSteps

*DIM,disY3, TABLE, loadSteps

*DIM,disZ3, TABLE, loadSteps

*DIM,disX5, TABLE, loadSteps

*DIM,disY5, TABLE, loadSteps

*DIM,disZ5, TABLE, loadSteps

!*****Reactions forces node

1*****

*DIM,momx1, TABLE, loadsteps

*DIM,momy1, TABLE, loadsteps

*DIM,momz1, TABLE, loadsteps

*DIM,fx1, TABLE, loadsteps

*DIM,fy1, TABLE, loadsteps

*DIM,fz1, TABLE, loadsteps

!*****Reactions forces node

2*****

*DIM,momx2, TABLE, loadsteps

*DIM,momy2, TABLE, loadsteps

Appendix C: (continued)

*DIM,momz2,TABLE,loadsteps

*DIM,fx2,TABLE,loadsteps

*DIM,fy2,TABLE,loadsteps

*DIM,fz2,TABLE,loadsteps

!*****Reactions forces node
5*****

*DIM,momx5,TABLE,loadsteps

*DIM,momy5,TABLE,loadsteps

*DIM,momz5,TABLE,loadsteps

*DIM,fx5,TABLE,loadsteps

*DIM,fy5,TABLE,loadsteps

*DIM,fz5,TABLE,loadsteps

*Do,nn,1,loadSteps

set,nn

!*****Displacements node
2,3,5*****

*GET,rotx,Node,nkp2,ROT,X

*SET,rotx2(nn),rotx

*GET,roty,Node,nkp2,ROT,Y

*SET,roty2(nn),roty

*GET,rotz,Node,nkp2,ROT,Z

*SET,rotz2(nn),rotz

*GET,disX,Node,nkp2,U,X

*SET,disX2(nn),disX

*GET,disY,Node,nkp2,U,Y

*SET,disY2(nn),disY

*GET,disz,Node,nkp2,U,Z

*SET,disZ2(nn),disz

*GET,disX,Node,nkp3,U,X

*SET,disX3(nn),disX

*GET,disY,Node,nkp3,U,Y

*SET,disY3(nn),disY

*GET,disz,Node,nkp3,U,Z

*SET,disZ3(nn),disz

*GET,disX,Node,nkp5,U,X

*SET,disX5(nn),disX

Appendix C: (continued)

```
*GET,disY,Node,nkp5,U,Y
*SET,disY5(nn),disY
*GET,disz,Node,nkp5,U,Z
*SET,disZ5(nn),disz
!*****Reactions forces node
1*****
```

```
*GET,momx,Node,nkp1,RF,MX
*SET,momx1(nn),momx
*GET,fx,Node,nkp1,RF,FX
*SET,fx1(nn),fx
*GET,momy,Node,nkp1,RF,MY
*SET,momy1(nn),momy
*GET,fy,Node,nkp1,RF,FY
*SET,fy1(nn),fy
*GET,momz,Node,nkp1,RF,MZ
*SET,momz1(nn),momz
*GET,fz,Node,nkp1,RF,FZ
*SET,fz1(nn),fz
```

```
!*****Reactions forces node
2*****
```

```
*GET,momx,Node,nkp2,RF,MX
*SET,momx2(nn),momx
*GET,fx,Node,nkp2,RF,FX
*SET,fx2(nn),fx
*GET,momy,Node,nkp2,RF,MY
*SET,momy2(nn),momy
*GET,fy,Node,nkp2,RF,FY
*SET,fy2(nn),fy
*GET,momz,Node,nkp2,RF,MZ
*SET,momz2(nn),momz
*GET,fz,Node,nkp2,RF,FZ
*SET,fz2(nn),fz
```

```
!*****Reactions forces node
5*****
```

```
*GET,momx,Node,nkp5,RF,MX
*SET,momx5(nn),momx
*GET,fx,Node,nkp5,RF,FX
*SET,fx5(nn),fx
```

Appendix C: (continued)

```
*GET,momy,Node,nkp5,RF,MY
*SET,momy5(nn),momy
*GET,fy,Node,nkp5,RF,FY
*SET,fy5(nn),fy
*GET,momz,Node,nkp5,RF,MZ
*SET,momz5(nn),momz
*GET,fz,Node,nkp5,RF,FZ
*SET,fz5(nn),fz
```

```
*ENDDO
```

```
/output,forceplana2%_asp%aspect%,txt,,Append
```

```
!*****
*****
!*****FILE HEADER: BEAM
DATA*****
!*****
*****
```

```
*MSG,INFO,'h2','b2','R','E','beamlenght'
%-8C %-8C %-8C %-8C %-8C
```

```
*VWRITE,h2,b2,R,E2,beamlenght
% 16.8G %-16.8G %-16.8G %-16.8G %-16.8G
```

```
!*****
*****
!*****DISPLACEMENT DATA
SET*****
!*****
*****
```

```
*MSG,INFO,'rotX2','rotY2','rotZ2','disX2','disY2','disZ2'
%-8C %-8C %-8C %-8C %-8C %-8C
```

```
*VWRITE,rotx2(1),roty2(1),rotz2(1),disX2(1),disY2(1),disZ2(1)
% 16.8G %-16.8G %-16.8G %-16.8G %-16.8G %-16.8G
```

```
*MSG,INFO,'disX3','disY3','disZ3','disX5','disY5','disZ5'
%-8C %-8C %-8C %-8C %-8C %-8C
```

Appendix C: (continued)

```
*VWRITE,disX3(1),disY3(1),disZ3(1),disX5(1),disY5(1),disZ5(1)
% 16.8G %-16.8G %-16.8G %-16.8G %-16.8G %-16.8G
!*****
*****
!*****REACTIONS AT NODE
2*****
!*****
*****
```

```
*MSG,INFO,'momx2','momy2','momz2','fx2','fy2','fz2'
%-8C %-8C %-8C %-8C %-8C %-8C
```

```
*VWRITE,momx2(1),momy2(1),momz2(1),fx2(1),fy2(1),fz2(1)
% 16.8G %-16.8G %-16.8G %-16.8G %-16.8G %-16.8G
```

```
!*****
*****
!*****REACTIONS AT NODE
5*****
!*****
*****
```

```
*MSG,INFO,'momx5','momy5','momz5','fx5','fy5','fz5'
%-8C %-8C %-8C %-8C %-8C %-8C
```

```
*VWRITE,momx5(1),momy5(1),momz5(1),fx5(1),fy5(1),fz5(1)
% 16.8G %-16.8G %-16.8G %-16.8G %-16.8G %-16.8G
```

```
!*****
*****
!*****REACTIONS AT NODE
1*****
!*****
*****
```

```
*MSG,INFO,'momx1','momy1','momz1','fx1','fy1','fz1'
%-8C %-8C %-8C %-8C %-8C %-8C
```

Appendix C: (continued)

```
*VWRITE,momx1(1),momy1(1),momz1(1),fx1(1),fy1(1),fz1(1)
% 16.8G %-16.8G %-16.8G %-16.8G %-16.8G %-16.8G
!*****
*****
/output

FINISH

*ENDDO
*ENDDO
```

Appendix D: MATLAB Code for a Specific Horizontal Buckling End-Loaded Beam

```

clear all
%filename =
['180+forceplanar_arc%arclength%_asp',num2str(aspect),'.txt'];
%filename = '180_FO~1.txt';
filename = ['forceplana2%_asp%aspect%', '.txt'];
%string1 = 'C:\DOCUME~1\despinos\';
%fid1 = fopen([string1,filename]); % opens the file
string1 = 'C:\Documents and Settings\Diego\Desktop\ThesisHome';
fid1 = fopen(filename);
%%%%%%%%%%%%%%%%%%%%%%%%%%%%%%%%%%%%%%%%%%%%%%%%%%%%%%%%%%%%%%%%%%%%%%%%%
%%%%%%%%%%%%%%%%%%%%%%%%%%%%%%%%%%%%%%%%%%%%%%%%%%%%%%%%%%%%%%%%%%%%%%%%%

ABT = fread(fid1); % reads the file into
variable ABT
fclose(fid1); %closes the data file

BT = native2unicode(ABT)'; %changes data from
machine code to text

end1stheader = findstr('disZ2', GBT); % finds end of first
header
begin2ndheader = findstr('disX3', GBT); % finds beginning of
second header
end2ndheader = findstr('disZ5', GBT); % finds end of second
header
begin3ndheader = findstr('momx2', GBT);
end3ndheader = findstr('fz2', GBT);
begin4ndheader = findstr('momx5', GBT);
end4ndheader = findstr('fz5', GBT);
begin5ndheader = findstr('momx1', GBT);
end5ndheader = findstr('fz1', GBT);

DATA1 = str2num(GBT(end1stheader(end)+6:begin2ndheader(end)-1)); %
turns the data into a numerical matrix
DATA2 = str2num(GBT(end2ndheader(end)+6:begin3ndheader(end)-1)); %
turns the data into a numerical matrix
DATA3 = str2num(GBT(end3ndheader(end)+4:begin4ndheader(end)-1)); %
turns the data into a numerical matrix
DATA4 = str2num(GBT(end4ndheader(end)+4:begin5ndheader(end)-1)); %
turns the data into a numerical matrix
DATA5 = str2num(GBT(end5ndheader(end)+4:end)); %
turns the data into a numerical matrix

```

Appendix D: (continued)

```
%%%%%%%%%%%%%%%%%%%%%%%%%%%%%%%%%%%%%%%%%%%%%%%%%%%%%%%%%%%%%%%%%%%%%%%%FORCES, DISPLACEMENTS AND
MOMENTD%%%%%%%%%%%%%%%%%%%%%%%%%%%%%%%%%%%%%%%%%%%%%%%%%%%%%%%%%%%%%%%%%%%%%%%%
%%%%%%%%%%%%%%%%%%%%%%%%%%%%%%%%%%%%%%%%%%%%%%%%%%%%%%%%%%%%%%%%%%%%%%%%
```

```
roty2 = DATA1(:,2);
disx2 = DATA1(:,4);
disz2 = DATA1(:,6);
disx3 = DATA2(:,1);
disz3 = DATA2(:,3);
disx5 = DATA2(:,4);
momx2 = DATA3(:,1);
momy2 = DATA3(:,2);
momz2 = DATA3(:,3);
fx2   = DATA3(:,4);
fy2   = DATA3(:,5);
fz2   = DATA3(:,6);
momx5 = DATA4(:,1);
momy5 = DATA4(:,2);
momz5 = DATA4(:,3);
fx5   = DATA4(:,4);
fy5   = DATA4(:,5);
fz5   = DATA4(:,6);
momx1 = DATA5(:,1);
momy1 = DATA5(:,2);
momz1 = DATA5(:,3);
fx1   = DATA5(:,4);
fy1   = DATA5(:,5);
fz1   = DATA5(:,6);
```

```
%%%%%%%%DEFINING l,a,b,gamma,Captheta,theta0,torque%%%%%%%%
%%%%%%%%
```

```
l = 25;
a = l+disx2;
b = disz2;
gamma = -(a.^2 - 2*a*l+l^2+b.^2)./(2*a*l-2*l^2);
theta = atan2(b,a-(1-gamma)*l);
theta(1) = 0;
Torque = -momy1;
theta0 = roty2;
```

```
E = 169000;
h = 1;
b1 = 10;
l = 25;
I = (b1*h^3)/12;
```

```
M = (momy1*l^2)/(E*I);
M_max = max(M);
M = M/M_max;
R = normrnd(0.1,.1,[size(M)]);
```

Appendix D: (continued)

```
X = [ones(size(M(2:end))) 1./M(2:end) 1./M(2:end).^2 1.*M(2:end)
1.*M(2:end).^2];
Y = gamma(2:end);
B = inv(X'*X)*X'*Y;
```

```
%Gamma =
1./(B(1)+B(2)./M+B(3)./M.^2+B(4)./M.^3+B(5)./M.^4+B(6)./M.^5);
Gamma = B(1)+B(2)./M+B(3)./M.^2 +B(4).*M +B(5).*M.^2;
```

```
Csgamma=polyfit(M(2:end)*M_max,gamma(2:end),0);%%%%%%%%%
```

```
Theta = atan2(b,a-(1-Gamma)*1);
ThetaC= atan2(b,a-(1-Csgamma)*1);
```

figure (5)

```
clf
plot(M*M_max,gamma)
```

```
epsilon = gamma(2:end)-Gamma(2:end);
SST = sum((gamma(2:end)-mean(gamma(2:end))).^2);
SSE = sum(epsilon.^2);
s_squared = SSE/(length(gamma(2:end))-length(B));
s = sqrt(s_squared);
rsqrd = 1- SSE/SST;
```

```
Var_b = inv(X'*X)*s_squared;
X_ortho = X'*X;
[V,D] = eig(X_ortho);
```

```
X2(:,1) = X*V(:,1);
X2(:,2) = X*V(:,2);
X2(:,3) = X*V(:,3);
X2(:,4) = X*V(:,4);
X2(:,5) = X*V(:,5);
```

```
C = inv(X2'*X2)*X2'*Y;
%Gamma2 =
C(1)*X2(:,1)+C(2)*X2(:,2)+C(3)*X2(:,3)+C(4)*X2(:,4)+C(5)*X2(:,5);
Gamma2 =
C(1)*X2(:,1)+C(2)*X2(:,2)+C(3)*X2(:,3)+C(4)*X2(:,4)+C(5)*X2(:,5);
Theta2 = atan2(b(2:end),a(2:end)-(1-Gamma2)*1);
```

```
epsilon2 = gamma(2:end)-Gamma2;
SSE2 = sum(epsilon2.^2);
s_squared2 = SSE2/(length(gamma(2:end))-length(C));
s2 = sqrt(s_squared2);
```

Appendix D: (continued)

```

rsqrd2 = 1- SSE2/SST;

Var_c = inv(X2'*X2)*s_squared2;
sc(1) = sqrt(Var_c(1,1));
sc(2) = sqrt(Var_c(2,2));
sc(3) = sqrt(Var_c(3,3));
sc(4) = sqrt(Var_c(4,4));
sc(5) = sqrt(Var_c(5,5));

B1_prime =
C(1)*V(1,1)+C(2)*V(1,2)+C(3)*V(1,3)+C(4)*V(1,4)+C(5)*V(1,5); % compare
with B(1)
B2_prime =
C(1)*V(2,1)+C(2)*V(2,2)+C(3)*V(2,3)+C(4)*V(2,4)+C(5)*V(2,5); % compare
with B(2)
B3_prime =
C(1)*V(3,1)+C(2)*V(3,2)+C(3)*V(3,3)+C(4)*V(3,4)+C(5)*V(3,5); % compare
with B(3)
B4_prime =
C(1)*V(4,1)+C(2)*V(4,2)+C(3)*V(4,3)+C(4)*V(4,4)+C(5)*V(4,5); % compare
with B(4)
B5_prime =
C(1)*V(5,1)+C(2)*V(5,2)+C(3)*V(5,3)+C(4)*V(5,4)+C(5)*V(5,5); % compare
with B(5)

B_var(1) = sum(sc.*V(1,:)).^2;
B_var(2) = sum(sc.*V(2,:)).^2;
B_var(3) = sum(sc.*V(3,:)).^2;
B_var(4) = sum(sc.*V(4,:)).^2;
B_var(5) = sum(sc.*V(5,:)).^2;

B_std = sqrt(B_var);
% 95 % 2 sided confidence interval ie mean + or - interval

t_statistic = tinv(.975,length(Y)-length(B));
CI = t_statistic*B_std
Gamma_minus = B(1)-CI(1)+(B(2)-CI(2))./M+(B(3)-CI(3))./M.^2 +(B(4)-
CI(4)).*M +(B(5)-CI(5)).*M.^2;
Gamma_plus = B(1)+CI(1)+(B(2)+CI(2))./M+(B(3)+CI(3))./M.^2
+(B(4)+CI(4)).*M +(B(5)+CI(5)).*M.^2;

%%%%%%%%%%%%%%%%%%%%%%%%%%%%%%%%%%%%%%%%%%%%%%%%%%%%%%%%%%%%%%%%%%%%%%%%%
%%%%%%%%%%%%%%%%%%%%%%%%%%%%%%%%%%%%%%%%%%%%%%%%%%%%%%%%%%%%%%%%%%%%%%%%%
figure(4)
plot([Gamma(2:end) Gamma_minus(2:end) Gamma_plus(2:end)]);

```

Appendix D: (continued)

```

%%%%%%%%%%%%%FIGURE 1 a vs b
%%%%%%%%%%%%%%%%%%%%%%%%%%%%%%%%%%%%%%%%%%%%%%%%%%%%%%%%%

%%%%%%%%%%%%%%%%%%%%%%%%%%%%%%%%%%%%%%%%%%%%%%%%%%%%%%%%%
figure(1)
clf
plot(a/l,b/l,'b*',((1-
Gamma2(2:end))+Gamma2(2:end).*cos(Theta2(2:end))),Gamma2(2:end).*sin(Th
eta2(2:end)),'R',((1-
Csgamma)+Csgamma*cos(Theta2)),Csgamma*sin(Theta2),'G-');

%%%%%%%%%%%%%FIGURE 2 M vs theta
%%%%%%%%%%%%%%%%%%%%%%%%%%%%%%%%%%%%%%%%%%%%%%%%%%%%%%%%%
%%%%%%%%%%%%%%%%%%%%%%%%%%%%%%%%%%%%%%%%%%%%%%%%%%%%%%%%%
figure(2)
clf
plot(M,theta*180/pi,'b*',M(2:end),Theta2*180/pi,'R',M(2:end),ThetaC(2:e
nd)*180/pi,'G-');

%%%%%%%%%%%%%FIGURE 3 M vs gamma
%%%%%%%%%%%%%%%%%%%%%%%%%%%%%%%%%%%%%%%%%%%%%%%%%%%%%%%%%
%%%%%%%%%%%%%%%%%%%%%%%%%%%%%%%%%%%%%%%%%%%%%%%%%%%%%%%%%

figure(3)
plot(gamma,M*M_max,'b*',Gamma2,M(2:end)*M_max,'R',Csgamma,M*M_max,'Gs-
');
mytexstr = '$\frac{M^2}{EI}$';
Gc=
ylabel(mytexstr,'interpreter','latex','fontsize',10,'units','norm');
G4c = legend('Data','\gamma*','\gamma');

%%%%%%%%%%%%%ERROR %%%%%%%%%%%%%%%%%%%%%%%%%%%%%%%%%%%%%%%%%%%%%%%%%%%%%%%%%%
%%%%%%%%%%%%%%%%%%%%%%%%%%%%%%%%%%%%%%%%%%%%%%%%%%%%%%%%%

erroro = ( a(2:end)/l - ((1-Gamma2)+Gamma2.*cos(Theta2))).^2 +
(b(2:end)/l - Gamma2.*sin(Theta2)).^2;
%disp_mag = (((1-Gamma2)+Gamma2.*cos(Theta2))-
a(round(end/3))/l).^2+(Gamma2.*sin(Theta2)-b(round(end/3))/l).^2).^5;

total_erroro = trapz(M(2:end),erroro);
%+trapz(Gamma2(2:end),erroro(2:end));
%total_erroro = sqrt(max(erroro(2:end)./diff(M)))

rsqrd2
Csgamma
total_erroro

```

Appendix E: ANSYS Batch Code for a Specific Horizontal Buckling End-Loaded Curved Beam

```

!*****
*****
/CONFIG,NRES,10000
!/CWD,'C:\Documents and Settings\despinos\Desktop\Work'
!/INPUT,'C:\Documents and
Settings\despinos\Desktop\ThesisDiego\AnsysCode\curvebeam3diffarcs','txt'
!*****
*****

!*****
*****
!*****Set Up Model
Variables*****
*
!*****
*****
!*DO,asp, .1,.7,.3
asp =.1
aspect = 10*asp
!*DO,beamlenght,10,20,1
*DO,LAMBDAg,15,105,15
R=100
Lambda=LAMBDAg*PI/180
arclength=R*Lambda
/PREP7
LCLEAR, ALL
LDELE, ALL

KDELE, ALL

PI=acos(-1.)

h1=.1
b1=1
b2=5.7
h2=2

```

Appendix E: (continued)

!***** Area properties

$$A1 = h1*b1$$

$$Iz1 = 1/12*b1*h1*h1*h1$$

$$Iy1 = 1/12*h1*b1*b1*b1$$

$$E1 = 300000$$

!*****

$$A2 = h2*b2$$

$$Iy2 = 1/12*h2*b2*b2*b2$$

$$Iz2 = 1/12*b2*h2*h2*h2$$

$$E2 = 169000$$

!*****Declare an element type: Beam 4 (3D
Elastic)*****

ET,1,BEAM4
KEYOPT,1,2,1
KEYOPT,1,6,1

!*****Set Real Constants and Material
Properties*****

R,1,A1,Iy1,Iz1,h1,b1, , !Check on the assumptions being made

R,2,A2,Iy2,Iz2,h2,b2, ,

MPTEMP,1,0
MPDATA,EX,1,,E1
MPDATA,PRXY,1,,0.35 ! Material properties for material 1 and 2

MPTEMP,1,0
MPDATA,EX,2,,E2

Appendix E: (continued)

MPDATA,PRXY,2,,0.35

!*****

xcoor=R*cos((90*PI/180)-(arclength/R))
ycoor=R*sin((90*PI/180)-(arclength/R))
midx = R*cos((90*PI/180)-(arclength/(2*R)))
midy = R*sin((90*PI/180)-(arclength/(2*R)))
fourthx =R*cos((90*PI/180)-(arclength/(4*R)))
fourthy =R*sin((90*PI/180)-(arclength/(4*R)))
fourthx2 =R*cos((90*PI/180)-((arclength*3)/(4*R)))
fourthy2 =R*sin((90*PI/180)-((arclength*3)/(4*R)))

!*****Create Keypoints 1 through 11: K(Point #, X-Coord, Y-Coord, Z-Coord)*****

K,1, 0,0,0,
K,2, 0,R,0
K,3, xcoor,ycoor,0
k,4, midx, midy,h2
K,5, midx,midy,(h2)+1
K,6, midx*(R-1)/R,midy*(R-1)/R,h2
!!?????
!K,7, midx-midy/R,midy+midx/R,h2
!K,7, midx*(R+1)/R,midy*(R+1)/R,h2
K,7, midx+cos(arclength/(2*R)),midy-sin(arclength/(2*R)),h2

k,8, fourthx,fourthy,h2/2
k,9, fourthx,fourthy,(h2/2)+1
k,10, fourthx*(R-1)/R,fourthy*(R-1)/R,h2/2
!!?????
!k,11, fourthx-fourthy/R,fourthy+fourthx/R,h2/2
!k,11, fourthx*(R+1)/R,fourthy*(R+1)/R,h2/2
k,11, fourthx+cos(arclength/(4*R)),fourthy-sin(arclength/(4*R)),h2/2

k,12, fourthx2,fourthy2,h2/2

Appendix E: (continued)

```

k,13, fourthx2,fourthy2,(h2/2)+1
k,14, fourthx2*(R-1)/R,fourthy2*(R-1)/R,h2/2
    !!!?????
!k,15, fourthx2-fourthy2/R,fourthy2+fourthx2/R,h2/2
!k,15, fourthx2*(R+1)/R,fourthy2*(R+1)/R,h2/2
k,15, fourthx2+cos((arclength*3)/(4*R)),fourthy2-sin((arclength*3)/(4*R)),h2/2

```

```

!*****Create Beam using Lines and an Arc and divide into
segments*****

```

```

LSTR, 4,5 !line 1
LSTR, 4,6 !line 2 ! Draws lines connecting keypoints
LSTR, 4,7 !line 3
LSTR, 8,9 !line 4
LSTR, 8,10 !line 5
LSTR, 8,11 !line 6
LSTR, 12,13 !line 7
LSTR, 12,14 !line 8
LSTR, 12,15 !line 9
LESIZE, ALL,,1

LARC, 2,8,1,R, !arc 10
LARC, 8,4,1,R, !arc 11
LARC, 4,12,1,R, !arc 12
LARC, 12,3,1,R, !arc 13

LESIZE, 10,,30
LESIZE, 11,,30
LESIZE, 12,,30
LESIZE, 13,,30

```

```

!*****MESH*****
*****

```

```

!rigid part skew axis!!

```

```

real, 1 ! Use real constant set 1
type, 1 ! Use element type 1
mat, 1 ! use material property set 1
LMESH, 1,9 ! mesh lines 1-9

```

Appendix E: (continued)

!copliant arc!

```
real,    2          ! Use real constant set 2
type,    1          ! Use element type 1
mat,     2          ! use material property set 2
LMESH,   10,13     ! mesh line 10,13
```

!*****Get Node Numbers at chosen

keypoints*****

ksel,s,kp,,2

nslk,s

*get,nkp2,node,0,num,max
part of an array parameter

!Retrieves a value and stores it as a scalar parameter or

nsl,all

ksel,all

ksel,s,kp,,3

nslk,s

*get,nkp3,node,0,num,max
nsl,all

ksel,all

ksel,s,kp,,4

nslk,s

*get,nkp4,node,0,num,max
part of an array parameter

!Retrieves a value and stores it as a scalar parameter or

nsl,all

ksel,all

ksel,s,kp,,5

nslk,s

*get,nkp5,node,0,num,max
nsl,all

ksel,all

ksel,s,kp,,6

nslk,s

*get,nkp6,node,0,num,max
nsl,all

ksel,all

ksel,s,kp,,7

Appendix E: (continued)

nslk,s
*get,nkp7,node,0,num,max
nsl,all
ksel,all

ksel,s,kp,,8
nslk,s
*get,nkp8,node,0,num,max
part of an array parameter
nsl,all
ksel,all

!Retrieves a value and stores it as a scalar parameter or

ksel,s,kp,,9
nslk,s
*get,nkp9,node,0,num,max
nsl,all
ksel,all

ksel,s,kp,,10
nslk,s
*get,nkp10,node,0,num,max
nsl,all
ksel,all

ksel,s,kp,,11
nslk,s
*get,nkp11,node,0,num,max
nsl,all
ksel,all

ksel,s,kp,,12
nslk,s
*get,nkp12,node,0,num,max
nsl,all
ksel,all

ksel,s,kp,,13
nslk,s
*get,nkp13,node,0,num,max
nsl,all
ksel,all

ksel,s,kp,,14

Appendix E: (continued)

```
nslk,s
*get,nkp14,node,0,num,max
nsl,all
ksel,all
```

```
ksel,s,kp,,15
nslk,s
*get,nkp15,node,0,num,max
nsl,all
ksel,all
```

FINISH

```
!*****
*****
!* ***** SOLUTION *****
*****
!* *****
*****
```

```
/SOL
ANTYPE,0 ! Specifies the analysis type and restart status and "0" means
that it Performs a static analysis. Valid for all degrees of freedom
```

```
NLGEOM,1 ! Includes large-deflection effects in a static or full transient
analysis
```

```
!CNVTOL,U,,0.000001,,0
!CNVTOL,F,,0.0001,,0
!Sets convergence values for nonlinear analyses
```

```
SOLCONTROL,ON
NEQIT,100
AUTOTS,ON
!* ***** Defines DOF constraints at
keypoints*****
```

```
DK,2, ,0, , , ,UX,UY,UZ,ROTX,ROTY,ROTz
```

```
DK,3, ,0, , , ,UZ,ROTY,ROTX
```

Appendix E: (continued)

```
!*****  
*****
```

```
increments=100  
loadsteps=70  
*DO,step,1,loadsteps,1  
theta=(step-1)*arclength/(R*increments)
```

```
!DDELE,12,ALL
```

```
!*****  
*****
```

```
newx=R*cos((PI/2-(arclength/R-theta)))  
newy=R*sin((PI/2-(arclength/R-theta)))
```

```
dispX=newx-xcoor  
dispY=newy-ycoor
```

```
DK,3,UX,dispX  
DK,3,UY,dispY  
DK,3,ROTZ,theta  
LSWRITE,step  
*ENDDO  
LSSOLVE,1,loadsteps
```

```
/STATUS,SOLU  
FINISH
```

```
!*****  
*****
```

```
!*****GET RESULTS  
*****
```

```
!*****  
*****
```

```
!*****Displacements nodes  
8,(9,10,11),4,(5,6,7),3,2,12,(13,14,15)*****  
/POST1  
*DIM,rotx8,TABLE,loadSteps  
*DIM,roty8,TABLE,loadSteps  
*DIM,rotz8,TABLE,loadSteps
```

Appendix E: (continued)

*DIM,disX8, TABLE,loadSteps
*DIM,disY8, TABLE,loadSteps
*DIM,disZ8, TABLE,loadSteps
*DIM,rotx9, TABLE,loadSteps
*DIM,roty9, TABLE,loadSteps
*DIM,rotz9, TABLE,loadSteps
*DIM,disX9, TABLE,loadSteps
*DIM,disY9, TABLE,loadSteps
*DIM,disZ9, TABLE,loadSteps
*DIM,rotx10, TABLE,loadSteps
*DIM,roty10, TABLE,loadSteps
*DIM,rotz10, TABLE,loadSteps
*DIM,disX10, TABLE,loadSteps
*DIM,disY10, TABLE,loadSteps
*DIM,disZ10, TABLE,loadSteps
*DIM,rotx11, TABLE,loadSteps
*DIM,roty11, TABLE,loadSteps
*DIM,rotz11, TABLE,loadSteps
*DIM,disX11, TABLE,loadSteps
*DIM,disY11, TABLE,loadSteps
*DIM,disZ11, TABLE,loadSteps
*DIM,rotx4, TABLE,loadSteps
*DIM,roty4, TABLE,loadSteps
*DIM,rotz4, TABLE,loadSteps
*DIM,disX4, TABLE,loadSteps
*DIM,disY4, TABLE,loadSteps
*DIM,disZ4, TABLE,loadSteps
*DIM,rotx5, TABLE,loadSteps
*DIM,roty5, TABLE,loadSteps
*DIM,rotz5, TABLE,loadSteps
*DIM,disX5, TABLE,loadSteps
*DIM,disY5, TABLE,loadSteps
*DIM,disZ5, TABLE,loadSteps
*DIM,rotx6, TABLE,loadSteps
*DIM,roty6, TABLE,loadSteps
*DIM,rotz6, TABLE,loadSteps
*DIM,disX6, TABLE,loadSteps
*DIM,disY6, TABLE,loadSteps
*DIM,disZ6, TABLE,loadSteps
*DIM,rotx7, TABLE,loadSteps
*DIM,roty7, TABLE,loadSteps
*DIM,rotz7, TABLE,loadSteps
*DIM,disX7, TABLE,loadSteps

Appendix E: (continued)

*DIM,disY7, TABLE,loadSteps
*DIM,disZ7, TABLE,loadSteps

!Point 3????

*DIM,rotz3, TABLE,loadSteps
*DIM,disX3, TABLE,loadSteps
*DIM,disY3, TABLE,loadSteps

*DIM,rotx12, TABLE,loadSteps
*DIM,roty12, TABLE,loadSteps
*DIM,rotz12, TABLE,loadSteps
*DIM,disX12, TABLE,loadSteps
*DIM,disY12, TABLE,loadSteps
*DIM,disZ12, TABLE,loadSteps
*DIM,rotx13, TABLE,loadSteps
*DIM,roty13, TABLE,loadSteps
*DIM,rotz13, TABLE,loadSteps
*DIM,disX13, TABLE,loadSteps
*DIM,disY13, TABLE,loadSteps
*DIM,disZ13, TABLE,loadSteps
*DIM,rotx14, TABLE,loadSteps
*DIM,roty14, TABLE,loadSteps
*DIM,rotz14, TABLE,loadSteps
*DIM,disX14, TABLE,loadSteps
*DIM,disY14, TABLE,loadSteps
*DIM,disZ14, TABLE,loadSteps
*DIM,rotx15, TABLE,loadSteps
*DIM,roty15, TABLE,loadSteps
*DIM,rotz15, TABLE,loadSteps
*DIM,disX15, TABLE,loadSteps
*DIM,disY15, TABLE,loadSteps
*DIM,disZ15, TABLE,loadSteps

!*****Reactions forces node
2*****

*DIM,momx2, TABLE,loadsteps
*DIM,momy2, TABLE,loadsteps
*DIM,momz2, TABLE,loadsteps
*DIM,fx2, TABLE,loadsteps

Appendix E: (continued)

*DIM,fy2, TABLE, loadsteps

*DIM,fz2, TABLE, loadsteps

!*****Reactions forces node
3*****

*DIM,momx3, TABLE, loadsteps

*DIM,momy3, TABLE, loadsteps

*DIM,momz3, TABLE, loadsteps

*DIM,fx3, TABLE, loadsteps

*DIM,fy3, TABLE, loadsteps

*DIM,fz3, TABLE, loadsteps

*Do,nn,1, loadSteps

set,nn

!*****Displacements node
8,(9,10,11),4,(5,6,7,)3,2,12,(13,14,15)*****

*GET,rotx,Node,nkp8,ROT,X

*SET,rotx8(nn),rotx

*GET,roty,Node,nkp8,ROT,Y

*SET,roty8(nn),roty

*GET,rotz,Node,nkp8,ROT,Z

*SET,rotz8(nn),rotz

*GET,disX,Node,nkp8,U,X

*SET,disX8(nn),disX

*GET,disY,Node,nkp8,U,Y

*SET,disY8(nn),disY

*GET,disz,Node,nkp8,U,Z

*SET,disZ8(nn),disz

*GET,rotx,Node,nkp9,ROT,X

*SET,rotx9(nn),rotx

*GET,roty,Node,nkp9,ROT,Y

*SET,roty9(nn),roty

*GET,rotz,Node,nkp9,ROT,Z

*SET,rotz9(nn),rotz

Appendix E: (continued)

*GET,disX,Node,nkp9,U,X
*SET,disX9(nn),disX
*GET,disY,Node,nkp9,U,Y
*SET,disY9(nn),disY
*GET,disz,Node,nkp9,U,Z
*SET,disZ9(nn),disz

*GET,rotx,Node,nkp10,ROT,X
*SET,rotx10(nn),rotx
*GET,roty,Node,nkp10,ROT,Y
*SET,roty10(nn),roty
*GET,rotz,Node,nkp10,ROT,Z
*SET,rotz10(nn),rotz

*GET,disX,Node,nkp10,U,X
*SET,disX10(nn),disX
*GET,disY,Node,nkp10,U,Y
*SET,disY10(nn),disY
*GET,disz,Node,nkp10,U,Z
*SET,disZ10(nn),disz

*GET,rotx,Node,nkp11,ROT,X
*SET,rotx11(nn),rotx
*GET,roty,Node,nkp11,ROT,Y
*SET,roty11(nn),roty
*GET,rotz,Node,nkp11,ROT,Z
*SET,rotz11(nn),rotz

*GET,disX,Node,nkp11,U,X
*SET,disX11(nn),disX
*GET,disY,Node,nkp11,U,Y
*SET,disY11(nn),disY
*GET,disz,Node,nkp11,U,Z
*SET,disZ11(nn),disz

*GET,rotx,Node,nkp4,ROT,X
*SET,rotx4(nn),rotx
*GET,roty,Node,nkp4,ROT,Y
*SET,roty4(nn),roty
*GET,rotz,Node,nkp4,ROT,Z
*SET,rotz4(nn),rotz

Appendix E: (continued)

*GET,disX,Node,nkp4,U,X
*SET,disX4(nn),disX
*GET,disY,Node,nkp4,U,Y
*SET,disY4(nn),disY
*GET,disz,Node,nkp4,U,Z
*SET,disZ4(nn),disz

*GET,rotx,Node,nkp5,ROT,X
*SET,rotx5(nn),rotx
*GET,roty,Node,nkp5,ROT,Y
*SET,roty5(nn),roty
*GET,rotz,Node,nkp5,ROT,Z
*SET,rotz5(nn),rotz

*GET,disX,Node,nkp5,U,X
*SET,disX5(nn),disX
*GET,disY,Node,nkp5,U,Y
*SET,disY5(nn),disY
*GET,disz,Node,nkp5,U,Z
*SET,disZ5(nn),disz

*GET,rotx,Node,nkp6,ROT,X
*SET,rotx6(nn),rotx
*GET,roty,Node,nkp6,ROT,Y
*SET,roty6(nn),roty
*GET,rotz,Node,nkp6,ROT,Z
*SET,rotz6(nn),rotz

*GET,disX,Node,nkp6,U,X
*SET,disX6(nn),disX
*GET,disY,Node,nkp6,U,Y
*SET,disY6(nn),disY
*GET,disz,Node,nkp6,U,Z
*SET,disZ6(nn),disz

*GET,rotx,Node,nkp7,ROT,X
*SET,rotx7(nn),rotx
*GET,roty,Node,nkp7,ROT,Y
*SET,roty7(nn),roty
*GET,rotz,Node,nkp7,ROT,Z
*SET,rotz7(nn),rotz

*GET,disX,Node,nkp7,U,X

Appendix E: (continued)

*SET,disX7(nn),disX
*GET,disY,Node,nkp7,U,Y
*SET,disY7(nn),disY
*GET,disz,Node,nkp7,U,Z
*SET,disZ7(nn),disz

!Point 3????

*GET,rotz,Node,nkp3,ROT,Z
*SET,rotz3(nn),rotz

*GET,disX,Node,nkp3,U,X
*SET,disX3(nn),disX
*GET,disY,Node,nkp3,U,Y
*SET,disY3(nn),disY

*GET,rotx,Node,nkp12,ROT,X
*SET,rotx12(nn),rotx
*GET,roty,Node,nkp12,ROT,Y
*SET,roty12(nn),roty
*GET,rotz,Node,nkp12,ROT,Z
*SET,rotz12(nn),rotz

*GET,disX,Node,nkp12,U,X
*SET,disX12(nn),disX
*GET,disY,Node,nkp12,U,Y
*SET,disY12(nn),disY
*GET,disz,Node,nkp12,U,Z
*SET,disZ12(nn),disz

*GET,rotx,Node,nkp13,ROT,X
*SET,rotx13(nn),rotx
*GET,roty,Node,nkp13,ROT,Y
*SET,roty13(nn),roty
*GET,rotz,Node,nkp13,ROT,Z
*SET,rotz13(nn),rotz

*GET,disX,Node,nkp13,U,X
*SET,disX13(nn),disX
*GET,disY,Node,nkp13,U,Y
*SET,disY13(nn),disY
*GET,disz,Node,nkp13,U,Z

Appendix E: (continued)

*SET,disZ13(nn),disz

*GET,rotx,Node,nkp14,ROT,X

*SET,rotx14(nn),rotx

*GET,roty,Node,nkp14,ROT,Y

*SET,roty14(nn),roty

*GET,rotz,Node,nkp14,ROT,Z

*SET,rotz14(nn),rotz

*GET,disX,Node,nkp14,U,X

*SET,disX14(nn),disX

*GET,disY,Node,nkp14,U,Y

*SET,disY14(nn),disY

*GET,disz,Node,nkp14,U,Z

*SET,disZ14(nn),disz

*GET,rotx,Node,nkp15,ROT,X

*SET,rotx15(nn),rotx

*GET,roty,Node,nkp15,ROT,Y

*SET,roty15(nn),roty

*GET,rotz,Node,nkp15,ROT,Z

*SET,rotz15(nn),rotz

*GET,disX,Node,nkp15,U,X

*SET,disX15(nn),disX

*GET,disY,Node,nkp15,U,Y

*SET,disY15(nn),disY

*GET,disz,Node,nkp15,U,Z

*SET,disZ15(nn),disz

!*****Reactions forces node

2*****

*GET,momx,Node,nkp2,RF,MX

*SET,momx2(nn),momx

*GET,fx,Node,nkp2,RF,FX

*SET,fx2(nn),fx

*GET,momy,Node,nkp2,RF,MY

*SET,momy2(nn),momy

*GET,fy,Node,nkp2,RF,FY

Appendix E: (continued)

```
*SET,fy2(nn),fy
*GET,momz,Node,nkp2,RF,MZ
*SET,momz2(nn),momz
*GET,fz,Node,nkp2,RF,FZ
*SET,fz2(nn),fz
```

```
!*****Reactions forces node
3*****
```

```
*GET,momx,Node,nkp3,RF,MX
*SET,momx3(nn),momx
*GET,fx,Node,nkp3,RF,FX
*SET,fx3(nn),fx
*GET,momy,Node,nkp3,RF,MY
*SET,momy3(nn),momy
*GET,fy,Node,nkp3,RF,FY
*SET,fy3(nn),fy
*GET,momz,Node,nkp3,RF,MZ
*SET,momz3(nn),momz
*GET,fz,Node,nkp3,RF,FZ
*SET,fz3(nn),fz
```

```
*ENDDO
```

```
/output,curvebeamarcsdevice%LAMBDA dg%,txt,,Append
```

```
!*****
*****
```

```
!*****FILE HEADER: BEAM
```

```
DATA*****
```

```
!*****
*****
```

```
*MSG,INFO,'t','w','R','E','arclength'
%-8C %-8C %-8C %-8C %-8C
```

```
*VWRITE,h2,b2,R,E2,arclength
%16.8G %-16.8G %-16.8G %-16.8G %-16.8G
```

```
!*****
*****
```

Appendix E: (continued)

```
!*****DISPLACEMENT DATA
SET*****
!*****
*****
```

```
*MSG,INFO,'rotX8','rotY8','rotZ8','disX8','disY8','disZ8'
%-8C %-8C %-8C %-8C %-8C %-8C
```

```
*VWRITE,rotx8(1),roty8(1),rotz8(1),disX8(1),disY8(1),disZ8(1)
% 16.8G %-16.8G %-16.8G %-16.8G %-16.8G %-16.8G
```

```
*MSG,INFO,'rotX9','rotY9','rotZ9','disX9','disY9','disZ9'
%-8C %-8C %-8C %-8C %-8C %-8C
```

```
*VWRITE,rotx9(1),roty9(1),rotz9(1),disX9(1),disY9(1),disZ9(1)
% 16.8G %-16.8G %-16.8G %-16.8G %-16.8G %-16.8G
```

```
*MSG,INFO,'rotX10','rotY10','rotZ10','disX10','disY10','disZ10'
%-8C %-8C %-8C %-8C %-8C %-8C
```

```
*VWRITE,rotx10(1),roty10(1),rotz10(1),disX10(1),disY10(1),disZ10(1)
% 16.8G %-16.8G %-16.8G %-16.8G %-16.8G %-16.8G
```

```
*MSG,INFO,'rotX11','rotY11','rotZ11','disX11','disY11','disZ11'
%-8C %-8C %-8C %-8C %-8C %-8C
```

```
*VWRITE,rotx11(1),roty11(1),rotz11(1),disX11(1),disY11(1),disZ11(1)
% 16.8G %-16.8G %-16.8G %-16.8G %-16.8G %-16.8G
```

```
*MSG,INFO,'rotX12','rotY12','rotZ12','disX12','disY12','disZ12'
%-8C %-8C %-8C %-8C %-8C %-8C
```

```
*VWRITE,rotx12(1),roty12(1),rotz12(1),disX12(1),disY12(1),disZ12(1)
% 16.8G %-16.8G %-16.8G %-16.8G %-16.8G %-16.8G
```

```
*MSG,INFO,'rotX13','rotY13','rotZ13','disX13','disY13','disZ13'
```

Appendix E: (continued)

%-8C %-8C %-8C %-8C %-8C %-8C

*VWRITE,rotx13(1),roty13(1),rotz13(1),disX13(1),disY13(1),disZ13(1)
% 16.8G %-16.8G %-16.8G %-16.8G %-16.8G %-16.8G

*MSG,INFO,'rotX14','rotY14','rotZ14','disX14','disY14','disZ14'
%-8C %-8C %-8C %-8C %-8C %-8C

*VWRITE,rotx14(1),roty14(1),rotz14(1),disX14(1),disY14(1),disZ14(1)
% 16.8G %-16.8G %-16.8G %-16.8G %-16.8G %-16.8G

*MSG,INFO,'rotX15','rotY15','rotZ15','disX15','disY15','disZ15'
%-8C %-8C %-8C %-8C %-8C %-8C

*VWRITE,rotx15(1),roty15(1),rotz15(1),disX15(1),disY15(1),disZ15(1)
% 16.8G %-16.8G %-16.8G %-16.8G %-16.8G %-16.8G

*MSG,INFO,'rotX4','rotY4','rotZ4','disX4','disY4','disZ4'
%-8C %-8C %-8C %-8C %-8C %-8C

*VWRITE,rotx4(1),roty4(1),rotz4(1),disX4(1),disY4(1),disZ4(1)
% 16.8G %-16.8G %-16.8G %-16.8G %-16.8G %-16.8G

*MSG,INFO,'rotX5','rotY5','rotZ5','disX5','disY5','disZ5'
%-8C %-8C %-8C %-8C %-8C %-8C

*VWRITE,rotx5(1),roty5(1),rotz5(1),disX5(1),disY5(1),disZ5(1)
% 16.8G %-16.8G %-16.8G %-16.8G %-16.8G %-16.8G

*MSG,INFO,'rotX6','rotY6','rotZ6','disX6','disY6','disZ6'
%-8C %-8C %-8C %-8C %-8C %-8C

*VWRITE,rotx6(1),roty6(1),rotz6(1),disX6(1),disY6(1),disZ6(1)
% 16.8G %-16.8G %-16.8G %-16.8G %-16.8G %-16.8G

*MSG,INFO,'rotX7','rotY7','rotZ7','disX7','disY7','disZ7'
%-8C %-8C %-8C %-8C %-8C %-8C

Appendix E: (continued)

*VWRITE,rotx7(1),roty7(1),rotz7(1),disX7(1),disY7(1),disZ7(1)
% 16.8G %-16.8G %-16.8G %-16.8G %-16.8G %-16.8G

!!POINTS 3 AND 2?????

*MSG,INFO,'rotZ3','disX3','disY3'
%-8C %-8C %-8C

*VWRITE,rotz3(1),disX3(1),disY3(1)
% 16.8G %-16.8G %-16.8G

```
!*****  
*****  
!*****REACTIONS AT NODE  
3*****  
!*****  
*****
```

*MSG,INFO,'momx3','momy3','momz3','fx3','fy3','fz3'
%-8C %-8C %-8C %-8C %-8C %-8C

*VWRITE,momx3(1),momy3(1),momz3(1),fx3(1),fy3(1),fz3(1)
% 16.8G %-16.8G %-16.8G %-16.8G %-16.8G %-16.8G

```
!*****  
*****  
!*****REACTIONS AT NODE  
2*****  
!*****  
*****
```

*MSG,INFO,'momx2','momy2','momz2','fx2','fy2','fz2'
%-8C %-8C %-8C %-8C %-8C %-8C

*VWRITE,momx2(1),momy2(1),momz2(1),fx2(1),fy2(1),fz2(1)
% 16.8G %-16.8G %-16.8G %-16.8G %-16.8G %-16.8G

Appendix E: (continued)

```
!*****  
*****  
!*****  
*****  
!*****  
*****
```

/output

FINISH

*ENDDO

*ENDDO

Appendix F: MATLAB Code for a Specific Horizontal Buckling End-Loaded

Curved Beam

```
clear all
filename = ['curvebeam3arcs_l105', '.txt'];
%string1 = 'C:\DOCUME~1\despinos\';
string1 = 'C:\Documents and Settings\Diego\Desktop\ThesisHome';
%fid1 = fopen([string1,filename]);
fid1 = fopen(filename);           % opens the file

%%%%%%%%%%%%%%%%%%%%%%%%%%%%%%%%%%%%%%%%%%%%%%%%%%%%%%%%%%%%%%%%%%%%%%%%%READS DATA FROM FILE%%%%%%%%%%%%%%%%%%%%%%%%%%%%%%%%%%%%%%%%%%%%%%%%%%%%%%%%%%%%%%%%%%%%%%%%%
%%%%%%%%%%%%%%%%%%%%%%%%%%%%%%%%%%%%%%%%%%%%%%%%%%%%%%%%%%%%%%%%%%%%%%%%%

ABT = fread(fid1);                % reads the file into
variable ABT
fclose(fid1);                    %closes the data file
GBT = native2unicode(ABT)';      %#ok<N2UNI> %changes

data from machine code to text
end1stheader = findstr('disZ8', GBT);    % finds end of first
header
begin2ndheader = findstr('rotX9', GBT);  % finds beginning of
second header
end2ndheader = findstr('disZ9', GBT);    % finds end of second

header
begin3ndheader = findstr('rotX10',GBT);
end3ndheader = findstr('disZ10', GBT);
begin4ndheader = findstr('rotX11', GBT);
end4ndheader = findstr('disZ11', GBT);
begin5ndheader = findstr('rotX12', GBT);
end5ndheader = findstr('disZ12', GBT);
begin6ndheader = findstr('rotX13', GBT);
end6ndheader = findstr('disZ13', GBT);
begin7ndheader = findstr('rotX14', GBT);
end7ndheader = findstr('disZ14', GBT);
begin8ndheader = findstr('rotX15', GBT);
end8ndheader = findstr('disZ15', GBT);
begin9ndheader = findstr('rotX4', GBT);
end9ndheader = findstr('disZ4', GBT);
begin10ndheader = findstr('rotX5', GBT);
end10ndheader = findstr('disZ5', GBT);
begin11ndheader = findstr('rotX6', GBT);
end11ndheader = findstr('disZ6', GBT);
begin12ndheader = findstr('rotX7', GBT);
end12ndheader = findstr('disZ7', GBT);
begin13ndheader = findstr('rotZ3', GBT);
end13ndheader = findstr('disY3', GBT);
```

Appendix F: (continued)

```
begin14ndheader = findstr('momx3', GBT);
end14ndheader   = findstr('fz3' , GBT);
begin15ndheader = findstr('momx2', GBT);
end15ndheader   = findstr('fz2' , GBT);
begin16ndheader = findstr('arclengt', GBT);
end16ndheader   = findstr('rotX8' , GBT);
```

```
%%%%%%%%%%%% turns the data into a numerical
matrix%%%%%%%%
```

```
DATA1 = str2num(GBT(end1stheader(end)+6:begin2ndheader(end)-1));
DATA2 = str2num(GBT(end2ndheader(end)+6:begin3ndheader(end)-1));
DATA3 = str2num(GBT(end3ndheader(end)+7:begin4ndheader(end)-1));
DATA4 = str2num(GBT(end4ndheader(end)+7:begin5ndheader(end)-1));
DATA5 = str2num(GBT(end5ndheader(end)+7:begin6ndheader(end)-1));
DATA6 = str2num(GBT(end6ndheader(end)+7:begin7ndheader(end)-1));
DATA7 = str2num(GBT(end7ndheader(end)+7:begin8ndheader(end)-1));
DATA8 = str2num(GBT(end8ndheader(end)+7:begin9ndheader(end)-1));
DATA9 = str2num(GBT(end9ndheader(end)+7:begin10ndheader(end)-1));
DATA10 = str2num(GBT(end10ndheader(end)+6:begin11ndheader(end)-1));
DATA11 = str2num(GBT(end11ndheader(end)+6:begin12ndheader(end)-1));
DATA12 = str2num(GBT(end12ndheader(end)+6:begin13ndheader(end)-1));
DATA13 = str2num(GBT(end13ndheader(end)+6:begin14ndheader(end)-1));
DATA14 = str2num(GBT(end14ndheader(end)+6:begin15ndheader(end)-1));
DATA15 = str2num(GBT(end15ndheader(end)+4:end));
DATA16 = str2num(GBT(begin16ndheader(end)+8:end16ndheader(end)-1));
```

```
%%%%%%%%%%%%FORCES, DISPLACEMENTS AND
MOMENTD%%%%%%%%
```

```
%%%%%%%%%%%%
%%%%%%%%%
```

```
rotx8 = DATA1(:,1);
roty8 = DATA1(:,1);
rotz8 = DATA1(:,3);
disx8 = DATA1(:,4);
disy8 = DATA1(:,5);
disz8 = DATA1(:,6);
```

```
rotx9 = DATA2(:,1);
roty9 = DATA2(:,1);
rotz9 = DATA2(:,3);
disx9 = DATA2(:,4);
disy9 = DATA2(:,5);
disz9 = DATA2(:,6);
```

```
rotx10 = DATA3(:,1);
roty10 = DATA3(:,1);
rotz10 = DATA3(:,3);
disx10 = DATA3(:,4);
disy10 = DATA3(:,5);
disz10 = DATA3(:,6);
```

Appendix F: (continued)

```
rotx11 = DATA4(:,1);  
roty11 = DATA4(:,1);  
rotz11 = DATA4(:,3);  
disx11 = DATA4(:,4);  
disy11 = DATA4(:,5);  
disz11 = DATA4(:,6);
```

```
rotx12 = DATA5(:,1);  
roty12 = DATA5(:,1);  
rotz12 = DATA5(:,3);  
disx12 = DATA5(:,4);  
disy12 = DATA5(:,5);  
disz12 = DATA5(:,6);
```

```
rotx13 = DATA6(:,1);  
roty13 = DATA6(:,1);  
rotz13 = DATA6(:,3);  
disx13 = DATA6(:,4);  
disy13 = DATA6(:,5);  
disz13 = DATA6(:,6);
```

```
rotx14 = DATA7(:,1);  
roty14 = DATA7(:,1);  
rotz14 = DATA7(:,3);  
disx14 = DATA7(:,4);  
disy14 = DATA7(:,5);  
disz14 = DATA7(:,6);
```

```
rotx15 = DATA8(:,1);  
roty15 = DATA8(:,1);  
rotz15 = DATA8(:,3);  
disx15 = DATA8(:,4);  
disy15 = DATA8(:,5);  
disz15 = DATA8(:,6);
```

```
rotx4 = DATA9(:,1);  
roty4 = DATA9(:,1);  
rotz4 = DATA9(:,3);  
disx4 = DATA9(:,4);  
disy4 = DATA9(:,5);  
disz4 = DATA9(:,6);
```

```
rotx5 = DATA10(:,1);  
roty5 = DATA10(:,1);  
rotz5 = DATA10(:,3);  
disx5 = DATA10(:,4);  
disy5 = DATA10(:,5);  
disz5 = DATA10(:,6);
```

Appendix F: (continued)

```
rotx6 = DATA11(:,1);
roty6 = DATA11(:,1);
rotz6 = DATA11(:,3);
disx6 = DATA11(:,4);
disy6 = DATA11(:,5);
disz6 = DATA11(:,6);

rotx7 = DATA12(:,1);
roty7 = DATA12(:,1);
rotz7 = DATA12(:,3);
disx7 = DATA12(:,4);
disy7 = DATA12(:,5);
disz7 = DATA12(:,6);

rotZ3 = DATA13(:,1);
disx3 = DATA13(:,2);
disy3 = DATA13(:,3);

momx3 = DATA14(:,1);
momy3 = DATA14(:,2);
momz3 = DATA14(:,3);
fx3   = DATA14(:,4);
fy3   = DATA14(:,5);
fz3   = DATA14(:,6);

momx2 = DATA15(:,1);
momy2 = DATA15(:,2);
momz2 = DATA15(:,3);
fx2   = DATA15(:,4);
fy2   = DATA15(:,5);
fz2   = DATA15(:,6);

arclength = DATA16(:,5);
R = DATA16(:,3);
h2 = DATA16(:,1);

x2 = zeros(70,1);
y2 = zeros(70,1);
z2 = zeros(70,1);

x3 = R*sin(arclength/R)+disx3;
y3 = R*cos(arclength/R)+disy3;
z3 = zeros(70,1);
R3 = sqrt(x3.^2+y3.^2);

x4 = R*sin(arclength/(2*R))+disx4;
y4 = R*cos(arclength/(2*R))+disy4;
z4 = 0+disz4;
R4 = sqrt(x4.^2+y4.^2+z4.^2);
```

Appendix F: (continued)

```
x8 = R*sin(arclength/(4*R))+disx8;
y8 = R*cos(arclength/(4*R))+disy8;
z8 = h2/2+disz8;
R8 = sqrt(x8.^2+y8.^2+z8.^2);

x12 = R*sin((arclength*3)/(4*R))+disx12;
y12 = R*cos((arclength*3)/(4*R))+disy12;
z12 = h2/2+disz12;
R12 = sqrt(x12.^2+y12.^2+z12.^2);

x13 = R*sin((arclength*3)/(4*R))+disx13;
y13 = R*cos((arclength*3)/(4*R))+disy13;
z13 = h2/2+1+disz13;

x14 = R*sin((arclength*3)/(4*R))*(R-1)/R+disx14;
y14 = R*cos((arclength*3)/(4*R))*(R-1)/R+disy14;
z14 = h2/2+disz14;

x15 = R*sin((arclength*3)/(4*R))+cos((arclength*3)/(4*R))+disx15;
y15 = R*cos((arclength*3)/(4*R))-sin((arclength*3)/(4*R))+disy15;
z15 = h2/2+disz15;

%%thetas with number are moving on plane phis with number are vertical
%%angle out plane
theta3=atan2(y3,x3);

theta8=atan2(y8,x8);
phi8=atan2(z8,sqrt(x8.^2+y8.^2));

theta12=atan2(y12,x12);
phi12=atan2(z12,sqrt(x12.^2+y12.^2));

theta4=atan2(y4,x4);
phi4=atan2(z4,sqrt(x4.^2+y4.^2));

Dx = [x15-x12 y15-y12 z15-z12]'; %Stick original parallel with Cx
Dz = [x13-x12 y13-y12 z13-z12]'; %Stick original parallel with Cz
%Dy= [x14-x12 y14-y12 z14-z12]'; %Stick original antiparallel with Cy
Dy = [x12-x14 y12-y14 z12-z14]'; %use opposite of stick direction

A = eye(3);%identity Matrix

for i = 1:length(rotz12)

R_B = [ cos( theta12(i)-(pi/2)) -sin(theta12(i)-(pi/2)) 0 ;
        sin(theta12(i)-(pi/2))  cos( theta12(i)-(pi/2)) 0 ;
        0 0 1];
%%%Beta out plane angle of point 12 = phi 12
BETA = atan2(z12,sqrt(x12.^2+y12.^2));
```

Appendix F: (continued)

```
R_C = [1 0 0;0 cos(BETA(i)) -sin(BETA(i)) ;0 sin(BETA(i))
cos(BETA(i))];

Bx(:,i) = R_C*A(:,1);
By(:,i) = R_C*A(:,2);
Bz(:,i) = R_C*A(:,3);

Cx(:,i) = R_B*Bx(:,i);
Cy(:,i) = R_B*By(:,i);
Cz(:,i) = R_B*Bz(:,i);

RR = [Dx(:,i) Dy(:,i) Dz(:,i)]*inv([Cx(:,i) Cy(:,i) Cz(:,i)]);

ROT(i, :, :) = RR;

v1(i)=RR(1,2)*RR(2,3)-(RR(2,2)-1)*RR(1,3);
v2(i)=RR(2,1)*RR(1,3)-(RR(1,1)-1)*RR(2,3);
v3(i)=(RR(1,1)-1)*(RR(2,2)-1)-(RR(1,2)*RR(2,3));

V=[v1(i) v2(i) v3(i)];
TRC=trace(RR);
CDROT MAG(i)=acos((TRC-1)/2);% Acording to plannar case CDROT MAG=theta0

end

%Shows Position of the axis of rotation with respec to point 12.
figure(1)
quiver3(x12,y12,z12,v1,v2,v3)
%plot(rotZ3,[x12,y12-100,z12,v1',v2',v3'])

%Shows Linear relationship between Theta0 and RotZ3
figure(2)
clf
hold on
plot(rotZ3,CDROT MAG)

%If Cy and Dy are matching then RR is a rotacion about the Cy
figure(3)
clf
hold on
%quiver3(x12,y12,z12,v1,v2,v3)
plot(rotZ3,Cy(1,:))
plot(rotZ3,Cy(2,:), 'g')
plot(rotZ3,Cy(3,:), 'r')
plot(rotZ3,Dy(1,:), 'c')
```

Appendix F: (continued)

```
plot(rotZ3,Dy(2,:), 'm')
plot(rotZ3,Dy(3,:), 'y')
plot(rotZ3,x12/R, 'c*')
plot(rotZ3,y12/R, 'm*')
plot(rotZ3,z12/R, 'y*')

% Cy -Radial, Cz - longitude, Cx - latitude, Psi-angle b/w C and D
Psiy= acos(dot(Cy,Dy)./(sqrt(dot(Cy,Cy)).*sqrt(dot(Dy,Dy))))*180/pi;
Psix=
real(acos(dot(Cx,Dx)./(sqrt(dot(Cx,Cx)).*sqrt(dot(Dx,Dx)))))*180/pi;
Psiz= acos(dot(Cz,Dz)./(sqrt(dot(Cz,Cz)).*sqrt(dot(Dz,Dz))))*180/pi;

rot_val(:,1) =
real(acos((dot(Cx,Dx)./(sqrt(dot(Cx,Cx)).*sqrt(dot(Dx,Dx)))))*180/pi;
rot_val(:,2) =
asin((dot(Cx,Dz)./(sqrt(dot(Cx,Cx)).*sqrt(dot(Dx,Dx)))))*180/pi;
rot_val(:,3) =
acos((dot(Cz,Dz)./(sqrt(dot(Cx,Cx)).*sqrt(dot(Dx,Dx)))))*180/pi;
rot_val(:,4) = -
asin((dot(Cz,Dx)./(sqrt(dot(Cx,Cx)).*sqrt(dot(Dx,Dx)))))*180/pi;

%Psi-angle b/w C and D-- b/w cy and dy must be zero because radial
direction no twist!
figure(4)
clf
hold on
plot(Psiy, 'r-*)
plot(Psix, 'b-*)
plot(Psiz, 'g-*)

% Checks radial displacement of keypoints
figure(5)
clf
hold on
plot(R4/R, 'r')
plot(R8/R, 'b')
plot(R12/R, 'm')
plot(R3/R, 'k')

%normal vector to Cy, and Dy, X,Z
CDY=cross(Cy,Dy)./([1;1;1]*(sin(Psiy*pi/180).*(sqrt(dot(Cy,Cy)).*sqrt(d
ot(Dy,Dy)))));
CDX=cross(Cx,Dx);
CDZ=cross(Cz,Dz);

%vectors from center of sphere to point 12 must match Cy and Dy
figure(6)
clf
hold on
quiver3(zeros(1,70),zeros(1,70),zeros(1,70),(x12)/R,(y12)/R,(z12)/R, 'b'
)
```

Appendix F: (continued)

```
quiver3(zeros(1,70),zeros(1,70),zeros(1,70),Cy(1,:),Cy(2,:),Cy(3,:), 'r'
)
quiver3(zeros(1,70),zeros(1,70),zeros(1,70),Dy(1,:),Dy(2,:),Dy(3,:), 'g'
)
view(3)
grid on

% checks quarter versus half symmetry for HKP leg, perfect half symmetry
not
% perfect quarter symmetry

error_theta8 =(90-theta8*180/pi)*4 - (90-theta3*180/pi);
error_theta4 =(90-theta4*180/pi)*2 - (90-theta3*180/pi);
error_theta12 =(90-theta12*180/pi)*4/3 - (90-theta3*180/pi);

figure(7)
clf
hold on
plot(error_theta12, 'r');
plot(error_theta4, 'b' );
plot(error_theta8, 'k');
% X axis will be captheta
ylabel('error (deg)')

error1=abs(theta4-theta8);
error2=abs(theta12-theta4);
error3=abs(theta8-pi/2);
error4=abs(theta3-theta12);

checcc=error1-error2
checcc2=error3-error4

%Shows errors between half symmetry and quarter symmetry thetas
figure(8)
clf
hold on
plot([1:70],[error1, error2, error3, error4 ])

figure(81)
clf
hold on
plot([1:70],[ error3, error4 ])

% checks quarter versus half symmetry for HKP leg
error_phi8 = phi8*180/pi*2 - phi4*180/pi;
error_phi12 = phi8*180/pi - phi12*180/pi;
error_phi4 =phi4*180/pi - phi12*180/pi*2;

error5=abs(phi4-phi8);
error6=abs(phi12-phi4);
```

Appendix F: (continued)

```
error7=phi8;
error8=phi12;

%Shows errors between half symmetry and quarter symmetry phis
figure(9)
clf
hold on
plot([1:70],[error5 error6 error7 error8]);

% checks quarter versus half symmetry for HKP leg
figure(10)
clf
hold on
plot(error_phi_a, 'r');
plot(error_phi_b, 'b');
plot(error_phi_c, 'k');
% X axis will be captheta
ylabel('error (deg)')

%Show the trajectory of points 12 4 and 8
figure(11)
clf
hold on
plot3(x8,y8,z8, 'r*',x4,y4,z4, 'b*',x12,y12,z12, 'g*');
grid on
axis equal
view(3)

scale=1/8;

%Shows that most of the force is apply in the x direction the y and z
%components of the force are close to 0
figure(12)
clf
hold on
plot(sqrt(fz3.^2+fx3.^2+fy3.^2))
hold on
plot(fx3, 'r')
plot(fy3, 'g')
plot(fz3, 'k')
grid on

%Shows the reaction forces vectors at the fix point 2
figure(13)
quiver3(x2,y2,z2,fx2,fy2,fz2)
view(3)
hold on

%Show that mom x and y are equal and apposite at points 2 and 3
figure(14)
clf
hold on
```

Appendix F: (continued)

```
quiver(x2,y2,momx3,momy3,0,'b.')
quiver(x2,y2,momx2,momy2,0,'r.')
view(3)
hold on
grid on

%Shows the moment vector behavior on point 3 as it moves
figure(15)
quiver3(x3,y3,z3,momx3,momy3,momz3,0)
view(3)
hold on

%beta and alpha are radians
% %beta = phi8;
% %alpha= pi/2-theta8
%
% %l = 100;
% %a= l+disx8;
% %b =disz8;
%PHI =arclength/R - alpha

%beta and alpha are radians

%CHANGED DEFFINITION OF ALPHA AND BETA!!!!
alpha= (theta4-theta3)/2;%%change of theta of curved beam center

%%% beta lower case half of out plane angle of center of beam = BETA
of
%%% point 12 because of symetry there are some error between half
symetry
%%% and quater symetry!!!
beta = phi4/2;

PHI = alpha(1)-alpha;%not vertical phi change in alpha!!!

%%%%%%%%%%%%%%%%%%%%%%%%%%%%%%%%%%%%%%%%%%%%%%%%%%%%%%%%%%%%%%%%%%%%%%%%
%%%%%%%%%%%%%%%%%%%%%%%%%%%%%%%%%%%%%%%%%%%%%%%%%%%%%%%%%%%%%%%%%%%%%%%%
%%%%%%%%%%%%%%%%%%%%%%%%%%%%%%%%%%%%%%%%%%%%%%%%%%%%%%%%%%%%%%%%%%%%%%%%
%%%%%%%%%%%%%%%%%%%%%%%%%%%%%%%%%%%%%%%%%%%%%%%%%%%%%%%%%%%%%%%%%%%%%%%%

gamma = 4*R/arclength*atan2(1-cos(beta).*cos(PHI),cos(beta).*sin(PHI));
%planar gamma = -(a.^2 - 2*a*l+l^2+b.^2)./(2*a*l-2*l^2);

theta = atan2(tan(beta),sin((gamma*arclength/(4*R))-PHI));
%atan2(b,a-(1-gamma)*l);
```

Appendix F: (continued)

```
lambda=arclength/(R*4);

% Phi=atan2(1-
cos(theta),cot(gamma*lambda)+(cos(theta).*tan(gamma*lambda)))
% Beta=asin(sin(gamma*lambda).*sin(theta))
% Alpha=lambda-Phi

% figure(12)
% clf
% hold on
% plot(PHI,alpha,'b*',Phi,alpha,'b')
% plot(beta,alpha,'g*',Beta,alpha,'g')
% plot(alpha,alpha,'r*',Alpha,alpha,'r')

% rotation of point 3---to find M12
r=[x12-x3 y12-y3 z12-z3];
M12 = cross(r,[fx3 fy3 fz3]);
mom12=[momx3 momy3 momz3]-M12;

momx12=mom12(:,1);
momy12=mom12(:,2);
momz12=mom12(:,3);

Magmom12=sqrt(momx12.^2+momy12.^2+momz12.^2);

MAXMagmom12=max(Magmom12);

M12=Magmom12/MAXMagmom12;

%Compares the behavior of the reaction moment vectors at point 12 and 3
as
%the mechanism moves
figure(16)
clf
hold on
quiver3(x12,y12,z12,momx12,momy12,momz12)
quiver3(x3,y3,z3,momx3,momy3,momz3, 'r')
view(3)

M_Mag = sqrt(momx3.^2+momy3.^2+momz3.^2);
M_Mag_max= max(M_Mag);

% M_theta = atan2(momy3,momx3)
% M_phi = atan2(momz3,sqrt(momy3.^2+momx3.^2))

%Shows most of the reaction force at 3 happens on the x direction,
%most of the reaction moment at 3 ias about the y
```

Appendix F: (continued)

```
% and the moments at 12 are close to zero
%momz12 represent twist about z axis must be close to zero
```

```
figure(17)
clf
hold on
plot(sqrt(fz3.^2+fx3.^2+fy3.^2))
plot(sqrt(momx12.^2+momy12.^2+momz12.^2), '--')
plot(sqrt(momx3.^2+momy3.^2+momz3.^2), '*')
hold on
plot(fx3, 'r')
plot(fy3, 'g')
plot(fz3, 'k')
plot(momx12, 'r--')
plot(momy12, 'g--')
plot(momz12, 'k--')
plot(momx3, 'r*')
plot(momy3, 'g*')
plot(momz3, 'k*')
```

```
theta(1) = 0;
theta0 = CDROT_MAG;
```

```
%Compares behavior of point 3 and 12
figure(18)
clf
hold on
plot3(x12,y12,z12, '*', x3,y3,0*x3, '*')
view(3)
```

```
theta(1) =0;
theta0 = CDROT_MAG;
```

```
E = 169000;
```

```
b2 =arclength/20;
```

```
I = (b2*h2^3)/12;
```

```
M = (M_Mag*arclength^2)/(E*I);% Nondimensionalization
M_max = max(M);
```

```
%Scales moment between 0 and 1
M = M/M_max;
R1 = normrnd(0.1,.1,[size(M)]);
```

Appendix F: (continued)

```

X = [ones(size(M(2:end))) 1./M(2:end) 1./M(2:end).^2 1.*M(2:end)
1.*M(2:end).^2];
Y = gamma(2:end);

B = inv(X'*X)*X'*Y;

%Gamma =
1./(B(1)+B(2)./M+B(3)./M.^2+B(4)./M.^3+B(5)./M.^4+B(6)./M.^5);
Gamma = B(1)+B(2)./M+B(3)./M.^2 +B(4).*M +B(5).*M.^2;

Csgamma=POLYFIT(M*M_max, gamma, 0);

%Theta = atan2(b,a-(1-Gamma)*1);
Theta = atan2(tan(beta),sin((Gamma*arclength/(4*R))-PHI));

%ThetaC= atan2(b,a-(1-.75)*1);
ThetaC = atan2(tan(beta),sin(( Csgamma*arclength/(4*R))-PHI));

%gives aproximation constant Ctheta (theta0=(Ctheta)*CAPtheta

Cstheta=POLYFIT(Theta(2:end), (theta0(2:end)./Theta(2:end))', 0);

figure(19)
clf
hold on

plot(Theta(2:end)*180/pi, theta0(2:end)./Theta(2:end)', 'b', Theta(2:end)*
180/pi, Cstheta.*ones(69,1)', 'r')

%OJO FOR THIS ARC 105%%%%%%%%%%%%%%%%%%%%%%%%%%%%%%%%%%%%%%%%%%%%%%%%%%%%%%%%%%%%%%%%%%%%%%%%
%Ctheta=1.3427%%%%%%%%%%%%%%%%%%%%%%%%%%%%%%%%%%%%%%%%%%%%%%%%%%%%%%%%%%%%%%%%%%%%%%%%

%%Shows the aproximation of theta0=Ctheta*Theta%%%%%%%%
figure(20)
clf
hold on
plot(Theta(2:end)*180/pi, theta0(2:end)*180/pi, 'r')
plot(Theta(2:end)*180/pi, Theta(2:end)*Cstheta*180/pi, 'b')

epsilon = gamma(2:end)-Gamma(2:end);
SST = sum((gamma(2:end)-mean(gamma(2:end))).^2);
SSE = sum(epsilon.^2);

```

Appendix F: (continued)

```
s_squared = SSE/(length(gamma(2:end))-length(B));
s = sqrt(s_squared);
rsqrd = 1- SSE/SST;

Var_b = inv(X'*X)*s_squared;
X_ortho = X'*X;
[V,D] = eig(X_ortho);

X2(:,1) = X*V(:,1);
X2(:,2) = X*V(:,2);
X2(:,3) = X*V(:,3);
X2(:,4) = X*V(:,4);
X2(:,5) = X*V(:,5);

C = inv(X2'*X2)*X2'*Y;
%Gamma2 =
C(1)*X2(:,1)+C(2)*X2(:,2)+C(3)*X2(:,3)+C(4)*X2(:,4)+C(5)*X2(:,5);
Gamma2 =
C(1)*X2(:,1)+C(2)*X2(:,2)+C(3)*X2(:,3)+C(4)*X2(:,4)+C(5)*X2(:,5);

%Theta2 = atan2(b(2:end),a(2:end)-(1-Gamma2)*1);

epsilon2 = gamma(2:end)-Gamma2;
SSE2 = sum(epsilon2.^2);
s_squared2 = SSE2/(length(gamma(2:end))-length(C));
s2 = sqrt(s_squared2);
rsqrd2 = 1- SSE2/SST

Var_c = inv(X2'*X2)*s_squared2;

B1_prime =
C(1)*V(1,1)+C(2)*V(1,2)+C(3)*V(1,3)+C(4)*V(1,4)+C(5)*V(1,5); % compare
with B(1)
B2_prime =
C(1)*V(2,1)+C(2)*V(2,2)+C(3)*V(2,3)+C(4)*V(2,4)+C(5)*V(2,5); % compare
with B(2)
B3_prime =
C(1)*V(3,1)+C(2)*V(3,2)+C(3)*V(3,3)+C(4)*V(3,4)+C(5)*V(3,5); % compare
with B(3)
B4_prime =
C(1)*V(4,1)+C(2)*V(4,2)+C(3)*V(4,3)+C(4)*V(4,4)+C(5)*V(4,5); % compare
with B(4)
B5_prime =
C(1)*V(5,1)+C(2)*V(5,2)+C(3)*V(5,3)+C(4)*V(5,4)+C(5)*V(5,5); % compare
with B(5)

B_var(1) =
abs(sqrt(Var_c(1,1))*V(1,1)+sqrt(Var_c(2,2))*V(1,2)+sqrt(Var_c(3,3))*V(
1,3)+sqrt(Var_c(4,4))*V(1,4)+sqrt(Var_c(5,5))*V(1,5));
```

Appendix F: (continued)

```

B_var(2) =
abs(sqrt(Var_c(1,1))*V(2,1)+sqrt(Var_c(2,2))*V(2,2)+sqrt(Var_c(3,3))*V(
2,3)+sqrt(Var_c(4,4))*V(2,4)+sqrt(Var_c(5,5))*V(2,5));
    B_var(3) =
abs(sqrt(Var_c(1,1))*V(3,1)+sqrt(Var_c(2,2))*V(3,2)+sqrt(Var_c(3,3))*V(
3,3)+sqrt(Var_c(4,4))*V(3,4)+sqrt(Var_c(5,5))*V(3,5));
    B_var(4) =
abs(sqrt(Var_c(1,1))*V(4,1)+sqrt(Var_c(2,2))*V(4,2)+sqrt(Var_c(3,3))*V(
4,3)+sqrt(Var_c(4,4))*V(4,4)+sqrt(Var_c(5,5))*V(4,5));
    B_var(5) =
abs(sqrt(Var_c(1,1))*V(5,1)+sqrt(Var_c(2,2))*V(5,2)+sqrt(Var_c(3,3))*V(
5,3)+sqrt(Var_c(4,4))*V(5,4)+sqrt(Var_c(5,5))*V(5,5));

    B_std = sqrt(B_var);
    % 95 % 2 sided confidence interval ie mean + or - interval

    t_statistic = tinv(.975,length(Y)-length(B));
    CI = t_statistic*B_std
    Gamma_minus = B(1)-CI(1)+(B(2)-CI(2))./M+(B(3)-CI(3))./M.^2 +(B(4)-
CI(4)).*M +(B(5)-CI(5)).*M.^2;
    Gamma_plus = B(1)+CI(1)+(B(2)+CI(2))./M+(B(3)+CI(3))./M.^2
+(B(4)+CI(4)).*M +(B(5)+CI(5)).*M.^2;

%%%%%%%%%%%%%%%%%%%%%%%%%%%%%%%%%%%%%%%%%%%%%%%%%%%%%%%%%%%%%%%%%%%%%%%%
%%%%%%%%%%%%%%%%%%%%%%%%%%%%%%%%%%%%%%%%%%%%%%%%%%%%%%%%%%%%%%%%%%%%%%%%

%%%%%%%%%%%%%%%%%%%%%%%%%%%%%%%%%%%%%%%%%%%%%%%%%%%%%%%%%%%%%%%%%%%%%%%%
%%%%%%%%%%%%%%%%%%%%%%%%%%%%%%%%%%%%%%%%%%%%%%%%%%%%%%%%%%%%%%%%%%%%%%%%
figure(41)
clf
plot(Gamma(2:end),M(2:end)*M_max,'b',
Gamma_minus(2:end),M(2:end)*M_max,'r',
Gamma_plus(2:end),M(2:end)*M_max,'g');

    %%%%Calculations Using model
lambda=arclength/(R*4);
Phi=atan2(1-
cos(Theta),cot(Gamma*lambda)+(cos(Theta).*tan(Gamma*lambda)));
Beta=asin(sin(Gamma*lambda).*sin(Theta));
Alpha=lambda-Phi;

%Shows that the equality of Phi, Beta and Alpha when found using gamma
vs.
%the ones obtain using the data guiven by ansys
figure(21)
clf
hold on
plot(PHI(2:end),alpha(2:end),'b*',Phi(2:end),alpha(2:end),'k')
plot(beta(2:end),alpha(2:end),'g*',Beta(2:end),alpha(2:end),'k')
plot(alpha(2:end),alpha(2:end),'r*',Alpha(2:end),alpha(2:end),'k')

```

Appendix F: (continued)

```
%Show range of gammas
figure(22)
plot([Gamma(2:end) Gamma_minus(2:end) Gamma_plus(2:end)])

%%%%%%%%%%%%%%%%%%%%%%%%%%%%%%%%%%%%%%%%%%%%%%%%%%%%%%%%%%%%%%%%%%%%%%%%
%%%%%%%%%%%%%FIGURE 1 alpha vs beta
%%%%%%%%%%%%%%%%%%%%%%%%%%%%%%%%%%%%%%%%%%%%%%%%%%%%%%%%%%%%%%%%%%%%%%%%

%%%%%%%%%%%%%%%%%%%%%%%%%%%%%%%%%%%%%%%%%%%%%%%%%%%%%%%%%%%%%%%%%%%%%%%%

figure(23);
clf
plot(alpha,beta, 'b*', Alpha(2:end),Beta(2:end), 'r', (lambda-atan2(1-
cos(ThetaC),cot( Csgamma*lambda)+(cos(ThetaC).*tan(
Csgamma*lambda))))),asin(sin( Csgamma*lambda).*sin(ThetaC)), 'g-');

%%%%%%%%%%%%%%%%%%%%%%%%%%%%%%%%%%%%%%%%%%%%%%%%%%%%%%%%%%%%%%%%%%%%%%%%
%%%%%%%%%%%%%FIGURE 2 M vs theta
%%%%%%%%%%%%%%%%%%%%%%%%%%%%%%%%%%%%%%%%%%%%%%%%%%%%%%%%%%%%%%%%%%%%%%%%
%%%%%%%%%%%%%%%%%%%%%%%%%%%%%%%%%%%%%%%%%%%%%%%%%%%%%%%%%%%%%%%%%%%%%%%%

figure(24);
clf
plot(M,theta*180/pi, 'b*',M(2:end),Theta(2:end)*180/pi, 'R',M(2:end),Thet
aC(2:end)*180/pi, 'G-');

%%%%%%%%%%%%%%%%%%%%%%%%%%%%%%%%%%%%%%%%%%%%%%%%%%%%%%%%%%%%%%%%%%%%%%%%
%%%%%%%%%%%%%FIGURE 3 M vs gamma
%%%%%%%%%%%%%%%%%%%%%%%%%%%%%%%%%%%%%%%%%%%%%%%%%%%%%%%%%%%%%%%%%%%%%%%%
%%%%%%%%%%%%%%%%%%%%%%%%%%%%%%%%%%%%%%%%%%%%%%%%%%%%%%%%%%%%%%%%%%%%%%%%

figure(25);
clf
plot(gamma,M*M_max, 'b*',Gamma(2:end),M(2:end)*M_max, 'R',
Csgamma,M*M_max, 'G*');
% G3c = ylabel('\gamma');
% set(G3c,'Rotation',0,'fontsize',12)
% mytexstr = '$\frac{M l^2}{EI}$';
% Gc=
xlabel(mytexstr,'interpreter','latex','fontsize',12,'units','norm');
G4c = legend('Data','\gamma*','\gamma');

% hold on

%%%%%%%%%%%%%%%%%%%%%%%%%%%%%%%%%%%%%%%%%%%%%%%%%%%%%%%%%%%%%%%%%%%%%%%%
%%%%%%%%%%%%%ERROR %%%%%%%%%%%%%%%%%%%%%%%%%%%%%%%%%%%%%%%%%%%%%%%%%%%%%%%%%%%%%%%%%%%%%%%%%
%%%%%%%%%%%%%%%%%%%%%%%%%%%%%%%%%%%%%%%%%%%%%%%%%%%%%%%%%%%%%%%%%%%%%%%%

erroro = (alpha - Alpha).^2 + (beta - Beta).^2;
```

Appendix F: (continued)

```
%erroro = ( a/l - ((1-Gamma)+Gamma.*cos(Theta)).^2 +
(b/l - Gamma.*sin(Theta)).^2;
%disp_mag = (((1-Gamma)+Gamma.*cos(Theta))-
a(round(end/3))/l).^2+(Gamma.*sin(Theta)-b(round(end/3))/l).^2).^5;

total_erroro =
trapz(M(2:end),erroro(2:end));%+trapz(Gamma(2:end),erroro(2:end));
%total_erroro = sqrt(max(erroro(2:end)./diff(M)))

%%Define tangent force get rid of radial component does not do work
n_r3 = [x3 y3]./(sqrt(x3.^2+y3.^2)*[1 1]);
F3 = [fx3 fy3];
F_r3 = (dot(F3',n_r3)')*[1 1]).*n_r3;
Ft_3=F3-F_r3;

q=Ft_3(1:70)';
p=Ft_3(71:140)';

Ftan=sqrt(q.^2+p.^2);

%displacement vector! and its 1st derivative
Z3=[R*cos(pi/2-4*lambda+(4*PHI)) R*sin(pi/2-4*lambda+(4*PHI))];
dZ3=[-R*sin(pi/2-4*lambda+(4*PHI)) R*cos(pi/2-4*lambda+(4*PHI))];
Y1=dZ3(1:70)';
X1=dZ3(71:140)';
dZ4=sqrt(Y1.^2+X1.^2);

%check if displacement vector is correct
figure(26)
clf
hold on
plot(x3,y3,'r',Z3(:,1),Z3(:,2),'b');

d_Ctheta_Phi=(sec(Phi)).^2./((sin(Theta)./((cot(Gamma*lambda)+cos(Theta)
).*tan(Gamma*lambda)))+(1-
cos(Theta)).*(sin(Theta).*tan(Gamma*lambda)))/((cot(Gamma*lambda)+cos(
Theta).*tan(Gamma*lambda)).^2));
d_Phi_Ctheta=(sin(Theta)./((sec(Phi)).^2.*(cot(Gamma*lambda)+cos(Theta)
).*tan(Gamma*lambda)))+(1-
cos(Theta)).*(sin(Theta).*tan(Gamma*lambda)))/((sec(Phi)).^2.*(cot(Gam
ma*lambda)+cos(Theta).*tan(Gamma*lambda)).^2));

%d_Phi_Ctheta2=(1/(sec(Phi)).^2)'.*((sin(Theta)./((cot(Gamma*lambda)+cos
(Theta).*tan(Gamma*lambda)))+(1-
cos(Theta)).*(sin(Theta).*tan(Gamma*lambda)))/((cot(Gamma*lambda)+cos(
Theta).*tan(Gamma*lambda)).^2));

%Checking
```

Appendix F: (continued)

```
diff_T_P=diff(Theta(2:end))./diff(Phi(2:end));
%diff_T_P=(Theta(4:end)-Theta(2:end-2))./(Phi(4:end)-Phi(2:end-2))
diff_P_T=diff(Phi(2:end))./diff(Theta(2:end));
%diff_P_T=(Phi(4:end)-Phi(2:end-2))./(Theta(4:end)-Theta(2:end-2))

check1=diff_T_P-d_Ctheta_Phi(3:end);
check2=diff_P_T-d_Phi_Ctheta(3:end);
check3=(ones(69,1)./d_Ctheta_Phi(2:end))-d_Phi_Ctheta(2:end);
check4=(180/pi*acos(dot(dZ3',F_r3')./(dot(dZ3',dZ3').*dot(F_r3',F_r3'))
.^5))';

%%Check deffifferentiation of cap theta with respect to phi
figure(27)
clf
hold on
plot(diff_T_P,'r')
plot(d_Ctheta_Phi(3:end),'b')

%%Check deffifferentiation of phi with respect to cap theta
figure(28)
clf
hold on
plot(diff_P_T,'r')
plot(d_Phi_Ctheta(3:end),'b')

%WORK done by Ft
dWf=dot(Ft_3',dZ3');
dWf2=dot(F3',dZ3');
check5=(dWf-dWf2)';

%CALCULATE K

T=((dWf)'+momz3).*d_Phi_Ctheta);%% captheta in embedded in the
Torque!!!
T1=((dWf)').*d_Phi_Ctheta);
T2=(momz3).*d_Phi_Ctheta);
check6=T1+T2-T;

%Cap theta vs components of T
figure(29)
clf
hold on
plot(Theta(2:end)*180/pi,T1(2:end),'r')
plot(Theta(2:end)*180/pi,T2(2:end),'b')
plot(Theta(2:end)*180/pi,momz3(2:end),'g')

%CALCULATE CONSTA Ktheta, KF, KM NONDIMENSIONALIZATION
```

Appendix F: (continued)

```
Ttheta=(T*R*4*lambda)/(E*I);
TF=(T1*R*4*lambda)/(E*I);
TM=(T2*R*4*lambda)/(E*I);
check7=TF+TM-Ttheta;

[CsKTHE,s]=POLYFIT(Theta(2:end),Ttheta(2:end),2);
[CsKf,s1]=POLYFIT(Theta(2:end),TF(2:end),1);
[CsKm,s2]=POLYFIT(Theta(2:end),TM(2:end),2);

KTHEf = polyval(CsKTHE,Theta);
Kff = polyval(CsKf,Theta);
Kmf = polyval(CsKm,Theta);

%shows tah he function of Ttheta, Tm and Tf fits the data.
figure(30)
clf
hold on
plot(Theta(2:end)*180/pi ,Ttheta(2:end), 'b')
plot(Theta(2:end)*180/pi ,TF(2:end), 'r')
plot(Theta(2:end)*180/pi ,TM(2:end), 'g')
plot(Theta(2:end)*180/pi ,KTHEf(2:end), 'b*')
plot(Theta(2:end)*180/pi ,Kff(2:end), 'r*')
plot(Theta(2:end)*180/pi ,Kmf(2:end), 'g*')

%%shows the behavior of K and Ktheta, KF, KM
figure(31)
clf
hold on
plot(T(2:end), 'r')
plot(T1(2:end), 'c')
plot(T2(2:end), 'k')
plot(Ttheta(2:end), 'b')
plot(TF(2:end), 'm')
plot(TM(2:end), 'g')

%shows behavior of T and components wrt theta
figure(32)
clf
hold on
plot(Theta(2:end) ,Ttheta(2:end), 'b')
plot(Theta(2:end) ,TF(2:end), 'r')
plot(Theta(2:end) ,TM(2:end), 'g')
plot(Theta(2:end) ,dWf(2:end), 'k')
plot(Theta(2:end) ,momz3(2:end), 'c')

%%Finds componets fuctions of Ttheta
Km=Kmf*E*I./(R*4*lambda)
Kf=Kff*E*I./(R^2*4*lambda)
```

Appendix F: (continued)

```
%Find moment and force using componet function Km and Kf
Mom=(Km.*d_Ctheta_Phi);
Foc=(Kf.*d_Ctheta_Phi);

%%%plots nondimensionalized K componetss
figure(33)
clf
hold on
plot(TF(2:end),'r')
plot(TM(2:end),'b')

%%%plots function components of K theta
figure(34)
clf
hold on
plot(Kf(2:end),'r')
plot(Km(2:end),'b')

%plot moment from the data and the moment found using the model
figure(35)
clf
hold on
plot(Theta(2:end)*180/pi,Mom(2:end),'r')
plot(Theta(2:end)*180/pi,momz3(2:end),'b')
%plot(T2.*d_Ctheta_Phi,'k')%%%ASK Dr. Lusk

%plot force from the data and the force found using the model
figure(36)
clf
hold on
plot(Theta(2:end)*180/pi,Foc(2:end),'r')
plot(Theta(2:end)*180/pi,Ftan(2:end),'b')
%plot(T1/R.*d_Ctheta_Phi,'k')

R
h2
E
b2
I
lambda
Cstheta
Csgamma
total_erroro
CsKTHE
CsKf
CsKm

%%%TEST%%%%%%%%%
```

Appendix F: (continued)

```
Ctheta2= acos((-
tan(PHI).*cot(Gamma*lambda)+1)./(1+tan(PHI).*tan(Gamma*lambda)));%%%usi
ng model or data?
d_Ctheta_PHI=(sec(PHI)).^2./((sin(Ctheta2)./((cot(Gamma*lambda)+cos(Cth
eta2).*tan(Gamma*lambda)))+(1-
cos(Ctheta2)).*(sin(Ctheta2).*tan(Gamma*lambda)))/((cot(Gamma*lambda)+
cos(Ctheta2).*tan(Gamma*lambda)).^2)));
d_PHI_Ctheta2=(sin(Ctheta2)./((sec(PHI)).^2.*(cot(Gamma*lambda)+cos(Cth
eta2).*tan(Gamma*lambda)))+(1-
cos(Ctheta2)).*(sin(Ctheta2).*tan(Gamma*lambda)))/((sec(PHI)).^2.*(cot
(Gamma*lambda)+cos(Ctheta2).*tan(Gamma*lambda)).^2)));

CsKf2=9.1455.*Ctheta2-1.4521.*ones(70,1);
CsKm2=-2.4524.*Ctheta2.^2+3.5246.*Ctheta2-0.0498.*ones(70,1);
CsKTHE2=-0.3244.*Ctheta2.^2+8.9923*Ctheta2-0.1640.*ones(70,1);

errorf=(CsKf2-Kff)./Kff
errorm=(CsKm2-Kmf)./Kmf
errorKT=(CsKTHE2-KTHEf)./KTHEf

Kf2=CsKf2.*E*I./(R^2*4*lambda);
Km2=CsKm2.*E*I./(R*4*lambda);

errorf2=(Kf2-Kf)./Kf
errorm2=(Km2-Km)./Km

Foc2=Kf2.*d_Ctheta_PHI;
Mom2=Km2.*d_Ctheta_PHI;

Theterr=(Ctheta2-Theta)./Theta
Ferr=(Foc2-Foc)./Foc
Merr=(Mom2-Mom)./Mom

figure(37)
clf
hold on
plot(Foc(2:end),'r')
plot(Foc2(2:end),'b')%%%need a constant?

figure(38)
clf
hold on
plot(Mom(2:end),'r')
plot(Mom2(2:end),'b')

figure(39)
clf
hold on
plot(Ctheta2,Mom2,'r')
plot(Ctheta2,Foc2,'b')
```

Appendix F: (continued)

```
figure(40)
clf
hold on
plot(Theta(2:end),Mom(2:end),'r')
plot(Theta(2:end),Foc(2:end),'b')
plot(Theta(2:end),Ftan(2:end),'g')
plot(Theta(2:end),momz3(2:end),'k')
plot(Ctheta2(2:end),Mom2(2:end),'r*')
plot(Ctheta2(2:end),Foc2(2:end),'b*')

Zout=[R*cos(pi/2-2*lambda+(2*PHI)) R*sin(pi/2-2*lambda+(2*PHI))
R*sin(2*beta)]%%%use full mode devided by 2 ask!!
dZout=[-R*sin(pi/2-2*lambda+(2*PHI)) R*cos(pi/2-2*lambda+(2*PHI))
R*cos(2*beta)];
%%
%%%THE END

Csgamma
B
CI
rsqrd
total_erroro
Cstheta
CsKTHE
CsKf
CsKm
```

Appendix G: Tables of Summary of Results for a Specific Horizontal Buckling End-Loaded Curved Beam

Table G.1. Summary of results of curved beam with $\lambda = 15^\circ$

Constant γ	0.7781
b_{-2}	0.8105 ± 0.05847
b_{-1}	-0.0077 ± 0.02985
b_0	-0.0005 ± 0.00846
b_1	-0.0046 ± 0.06974
b_2	0.0001 ± 0.04877
Coefficient of determination R^2	99.96%
Total error	2.4977e-10%
C_g	1.2386
$T_\theta (\theta^*)$	$0.8410\theta^2 + 7.2766\theta - 0.0739$
$T_f (\theta^*)$	$8.7428\theta - 0.6312$
$T_m (\theta^*)$	$-0.0492\theta^2 + 0.0746\theta - 0.0048$

Appendix G: (continued)

Table G.2. Summary of results of curved beam with $\lambda = 30^\circ$

Constant γ	0.7812
b_{-2}	0.7441 ± 0.1764
b_{-1}	0.0235 ± 0.0979
b_0	0.0235 ± 0.0312
b_1	0.0634 ± 0.1999
b_2	-0.0278 ± 0.1344
Coefficient of determination R^2	99.92%
Total error	1.4426e-8%
C_g	1.2451
$T_\theta (\theta^*)$	$0.7486\theta^2 + 7.4219\theta - 0.0909$
$T_f (\theta^*)$	$8.7603\theta - 0.6694$
$T_m (\theta^*)$	$-0.1973\theta^2 + 0.2982\theta - 0.0183$

Table G.3. Summary of results of curved beam with $\lambda = 45^\circ$

Constant γ	0.7864
b_{-2}	0.4210 ± 0.3802
b_{-1}	0.1709 ± 0.2267
b_0	-0.0283 ± 0.0794
b_1	0.3792 ± 0.4098
b_2	-0.1446 ± 0.2647
Coefficient of determination R^2	99.54%
Total error	1.4710e-7%
C_g	1.2559
$T_\theta (\theta^*)$	$0.6064\theta^2 + 7.6418\theta - 0.1110$
$T_f (\theta^*)$	$8.7916\theta - 0.7361$
$T_m (\theta^*)$	$-0.4459\theta^2 + 0.6701\theta - 0.0378$

Appendix G: (continued)

Table G.4. Summary of results of curved beam with $\lambda = 60^\circ$

Constant γ	0.7938
b_{-2}	-0.8429 ± 0.7203
b_{-1}	0.7667 ± 0.4555
b_0	-0.1280 ± 0.1718
b_1	1.5518 ± 0.7422
b_2	-0.5493 ± 0.4614
Coefficient of determination R^2	98.89%
Total error	7.3009e-7%
C_g	1.2711
$T_\theta (\theta^*)$	$0.4304\theta^2 + 7.9087\theta - 0.1287$
$T_f (\theta^*)$	$8.8415\theta - 0.8413$
$T_m (\theta^*)$	$-0.7980\theta^2 + 1.1904\theta - 0.0600$

Table G.5. Summary of results of curved beam with $\lambda = 75^\circ$

Constant γ	0.8033
b_{-2}	-5.6781 ± 1.2942
b_{-1}	3.1644 ± 0.8605
b_0	-0.5591 ± 0.3448
b_1	5.8103 ± 1.2796
b_2	-1.9389 ± 0.7671
Coefficient of determination R^2	98.6%
Total error	2.4244e-6%
C_g	1.2908
$T_\theta (\theta^*)$	$0.1990\theta^2 + 8.2504\theta - 0.1502$
$T_f (\theta^*)$	$8.9062\theta - 0.9835$
$T_m (\theta^*)$	$-1.2459\theta^2 + 1.8406\theta - 0.0743$

Appendix G: (continued)

Table G.6. Summary of results of curved beam with $\lambda = 90^\circ$

Constant γ	0.8148
b_{-2}	-26.4491 ± 2.2828
b_{-1}	14.0351 ± 1.5874
b_0	-2.6508 ± 0.6697
b_1	23.2103 ± 2.1709
b_2	-7.3468 ± 1.2565
Coefficient of determination R^2	98.93%
Total error	6.3645e-6%
C_g	1.3147
$T_\theta (\theta^*)$	$-0.0520\theta^2 + 8.6129 \theta - 0.1615$
$T_f (\theta^*)$	$9.0057\theta - 1.1829$
$T_m (\theta^*)$	$-1.7981\theta^2 + 2.6234 \theta - 0.0747$

Table G.7. Summary of results of curved beam with $\lambda = 105^\circ$

Constant γ	0.8281
b_{-2}	-142.1823 ± 4.1447
b_{-1}	78.0177 ± 3.0046
b_0	-15.7772 ± 1.3276
b_1	115.4554 ± 3.7958
b_2	-34.7151 ± 2.1215
Coefficient of determination R^2	99.44%
Total error	1.5795e-5%
C_g	1.3427
$T_\theta (\theta^*)$	$-0.3244\theta^2 + 8.9923 \theta - 0.1640$
$T_f (\theta^*)$	$9.1455 \theta - 1.4521$
$T_m (\theta^*)$	$-2.4524\theta^2 + 3.5246 \theta - 0.0498$